# RELATIONSHIPS BETWEEN SATELLITE DERIVED OUTGOING LONGWAVE RADIATION (OLR) AND SOME IMPORTANT METEOROLOGICAL PARAMETERS

By

**WILLIAM NYAKWADA**

A THESIS SUBMITTED IN PART FULFILMENT FOR THE DEGREE OF MASTER OF
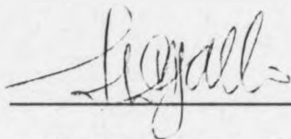
SCIENCE IN THE UNIVERSITY OF NAIROBI.

FEBRUARY 1991

This thesis is my original work and has not
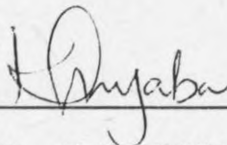been presented for a degree in any other University.

**WILLIAM NYAKWADA**

This thesis has been submitted for examination
with our approval as University supervisors

15/3/91

**PROFESSOR L.J. OGALLO**

15/3/91

**DR. E.K. ANYAMBA**

Department of Meteorology
University of Nairobi
P. O. Box 30197
NAIROBI
KENYA

## TABLE OF CONTENTS

## CHAPTER ONE

## CHAPTER TWO

**CHAPTER THREE**

## LIST OF FIGURES

# LIST OF TABLES

## ABSTRACT

The objective of this study was to determine relationships between satellite derived outgoing longwave radiation (OLR) and several meteorological parameters using correlation and regression analyses. The meteorological parameters included rainfall, rain-days, moisture budget, cloud cover, incoming radiation and surface temperature. Principal component analysis (PCA) was further used to study the spatial and temporal characteristics of OLR and rainfall.

The first step in the study involved the estimation of the few missing records. The quality of the estimated records was examined before they were included in the study. Both point and areally averaged records were used in the study for the four standard seasons namely March-May, June-August, September-November and December- February.

The results from correlation analysis revealed significant correlation between OLR and the various meteorological parameters. The correlations between point records were generally weak compared to those obtained for areal records.

The largest values of correlations obtained for point and areal rainfall were 0.88 and 0.97 respectively. Similarly, the largest values of correlations observed for rain-days, moisture budget, cloud cover, incoming radiation and surface temperature were 0.89, 0.89, 0.84, 0.93 and 0.72 respectively. The surface temperature had the weakest correlations at all stations and seasons.

The map patterns of longterm OLR values indicated large spatial and temporal fluctuations similar to those of centres of active convection. Some similarities in the spatial and temporal characteristics of the OLR and rainfall were evident from the PCA results. The spatial complexity of rainfall patterns in Kenya was also discernible from the PCA results which indicated that the six (6) significant rainfall rotated principal component (RPC) modes could account for about 75% of rainfall variance while the three (3) dominant OLR RPC modes accounted for about 89% of OLR variance over East Africa.

The results from regression analysis indicated that useful rainfall estimates could be derived from OLR records. The skill of regression equations was high for areally averaged records and over arid and/semi-arid areas. In most cases, however, OLR accounted for rainfall variance ranging from 50 to 79%.

## 1.0 INTRODUCTION

Most of the activities in East Africa are highly dependent on rainfall. However, anomalous rainfall events like droughts and floods often lead to loss of life and property. Its influence on rainfed agricultural and pastoral activities, on which the economy of the three states of East Africa depends, is immense. Rainfall is highly variable both in space and time, especially in the tropics where the variations in other Meteorological elements are comparatively small. The knowledge of rainfall distribution in space and time is, therefore, essential for solving problems related to all rain dependent activities. The understanding of its distribution in space and time is also important for the improvement of the general circulation models (GCM) since it is a good surface indicator of regions of convective activities and a measure of the released latent heat of condensation. It has been observed that latent heat released in the tropics, where above two-thirds of global precipitation occurs, has strong influence on the general circulation of both low and high latitudes (Simpson et al., 1988; Liebmann and Gruber, 1988).

While rainfall is that important it is one of the most difficult meteorological elements to measure, especially over the vast oceans, thick forests and deserts where raingauge network is sparse or non-existent. Over the oceans, rainfall has normally been estimated from observations at coastal and island stations which are likely to be influenced by orographically induced circulations.

The observations from raingauges are highly influenced by the shape of the gauges, their exposure to the wind and evaporation of the catch in the gauge in-between measurements. Convective rainfall, which dominates rainfall processes over the globe, is of small spatial scales and its accurate observation in space and time would require a dense network of raingauges. Such a dense network is not easy to achieve due to the high costs involved. Finances to establish such a network are not available to most of the developing countries.

In view of the above mentioned shortcomings of the use of standard raingauges, a lot of effort has been made to use remote sensing facilities (radar and satellite based sensors) to estimate rainfall. Remote sensing is the Art and Science of obtaining information about the object, area or phenomenon through the analysis of the data acquired by a device that is not in contact with the object, area or phenomenon under investigation.

Estimation of rainfall by radar improved the understanding of the distribution of the element in space and time. However, problems of attenuation and calibration limit the accuracy of radar for the determination of rainfall. Moreover, its fixed location and limited area of coverage (80 to 100 km) makes it unsuitable for global scale measurements over the oceans. Another drawback of radar methods is that for each specific rain rate a certain relationship between reflectivity and rainfall must be determined (Hudlow, 1979, Sulakvilidze and Dadali, 1965).

Due to the problems associated with the standard raingauges and radars, many attempts have been made to derive rainfall estimates from satellites. The advantages of the satellites include their ability to monitor large areas.

The limitations of satellite methods include huge expenses needed to set up a system, the interpretation of the satellite data and the need for ground truth data for comparison with satellite estimates. Also the derived relationships between satellite data and rainfall are not easily transferable from location to location. Despite these difficulties various methods that utilize satellite derived information have been developed. They include methods that use visible and infrared data (singly), microwave data and data from more than one spectral band (multispectral). The methods that use infrared data include those that use satellite derived outgoing longwave radiation (OLR). The details of these methods are given later in the text.

The outgoing longwave radiation (OLR) at the top of the atmosphere is known to be influenced by the incoming radiation, cloud cover, rain days, surface temperature and moisture budget (precipitation minus evaporation). Short and Wallace (1980) attributed diurnal variations in OLR to diurnal variations of surface temperature and cloudiness. Its large diurnal variation over dry lands has been attributed to daytime warming of the surface by the incoming solar radiation (Hartmann and Recker, 1986) and reduced soil moisture content (Liebmann and Gruber, 1988). Budyko (1969) established a linear relationship between OLR, surface temperature and cloud cover, and between OLR and the incoming

radiation. North (1975) found a linear relationship between OLR and surface temperature. Morrissey (1986) established the existence of a good correlation between OLR and the moisture budget.

The major objective of this study is to establish a relationship between rainfall and satellite derived outgoing longwave radiation (OLR) over Kenya. Such relationships may be used to estimate rainfall after some calibrations. In view of the above mentioned influence of the incoming radiation, cloud cover, rain-days surface temperature and moisture budget on OLR, the relationships between these elements and OLR over Kenya are investigated. The details of the objective are given in the following section.

## 1.1 OBJECTIVE OF STUDY

The major objective of the present study is to establish relationships between rainfall and satellite derived outgoing longwave radiation (OLR), which may be used to estimate both point and areal rainfall over Kenya. Relationships between OLR, and incoming radiation, cloud cover, surface temperature, moisture budget and rain-days are also investigated.

The study was divided into six stages. The first stage involved estimation of missing records. The second stage involved the testing of the quality of records. In the third stage rainfall was averaged over 2.5° x 2.5° latitude/ longitude squares and rainfall homogeneous regions adopted from Ogallo (1989).

In the fourth stage the spatial characteristics of OLR and rainfall were investigated using Principal Component Analysis (PCA). Also the characteristics of OLR fluctuations are inferred from the longterm means of OLR.

In the fifth stage correlations between point and areal rainfall are computed. Also computed are correlations between the other Meteorological parameters and OLR.

In the final stage, however, regression models for statistically significant relationship between OLR and rainfall are developed. The skills of the regression equations were determined from the analysis of variance (ANOVA) principles.

The details of the methods used in the analysis are discussed later in the text after the review of literature relevant to this study.

## 1.2 LITERATURE REVIEW

Several Scientists, institutions and organizations have explored the possibility of estimating rainfall using satellite derived information and surface observed rainfall. The methods that have been suggested include those that use

   (i)    Visible and infrared data, singly,

   (ii)   Microwave data and

   (iii)  Data from more than one spectral band
          (multispectral).

The development of the methods that belong to the first category is based on the relationships between areas of active convection and rainfall, and areas with high albedos (visible) and comparatively colder temperatures (infrared) (Kasahara et al.,1987). The methods in this category include

those suggested by Griffith et al. (1978), Stout et al.
(1979), Heinman et al. (1987), Doneaud et al. (1987), Arkin
(1979), Arkin and Meisner (1987), Barret et al. (1986),
Dugdale and Milford (1985, 1989), and Motell and Weare
(1987).

The method suggested by Griffith et al. (1978) uses
visible or infrared satellite imagery data to estimate
rainfall. The method uses the brightness (visible) and cloud
top temperature (infrared) threshholds to identify rain
clouds and areas covered by such clouds. The relationships
are developed between normalised cloud and radar echo areas.
The volumetric rain rate is finally determined from

$$R_V = I \, A_E \dots\dots\dots\dots\dots\dots\dots\dots (1)$$

Where $R_V$ is the rain volume per hour ($m^3 \, h^{-1}$) I is the
rain in units of $m^3 \, Km^{-2} \, h^{-1}$ (a function of echo growth
trend) and $A_E$ is echo area ($Km^2$) defined by $1mmh^{-1}$ rain rate.

Good results have been obtained by the method in the
tropics. The method is, however, complex especially with the
inclusion of cloud development stages.

While the Griffith et al. (1978) method involved two
steps to estimate rainfall, Stout et al. (1979) suggested a
more direct method which estimates volumetric rain rate from
the cloud area and its rate of change. The cloud areas are
identified as in the Griffith et al. (1978) method. Their
model may be expressed as

$$R_V = a_o \, A_c + a_1 \left\{ \frac{dA_c}{dt} \right\} \dots\dots\dots\dots\dots (2)$$

Where $A_c$ is the area of cloud, $dA_c/dt$ the rate of

change of cloud area, and $a_0$ and $a_1$ the regression coefficients.

The method requires satellite images taken at frequent time intervals which can only be obtained from geosynchronous satellites.

Heinmann et al. (1987) used Geostationery Operational Environmental Satellite (GOES) infrared data and manually digitized radar (MDR) to produce accumulated rainfall maps for Florida. The method assigns pixels with certain infrared temperatures an MDR value. This method suffers from the effects of cirrus and stratiform clouds which lead to over estimation of rain areas.

Doneaud et al. (1987) used a method which related area-time-integral of cloud areas, determined by infrared temperature threshhold, over alife-time of a storm to volumetric surface observed rainfall. The method is based on strong correlations between radar echo area coverage integrated over the lifetime of a storm and the radar estimated rain volume. It gives good results for convective rainfall. The effects of cirri, however, makes it difficult to identify the end times for the development of convective storms.

Arkin (1979) suggested a method which correlates the fraction of the area of a fixed region covered by clouds at a certain cloud top temperature to surface observed rainfall. The method assumes that areas of active convection and rainfall appear colder than inactive areas. Richards and Arkin (1981) investigated the skill of this method on varying spatial and temporal averaging scales, and threshhold

temperatures. They found that the skill of this method improved with the increase in spatial and temporal averaging scales. The method was found to be insensitive to changes in the threshhold temperature in some temperature ranges. The best relationships were observed for $2.5^O$ x $2.5^O$ latitude/longitude squares and a temperature threshhold of 235K.

Arkin and Meisner (1987) suggested a method which estimates rainfall from the product of the mean fractional cloud coverage of clouds colder than 235K in $2.5^O$ x $2.5^O$ latitude/longitude box, the length of the averaging period in hours and a constant. The method, commonly referred to as GOES precipitation Index (GPI) can be expressed as

$$GPI = SF_ct \dots\dots\dots\dots\dots\dots\dots\dots (3)$$

Where GPI is the estimated rainfall in mm, $F_C$ is the fractional cloud cover (varying between 0 and 1 and t is the length of the period (hours) for which $F_C$ was the mean fractional cover. S is the slope which is estimated by regressing surface observed rainfall on the fractional cloud cover. It was fixed at $3mmh^{-1}$ in their work. This method gives good results in the regions and seasons dominated by convective rainfall.

It is known that clouds with equal cloud top temperatures can give different amounts of rainfall due to the effects of orography, windshear, and moisture conditions (Turpeinen, 1986). Owing to this the ESOC (European Space Operation Centre) Precipitation Index (EPI) scheme (Turpeinen, 1986; Turpeinen et al;1987) suggested an improvement on Arkin's (1979) method by incorporating the

upper tropospheric humidity (UTH). In the EPI method, the determined fractional cloud cover at a temperature colder than 235K (EPI) are segregated into three categories depending on the level of UTH during the period of observation. The segregated EPI's form multiple predictors of rainfall. Good results have been obtained by this method in the tropics, including Africa (Turpeinen, 1986; Turpeinen et al, 1987; Turpeinen and Diallo, 1989). The method has also given good results over the highly convective western facing slopes of Kenya (Turpeinen et al.,1987). The method was not applied to the eastern facing slopes of Kenya due to high cloud top temperatures in the region imposed by frequent orographic rainfall.

The Polar-Orbiter-Effective Rainfall Monitoring Integrative Technique (PERMIT) (Barret et al., 1986) uses four infrared image slots per day and appropriate temperature threshold to map daily rain areas. Then the rain /no-rain areas of the month are aggregated to form a map of PERMIT - estimated rain days for respective months. The final rainfall estimates are obtained by relating the surface observed rainfall to the first PERMIT rainfall estimates. The first PERMIT rainfall estimates are obtained by multiplying the PERMIT rain-days by mean rainfall per rain day obtained from climatological maps. The method was developed from a more data demanding Agricultural Drought Monitoring Technique (ADMIT), discussed later in the text. Barret and Power (1986) found ADMIT to have higher skill than PERMIT over the Sahel.

Dugdale and Milford (1985, 1989) and Ouma (1988) related Cold Cloud Duration (CCD) derived from satellite data to surface observed rainfall to estimate rainfall over parts of Africa. Flitcroft et al.(1986) used the same method to estimate rainfall over the Sahel. They indicated sparse rainfall network in the region to be a limiting factor.

Motell and Weare (1987) suggested a method which uses satellite derived outgoing longwave radiation (OLR) to estimate rainfall. This method which was adopted in this study is discussed later in the text.

The methods discussed by Ouma (1988) fall in this category.
All the methods discussed in this first category suffer from the difficulty of separating non-precipitating thick cirrus and stratus clouds from the precipitating clouds.

The methods that are based on microwave technique use measurements in microwave frequencies to estimate rainfall. Microwave frequencies have advantage over visible and infrared frequencies due to their capability to penetrate through precipitating and non-precipitating low clouds (Yeh and Liou, 1983). The methods that belong to this category can be grouped into two classes namely passive and active microwave methods. The passive microwave methods use the intensity of radiation emitted. The active microwave methods use the reflected portion of the beam directed to clouds to estimate rainfall.

Most of microwave satellite methods belong to the first type. They include those suggested by Wilheit et al. (1976, 1977), Spencer (1984) and Rodgers and Siddalingaiah (1983).

The passive microwave methods are developed on the basis of absorption and scattering of microwave radiation by cloud hydrometers. The methods that use absorption properties of liquid rain drops utilize microwave measurements in frequencies below 22GHz where absorption dominates. The absorbed radiation is associated with the emitted radiation by Kirchoff's law. These methods require a background with low and uniform emissivity (e.g Oceans) to identify rain areas (Wilheit et al, 1976, 1977, Vonder Haar and Hillger, 1986; Houghton, 1979). Wilheit et al. (1976, 1977) used this method to interpret microwave measurement in terms of rain rates. The methods have limitations over land due to high emissivity which is highly variable due to surface roughness (Spencer, 1984; Wilheit, 1986). Spencer (1984), Rodgers and Siddalingaiah (1983) found that a combination of measurements in more than one microwave frequency had a higher skill in delineating rain areas than single frequency measurements over the land.

The methods that use the scattering properties of frozen cloud hydrometers employ measurements in frequencies greater than 60GHz (Wilheit, 1986). At such frequencies low brightness temperatures can be associated with convective rainfall. The method can be used to estimate rainfall over any background. However, it is more indirect than the absorption methods and suffers from the variability of the shapes and distribution of ice for individual rain rates.

In the frequencies ranging from 22 to 60GHz any form of attenuation (absorption or scattering) can dominate (Wilheit, 1986).

The passive microwave techniques suffer from non-linear relationship between rain rates and microwave irradiances which result in multiple rain rates for each microwave irradiance.

The tropical rainfall measuring mission (TRMM) intends to launch a radar on TRMM satellite which will make it possible to estimate rainfall from space by active microwave method (Simpson et al., 1988). The TRMM satellite is expected to have an altitude of 300km and an inclination of $30^{\circ}$ which will enable it to solve the beam filling problem and diurnal cycle effects suffered by polar orbiting satellites with microwave sensors. (Shin and North, 1988).

The multispectral methods use measurements in more than one frequency. The principle behind the development of multispectral methods is that a single spectral band may not be able to reveal all the properties of clouds. The methods include those that use visible, infrared and microwave data as multiple predictors. Simpson et al. (1988) suggested that in order to obtain useful quantitative rainfall estimates, it is necessary to have additional sensors to those operating in the visible and infrared portions of the spectrum. The tropical rainfall measuring mission (TRMM) (Simpson et al. 1988) intends to improve the measurements of tropical rainfall by utilizing information from passive microwave sensors, and visible and infrared portions of the spectrum.

The multispectral methods that use visible and infrared data as multiple predictors are based on the knowledge that while infrared temperature indirectly reveals the heights of cloud tops, the visible data informs on the depth of clouds,

their geometry and composition (Barret et al., 1986; Collier et al., 1989).

Lovejoy and Austin (1979) used GOES infrared and visible data as multiple predictors to estimate rainfall over Montreal. They found that infrared and visible data had a higher skill in separating rain from no-rain areas than single spectrum data. However, this combination had a poor skill in predicting rain rates.

The Agricultural Drought Monitoring Technique (ADMIT) (Barret et al., 1986) uses visible and infrared data as multiple predictors of rainfall. The method first classifies pixels into rain and no-rain using an established visible/infrared threshold curve. The first rainfall estimates are obtained as discussed in PERMIT. The final rainfall estimates are obtained by regressing the surface observed rainfall on the first satellite rainfall estimates. This method is capable of reducing the influence of diurnal circulations and non-precipitating cirroform and anvil expansion on rainfall estimates.

Negri and Adler (1987a) found that the explained variance of rainfall improved when infrared and visible data were used as independent multiple predictors. However, Negri and Alder (1987b) found that the results obtained from one parameter models (infrared or visible) were comparable to those obtained from multiple parameter model (infrared and visible). They attributed this to high correlations between visible brightness, mean cloud temperatures and cloud areas. The high correlation between visible and infrared data makes

visible data to be a redundant source of information since cold clouds are, in most cases, bright.

The problems associated with the methods that use visible and infrared data include those that arise from registration errors between visible and infrared images, instrument calibration, time difference between images, illumination geometry, the emission of equal irradiances by precipitating and non- precipitating clouds and lack of visible images at night (Collier et al., 1989; Negri and Adler, 1987b).

The methods that employ infrared and microwave data have been suggested by Yeh and Liou (1983), and Spencer (1984). Yeh and Liou (1983) used infrared and microwave data to infer various cloud parameters including water content. They obtained results which were qualitatively comparable to surface observed patterns. However, the quantities of rainfall derived from the estimated cloud water contents were higher than the surface observed rainfall amounts.

Spencer (1984) found that more variance of radar echo was explained when infrared and microwave measurements were employed as multiple predictors.

The methods discussed above are either involving or require the use of measurements from geostationery satellites. The methods that use satellite derived outgoing longwave radiation (OLR) are more direct and give good results in the tropics. The methods correlate rainfall to OLR values. They take advantage of easy interpretation of OLR in the tropics where low values of OLR correspond to regions of deep active convective clouds and high OLR values

correspond to cloudless regions or regions of maximum subsisdence (Gruber and Winston, 1978; Knutson et al., 1986; Hartman and Short, 1980; Morrissey, 1986; Murakami, 1980; Lau and Chan, 1983; Liebmann and Hartman, 1982; Short and Wallace, 1970, Slingo et al., 1987, Heddingnaus and Krueger, 1981).

Short and Wallace (1980) used this approach to infer diurnal variations of cloudiness and precipitation employing OLR data from NOAA polar orbiting satellites. They found that OLR exhibits diurnal oscillations similar to those exhibited by thermally driven convective clouds and precipitation. Lau and Chan (1983) used OLR data from NOAA polar orbiting satellite to derive the frequency of highly convective clouds (HCC) from which rainfall was estimated. They obtained the regression equation,

$$R = 0.05 + 66.7 \, N_c \quad \ldots \ldots \ldots \ldots (4)$$

Where R is rainfall rate in mm/month and $N_c$ is the number of days in a month in which the grid point daily OLR average falls below a threshold of $240 Wm^{-2}$.

Morrissey (1986) found a good correlation between OLR and rainfall.

Motell and Weare (1987) related OLR to surface observed rainfall to estimate rainfall over the pacific. They used NOAA archived digital OLR data which were related to surface rainfall at small tropical islands. They derived the equation,

$$R = 1763.847 - 6.107 \, (OLR) \ldots \ldots \ldots (5)$$

Where R is the rainfall estimate in mm/month, OLR is the mean monthly outgoing longwave radiation. They

restricted the heights of stations to 30m above mean sea level. When they used stations of higher altitude and latitude, they obtained relatively weak correlations. The weak correlations were attributed to the failure of relationships between OLR and rainfall in higher latitudes. However, the high altitudes of the stations used might also have affected the results. The relationships were found to be good equator-ward of $20^{\circ}$ latitude. They found the method to give better result than methods that use visible imagery over regions dominated by stratus clouds. While stratus clouds may have similar brightness as convective clouds, their cloud top temperatures are higher than those of active convective clouds. The method was also found to overpredict rainfall in low mean rainfall areas and underpredict in regions of high mean rainfall.

The limitations of methods which use OLR include the difficulty to isolate regions of active convection from regions of inactive thick cirrus clouds (the so called cirrus contamination) (Morrissey, 1986; Simpson et al., 1988). It is also difficult to separate regions of low OLR caused by orography and the presence of ice and snow from those of active convection. In regions of high orography the signals from deep convection are contaminated by the signals from the surface (Lau and Chan, 1983). While the elimination of cirrus contamination is not easy, the errors due to the influence of surface temperature are small in the tropics.

This method was adopted in this study due to its good results in the tropics and capability to give good rainfall estimates in regions of stratiform clouds. The eastern

facing slopes of Kenya receive most of their rainfall from stratiform clouds. The OLR values were related to point and areal rainfall. Relationships between OLR and other Meteorological parameters were also investigated from correlation and regression analyses.

In the next section the data used in this study are discussed.

## 1.3. DATA

In this section, the data used in this study are discussed. The data included satellite derived outgoing longwave radiation (OLR), rainfall, rain-days, cloud cover, evaporation, incoming radiation and surface temperature. The OLR data are discussed in the first part of this section. The second part of this section discusses the other surface observed Meteorological data. Evaporation was used to derive the moisture budget discussed in section 2.3.

## 1.3.1 SATELLITE DERIVED OUTGOING LONGWAVE RADIATION (OLR) DATA

The rainfall of East Africa, like that in other tropical regions, is dominantly from deep convective clouds. Some of these clouds extend as high as the tropopause level. They are, therefore, seen by satellites as regions of cold temperatures and low OLR. This,together with the fact that spatial variations of temperature in the tropics are small, makes it easier to interpret OLR data in the tropics. Low and high values of OLR generally correspond to deep active convective and cloudless regions, respectively (Janowiak et al., 1985; Short and Wallace, 1980; Gruber and Krueger, 1984;

Motell and Weare, 1987; Liebmann and Gruber, 1988; Knutson et al., 1986; Bess et al., 1989).

The monthly mean outgoing longwave radiation (OLR), as observed from NOAA polar orbiting satellites for the period 1974 to 1986, were used in this study. The total OLR data were derived from window channels measurements which have varied between 10.5 and 12.5 micrometers from satellite to satellite. The measurements in the window region ensure that OLR is a factor of only the brightness temperature of the radiating surface. In this window region, most clouds, except for thin cirrus, absorb essentially all the infrared radiation upwelling from beneath them, and emit radiation almost like perfect absorbers. In conditions of overcast, OLR measurements contain no direct information about the atmosphere below the cloud top (Pearson and Stogaitis, 1989; Fritz and Winston, 1962).

Various algorithms have been in use to derive the total OLR from window channel measurements. They include those of Gruber and Krueger (1984), Abel and Gruber (1979) and Ellingson and Ferraro (1983).

Changes in the methods of deriving the total OLR from window channel measurements, equator crossing times and window channels introduce inhomogeneity in the data (Janowiak et al., 1985, Hartmann and Short. 1980; Gruber and Krueger, 1984; Lau and Chan 1983).

The inhomegeneity caused by changes in the algorithms and window channels are easy to eliminate using the suggested algorithms (Janowiak et al.,1985). However, the inhomogeneity caused by different equator crossing times is

difficult to eliminate but may be minimized by taking the average of twice daily OLR measurements. Since monthly OLR data were used in this study, the inhomogeneity due to equator crossing time is considered negligible.

Eventhough NOAA polar orbiting satellites, like other asynchronous satellites, undersample small spatial and temporal scales, advantages of these satellite over the geosynchronous satellites include global coverage, high vertical resolution and minimum geometric distortion (Salby, 1989).

Garcia (1981) found that NOAA polar orbiting satellite data gave results comparable to those of high resolution geostationary satellite. NOAA polar orbiting data avail the longest continuous record of OLR vital for climatological analysis.

The monthly and seasonal OLR were used in this study. Both grid point and areally averaged values were used. The OLR were averaged over $2.5^{\circ}$ x $2.5^{\circ}$ latitude/longitude squares formed by joining the OLR grid points (figure 1b). The resolution of OLR was $2.5^{\circ}$ x $2.5^{\circ}$ latitude/longitude (figure 1a).

## 1.3.2 RAINFALL, EVAPORATION, INCOMING RADIATION, RAIN-DAYS, CLOUD COVER, AND SURFACE TEMPERATURE DATA

The monthly rainfall totals used in this study were obtained from 119 stations evenly distributed over Kenya (Figure 2a). The locations of the stations are indicated in table 1. The rainfall was also averaged over $2.5^{\circ}$ x $2.5^{\circ}$ latitude/longitude squares and climatological homogeneous region (figures 1b and 2b). The period of study was

restricted by the availability of OLR records. The OLR were available for the period 1974 to 1986.

Other records which were used included incoming radiation, cloud cover, rain-days, evaporation and surface temperature. The evaporation data were used to estimate the moisture budget discussed in section 2.3.

In the next section the climate of East Africa is discussed.

**Table 1:** THE LIST OF STATIONS USED IN THE ANALYSIS

| STATION NAME | Number | LOCATION Lat. | Long. (E) | ALTITUDE Ft. Above M.S.L |
|---|---|---|---|---|
| Lodwar Met. | 8635000 | $3^{\circ}07'N$ | $35^{\circ}37'$ | 1600 |
| Kupri Irrig. Sch | 8735005 | $2^{\circ}06'N$ | $35^{\circ}28'$ | 2300 |
| Oropoi Police Post | 8634007 | $3^{\circ}48'N$ | $34^{\circ}21'$ | 3000 |
| Chepunyal Chiefs office | 8835032 | $1^{\circ}36'N$ | $35^{\circ}17'$ | 7800 |
| Lokori | 8836009 | $1^{\circ}57'N$ | $36^{\circ}54'$ | 2500 |
| South Horr Catholic Mission | 8736000 | $2^{\circ}06'N$ | $36^{\circ}54'$ | 3600 |
| Tuum Pri. School | 8736001 | $2^{\circ}09'N$ | $36^{\circ}47'$ | 4800 |
| Maikona Catholic Mission | 8737005 | $2^{\circ}56'N$ | $37^{\circ}38'$ | 2000 |
| Baragoi D.O's office | 8836001 | $1^{\circ}36'N$ | $36^{\circ}48'$ | 4500 |
| Laisamis Police post | 8638000 | $1^{\circ}36'N$ | $37^{\circ}48'$ | 1904 |
| Sololo Police Post | 8638000 | $3^{\circ}33'N$ | $38^{\circ}39'$ | 2400 |
| North Horr Police Post | 8637000 | $3^{\circ}19'N$ | $37^{\circ}04'$ | 2200 |
| Sabarei Police Post | 8536000 | $4^{\circ}21'N$ | $36^{\circ}54'$ | 2500 |
| Ileret Police Post | 8536001 | $4^{\circ}19'N$ | $36^{\circ}14'$ | 1400 |
| Marsabit Met. | 8738000 | $2^{\circ}19'N$ | $37^{\circ}59'$ | 4413 |
| Buna Police Post | 8739000 | $2^{\circ}48'N$ | $39^{\circ}01'$ | 2000 |
| Moyale Met | 8639000 | $3^{\circ}32'N$ | $39^{\circ}03'$ | 3650 |
| Wajir Met. | 8840000 | $1^{\circ}45'N$ | $40^{\circ}04'$ | 800 |
| Rhamu Police Post | 8641001 | $3^{\circ}56'N$ | $41^{\circ}14'$ | 980 |
| Elwak | 8740000 | $3^{\circ}47'N$ | $40^{\circ}57'$ | 1200 |
| Gurar Police post | 8639001 | $3^{\circ}22'N$ | $39^{\circ}35'$ | 3000 |
| Mandera Met. | 8641000 | $3^{\circ}56'N$ | $41^{\circ}52'$ | 1085 |
| Kitale Met. | 8834098 | $1^{\circ}01'N$ | $34^{\circ}59'$ | 6100 |
| Leissa Farm | 8835039 | $1^{\circ}10'N$ | $35^{\circ}02'$ | 6000 |
| Kisumu Met. | 9034025 | $0^{\circ}06'S$ | $34^{\circ}45'$ | 3769 |
| Port Victoria | 8933026 | $0^{\circ}07'N$ | $33^{\circ}59'$ | 4100 |
| Rusinga Hydromet. | 9034103 | $0^{\circ}25'S$ | $34^{\circ}08'$ | 4860 |
| Maji Mazuri | 9035028 | $0^{\circ}01'S$ | $34^{\circ}42'$ | 7680 |
| Kericho DC's Office | 9035003 | $0^{\circ}23'S$ | $35^{\circ}17'$ | 6500 |
| Jamji | 9035001 | $0^{\circ}29'S$ | $35^{\circ}11'$ | 6000 |
| Kericho Met | 9035279 | $0^{\circ}22'S$ | $35^{\circ}21'$ | 7160 |
| Nakuru Met. | 9036261 | $0^{\circ}16'S$ | $36^{\circ}04'$ | 6141 |
| Narok | 9135001 | $1^{\circ}06'S$ | $35^{\circ}52'$ | 5200 |
| Bondo water | 9034036 | $0^{\circ}03'S$ | $34^{\circ}17'$ | 4000 |
| U.O. East Africa | 8935062 | $0^{\circ}15'S$ | $35^{\circ}05'$ | 6500 |
| Chorllim ADC | 8834013 | $1^{\circ}02'N$ | $34^{\circ}48'$ | 6500 |
| Namandala Farm | 8834017 | $1^{\circ}03'N$ | $34^{\circ}56'$ | 6000 |
| Kaibubich | 8835031 | $1^{\circ}12'N$ | $35^{\circ}17'$ | 9000 |
| Cherengani | 8835034 | $1^{\circ}03'N$ | $35^{\circ}19'$ | 7300 |
| Nzoia Sugar | 8934138 | $0^{\circ}45'N$ | $34^{\circ}56'$ | 5980 |
| Lugari Forest | 8934016 | $0^{\circ}40'N$ | $34^{\circ}54'$ | 5544 |
| Nangina Catholic Mission | 8934030 | $0^{\circ}17'N$ | $34^{\circ}06'$ | 4000 |

| | | | | |
|---|---|---|---|---|
| Kabgendi | 8935001 | 0°02'N | 35°18' | 6200 |
| Kapsowar | 8935002 | 0°59'N | 35°33' | 7500 |
| Kapsiwowi | 8935130 | 0°07'N | 35°36' | 8500 |
| N/Hill | 8935160 | 0°03'N | 35°09' | 6700 |
| Kissi D.O's office | 9034001 | 0°03'N | 34°09' | 5800 |
| Miwani Sugar II | 9034007 | 0°03'S | 34°57' | 4670 |
| Miwani I | 9034012 | 0°03'S | 34°58' | 4000 |
| Lumut Chiefs office | 8835017 | 1°25'N | 35°33' | 3200 |
| South Marmet | 8936023 | 0°03'N | 36°22' | 7600 |
| Naivasha D.O office | 9036002 | 0°43'S | 36°26' | 6234 |
| Nyeri M.O.W. | 9035017 | 0°02'S | 37°57' | 6000 |
| Muchene | 8937078 | 0°06'S | 37°32' | 7400 |
| Kitito | 9037016 | 0°59'S | 37°18' | 4800 |
| Meru Met. | 8937065 | 0°05'N | 37°39' | 6000 |
| Poror Forest post | 8836003 | 1°14'N | 37°36' | 7900 |
| Nanyuki Met. | 8937022 | 0°03'N | 37°02' | 6200 |
| Ragati Forest St. | 9037015 | 0°23'S | 37°02' | 6600 |
| Rumuruti | 8936001 | 0°16'N | 36°34' | 6090 |
| Mutara | 8936014 | 0°07'N | 36°42' | 6000 |
| Nginyang | 8936020 | 0°57'N | 36°01' | 3000 |
| Garissa Met. | 9039000 | 0°25'S | 39°38' | 420 |
| Balambala P.P. | 9039001 | 0°02'S | 39°04' | 625 |
| Bura Pol. St. | 9139000 | 1°06'S | 39°57' | 370 |
| Masalani P.P. | 9140007 | 1°47'S | 40°06' | 200 |
| Tana River Exp. | 9140006 | 1°42'S | 40°07' | 300 |
| Muddo Gashi | 8939000 | 0°45'N | 39°11' | 800 |
| Liboi | 8940003 | 0°22'N | 40°52' | 300 |
| Muddo Gashi Police post | 8939000 | 0°45'N | 39°11' | 800 |
| Makindu Met | 9237000 | 2°17'S | 37°50' | 3280 |
| Voi Met | 9338001 | 3°24'S | 38°34' | 1837 |
| Masangoleni | 9238005 | 2°22'S | 38°09' | 2300 |
| Bachuma Range Res. | 9338022 | 3°48'S | 38°57' | 1300 |
| Dagoretti Met. HQS. | 9136164 | 1°18'S | 36°45' | 5900 |
| Nairobi Water | 9136158 | 1°17'S | 36°50' | 7800 |
| Eastleigh Met. (MAB) | 9136087 | 1°16'S | 36°52' | 5371 |
| Mdigo Farm | 9136096 | 1°22'S | 36°45' | 6200 |
| Jomo Kenyatta (JKIA) | 9136168 | 1°19'S | 36°55' | 5329 |
| Langata | 9136198 | 1°18'S | 36°52' | 5637 |
| Machakos D.C. | 9137010 | 1°31'S | 37°01' | 5015 |
| Mukuli Forest | 9137106 | 1°29'S | 37°05' | 5000 |
| Kitui Agriculture | 9138000 | 1°22'S | 38°01' | 3860 |
| Kitui Water | 9138014 | 1°22'S | 38°00' | 3570 |
| Olkutai Camp | 9237018 | 2°35'S | 37°15' | 4000 |
| Mtito Andei | 9238009 | 2°05'S | 38°08' | 300 |
| Bamba Res. | 9339016 | 2°32'S | 39°31' | 800 |
| Lamu Met. | 9240001 | 2°16'S | 40°54' | 10 |
| Lamu D.O. | 9240003 | 2°23'S | 40°26' | 65 |
| Malindi Met. | 9340009 | 3°14'S | 40°06' | 65 |
| Malindi Water | 9340005 | 3°10'S | 40°06' | 150 |
| Garsen Water | 9240010 | 2°16'S | 40°07' | 200 |
| Karawa Vet | 9240012 | 2°39'S | 40°12' | 16 |
| Lake Kenyatta | 9240014 | 2°24'S | 40°41' | 10 |
| Ganze Disp. | 9339012 | 3°32'S | 39°41' | 600 |
| Rabai Chief's Camp | 9339043 | 3°56'S | 39°34' | 539 |
| Mackinnon Road | 9339002 | 3°44'S | 39°03' | 1175 |
| Majiya Chumvi | 9339023 | 3°49'S | 39°23' | 800 |
| Mazeras Res. | 9339048 | 3°59'S | 39°33' | 535 |

| | | | | |
|---|---|---|---|---|
| Makamini Chief | 9339049 | 3$^o$59'S | 39$^o$15' | 650 |
| Kwale Agriculture | 9439001 | 4$^o$04'S | 39$^o$41' | 1294 |
| Gazi Sugar | 9439004 | 4$^o$25'S | 39$^o$30' | 150 |
| Mwangulu Chief's office | 9439027 | 4$^o$25'S | 39$^o$07' | 400 |
| Simba Hills | 9439043 | 4$^o$22'S | 39$^o$25' | 800 |
| Mombasa Old Obs. | 9439002 | 4$^o$04'S | 39$^o$41' | 53 |
| Kinango Agr. | 9439015 | 4$^o$08'S | 39$^o$19' | 1000 |
| Moi Airport (Mombasa) | 9439021 | 4$^o$02'S | 39$^o$37' | 185 |
| Acher's Post | 8937035 | 0$^o$13'N | 36$^o$23' | 6750 |
| Msabaha | 9340007 | 3$^o$16'S | 40$^o$03' | 300 |
| Buchuma | 9338022 | 3$^o$48'S | 38$^o$57' | 1300 |
| Mtwapa | 9339036 | 3$^o$56'S | 39$^o$44' | 70 |
| Thika Met. | 9137048 | 1$^o$01'S | 37$^o$06' | 4800 |
| Machakos Dam | 9137098 | 1$^o$33'S | 37$^o$14' | 5160 |
| KARI Muguga | 9136121 | 1$^o$13'S | 36$^o$38' | 6875 |
| Kisii Met | 9034080 | 0$^o$41'S | 34$^o$47' | 4200 |
| Marimanti | 9037160 | 1$^o$14'S | 37$^o$55' | 4000 |
| Koiwa | 9035260 | 0$^o$37'S | 35$^o$19' | 7400 |
| Hola | 9140006 | 1$^o$28'S | 40$^o$00' | 300 |
| Mumias | 8934133 | 0$^o$22'N | 34$^o$30' | 4270 |

14
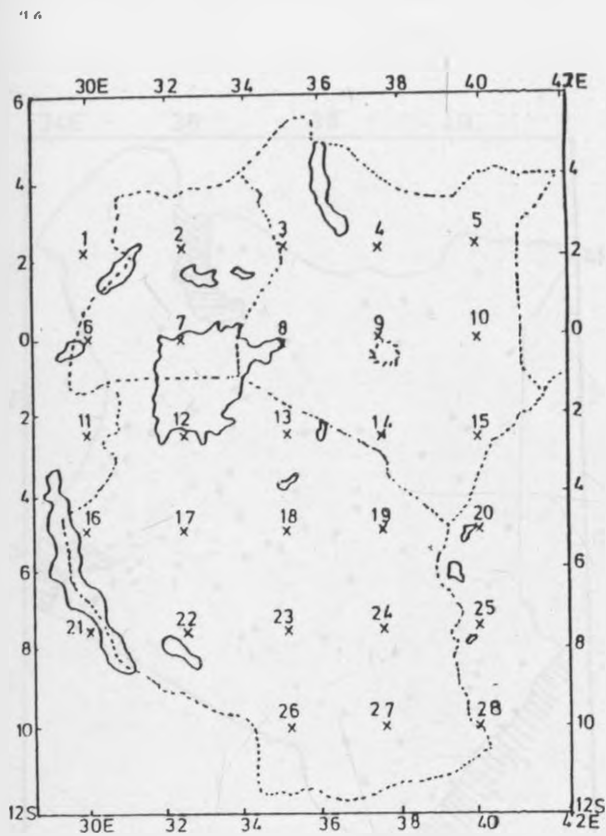


Figure 1a: OLR grid point locations over East Africa.
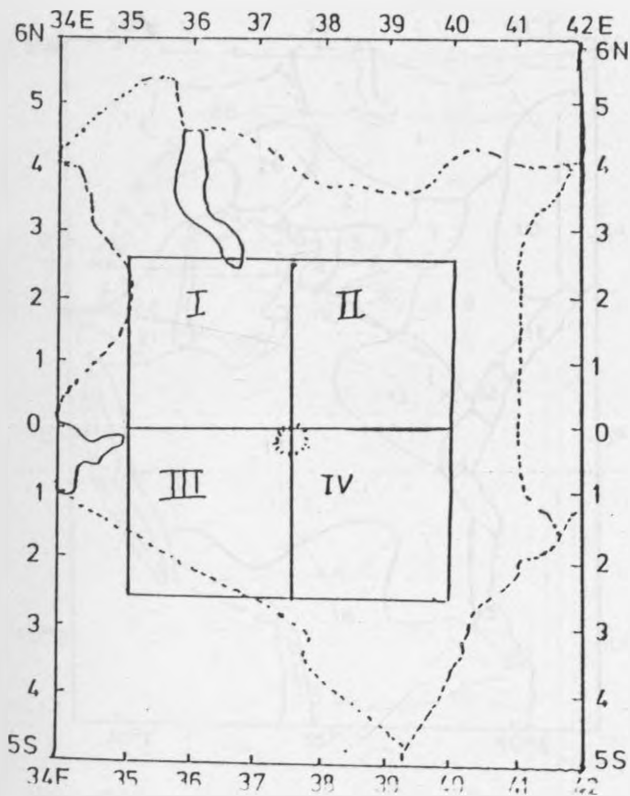


Figure 1b: 2.5° x 2.5°  Latitude/Longitude square grids located over Kenya
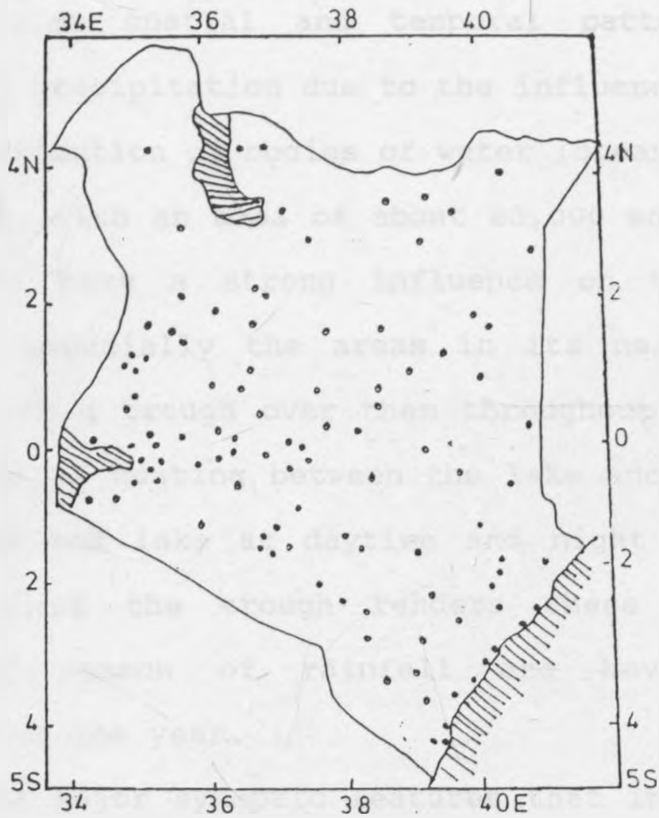
Figure 2a: The locations of Meteorological stations used in the study.
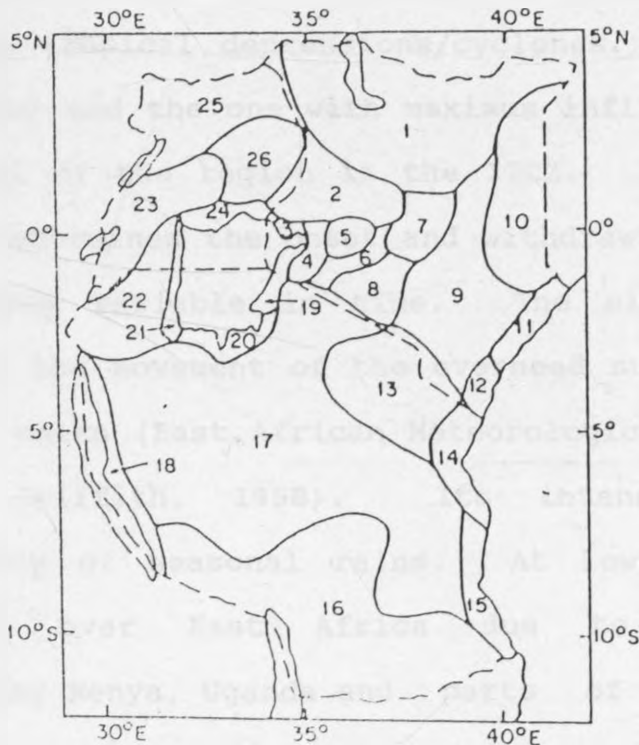


Figure 2b: Climatological homogeneous regions over East Africa (adopted from Ogallo, 1989).

## 1.4 THE CLIMATOLOGY OF RAINFALL OF EAST AFRICA

Eventhough East Africa lies in the equatorial belt, it has complex spatial and temporal patterns of daily and seasonal precipitation due to the influence of topography and the distribution of bodies of water (oceans and lakes). Lake Victoria, with an area of about 83,000 square kilometers, is known to have a strong influence on the climate of the region, especially the areas in its neighbourhood. These areas have a trough over them throughout the year caused by differential heating between the lake and land, located over the land and lake at daytime and night respectively. The presence of the trough renders these areas to have no distinct season of rainfall and have rainfall almost throughout the year.

The major synoptic features that influence the weather of East Africa are the intertropical convergence Zone (ITCZ), Mascarene high, Arabian ridge, the tropical easterly waves and the tropical depressions/cyclones. Of these, the most important and the one with maximum influence on the seasonal rainfall of the region is the ITCZ. Its surface position, which determines the onset and withdrawal of seasonal rains, is highly variable in time. The migration of the ITCZ follows the movement of the overhead sun lagging it by four to six weeks (East African Meteorological Department (EAMD), 1962; Griffith, 1958). Its intensity determines the intensity of seasonal rains. At low levels, it is very diffuse over East Africa due to the influence of orography Kenya, Uganda and parts of Tanzania near the equator have two rainy seasons in a year associated with the

northward movement (March - May) and Southward retreat (September - November) of ITCZ, respectively.

During the June- August season (Northern summer) East Africa is under the influence of South East/South West Monsoon airmass. Most parts of Kenya and Tanzania receive little rainfall. This is mainly because the south east/south west monsoon airmass over East Africa is diffluent in the low levels and flows parallel to the coast and East African highlands. Also there is a quasi-permanent inversion near 700 Hectopascals (Hpa) over the region during this season. These factors inhibit the occurrence of widespread rainfall. However, Uganda and Western Kenya receive rainfall in this season associated with lake Victoria circulation and the dynamic trough over Central Africa (Anyamba, 1984). The areas are also influenced by the moist Congo airmass.

During the December-February season, the region is under the influence of North east monsoon airmass (Anyamba, 1984). Tanzania receives rainfall in this season associated with the ITCZ in Southern Africa. Also parts of the region near large water bodies receive rainfall due to the influence of local circulations. Most parts of Kenya and Uganda are dry during this season.

The easterly waves are known to influence the weather of the region. Most of their influence is felt along the coast (Fremming, 1970; Lumb, 1966). Njau (1982), Lumb (1966) and Fremming (1970) suggested a link between East African rainfall and easterly waves.

Tropical depressions/cyclones over south Indian ocean and Arabian sea influence the weather of the region either by

passing near or hitting parts of the region. They also have indirect influence on the weather of the region by changing the tracks of the airmasses influencing the weather in particular seasons.

The Congo airmass and remnants of extratropical weather systems which penetrate the region influence the weather of the region, especially during June-August season.

The sea surface temperatures (SST), through their influence on the position and intensity of ITCZ, have a significant influence on the weather of the region. The SST also determine favourable conditions for the formation of the tropical depression/cyclones whose influence on the weather of the region has been noted earlier in the text.

A detailed discussion of the climatology of rainfall of East Africa may be obtained in Asnani (1982), Asnani and Kinuthia (1979), Ogallo (1988, 1989), Brown and Cochome' (1973), Griffith (1958), Tomsett (1969), Trewartha (1961), Johnson and Morth(1960) and other texts.

## 2.0 METHODOLOGY

In this chapter, the various methods which were used in this study are discussed. The methods include those used to estimate missing records, moisture budget and areal rainfall, mass curves, Principal Component analysis (PCA), correlation and regression analyses.

## 2.1 ESTIMATION OF MISSING RECORDS

Most climatological records have gaps which must be filled before such data may be used for the continuous

studies like in the case of time series analysis. The methods which have been commonly used to estimate missing data include isopleth, isopercentile, correlation, arithmetic mean, regression, Thiessen polygon and Empirical Orthogonal Function (EOF) methods.

Only a brief account of arithmetic mean and regression methods which were used in this study are included here. The details of other methods can be obtained in many references including Basalirwa, (1979), WMO (1960, 1966, 1974), Grimmer (1963), Chow (1964), Shaw (1988), Thiessen (1911).

It is however important to note here that the choice of stations used was restricted to those with a maximum of 5% missing data, provided the missing data was not for consecutive years, to avoid dilution of the records (WMO, 1970, 1974).

## 2.1.1. ESTIMATION OF MISSING DATA FROM ARITHMETIC MEAN METHOD

The estimation of missing data by arithmetic mean method requires the knowledge of a neighbouring station which is best correlated to the station with missing data. Hence; under this method, the first step is to identify a neighbouring station which has the highest correlation with the station with missing records.

Correlation coefficient can quantify the degree of correlation between pairs of variables. In this study simple correlation coefficient (r) was used to determine the neighbouring station which was best correlated to the station with missing data. If r is significantly different from zero, then the pair of variables are significantly

correlated.

The neighbouring station with the highest correlation coefficient (r) and reliable record was used to estimate the missing records as shown in equation 6

$$X_{Aj} = \frac{X_{Bj} \cdot \overline{X}_A}{\overline{X}_B} \dots\dots\dots\dots\dots\dots\dots (6)$$

$X_{Aj}$ is the missing record of station A in the jth year, $X_{Bj}$ the record for station with reliable records B in year j, and $\overline{X}_A$ and $\overline{X}_B$ are the longterm averages for stations A and B, respectively based on the period of records available at A.

This method generally requires long period of records in order to generate stable averages for individual stations. It also requires relatively homogeneous distribution of station in the catchment. Such a network could include all the best correlated neighbouring stations which are required to estimate the missing records.

## 2.1.2 ESTIMATION OF MISSING RECORDS FROM THE REGRESSION METHOD

Like the arithmetic mean method, the method requires the identification of the best correlated neighbouring station to be used in the estimation of the missing records of the station with unreliable records. The method used in the previous section was used to identify the best correlated neighbouring station. A regression equation was then used to

express the relationship between the stations instead of using the arithmetic mean method as expressed in equation 6.

Equation 7 gives an example of linear regression equation which can be used to express the linear relationship between the two stations.

$$X_{Aj} = a + bX_{Bj} \ldots \ldots \ldots \ldots \ldots (7)$$

$X_{Aj}$ is the record of station A in the jth year, $X_{Bj}$ is record for station B in year j, and a and b are regression constants. The details of regression analysis will be discussed later in the text.

Once a and b have been determined from the available records, equation 7 can be used to estimate future missing values at station A ($X_{Aj}$) if the records at station B ($X_{Bj}$) are available.

Like the arithmetic mean method, this method gives good results only when the stations A and B are within the same homogeneous climatological zones.

## 2.2 QUALITY OF THE RECORDS

Most climatological records are characterised with inconsistencies which may be caused by changes in the location and exposure of the raingauge, technology, instrument type and microclimate. Errors associated with data collection, transmission and processing may also introduce heterogeneity into the records. The inclusion of estimated data into the records may also introduce heterogeneity into such records.

It is therefore, necessary to check for the quality of climatological records before such data are used in any climatological analyses.

The most commonly used methods of testing the quality of data include the run test, mass and residual mass curves methods. Only a brief account of mass curves analysis, which was used in this study, is included here. A brief discussion of double-mass curves method which can be used to homogenize heterogeneous records is also included. The details of the various methods may be obtained in various references including Ogallo (1981); Thom (1966) and WMO (1966).

## 2.2.1 MASS AND DOUBLE MASS CURVES

Mass curve analysis involves the plotting of cumulative climatological records against time. The patterns of these graphs can be used to test for the quality of the records. A single straight line is obtained for nearly error free (homogeneous) records. Other patterns indicate heterogeneity in the records.

If the records are heterogeneous, the next step would be to correct for heterogeneity. The method commonly used to adjust heterogeneous records is the double mass curves. The principles of the double-mass curves analysis are similar to those of mass curves. Double-mass curves analysis, however, plots the cumulative values of the heterogeneous records against the cumulative values of records from a homogeneous station or parameter. An example of double mass curve analysis is given in figure 3a. Two lines, AD and DE (figure 3a), are obtained for heterogeneous records while only a
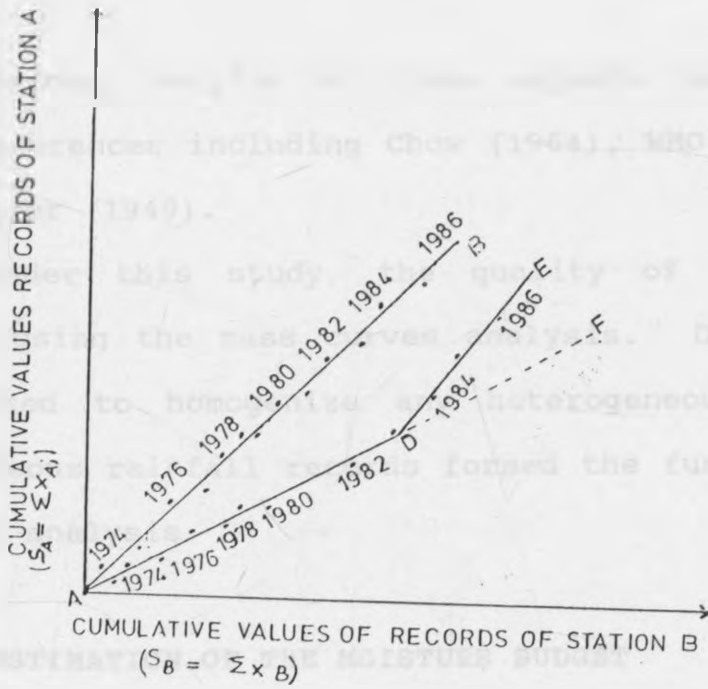
Figure 3a: An illustration of mass curves analysis.

single line (AB) is obtained for the homogeneous records. The slopes of the two lines, AD and DE, can be used to adjust the heterogeneous records. If the records lying on AD are known to be homogeneous, all later records which are lying on DE are adjusted to obtain homogeneous records which are lying on DF.

Further details of these methods can be obtained in many references including Chow (1964), WMO (1970, 1974, 1983) and Kohler (1949).

Under this study, the quality of all records were tested using the mass curves analysis. Double mass curves were used to homogenize any heterogeneous records. The homogeneous rainfall records formed the fundamental base for further analysis.

## 2.3.   ESTIMATION OF THE MOISTURE BUDGET

The moisture budget (MB) can be expressed as

$$MB = P - E \dots\dots\dots\dots\dots\dots (8)$$

Where P is the Precipitation and E is Evaporation

The moisture budget is expected to be large and positive in regions of active convection and rainfall (Morrissey, 1986). It is negatively correlated to OLR.

In this study, all stations, except for Kericho and Meru, had negative monthly moisture budgets. The dry days in-between the wet days limit the computation of monthly moisture budgets. It should also be noted that most rainfall of the region is received during particular periods of the day leading to high solar heating in clear sky conditions. Such heating may lead to high evaporation which may exceed

the received rainfall. The derived moisture budgets were correlated to OLR to investigate the relationships.

## 2.4 METHODS USED TO ESTIMATE AREAL RAINFALL

The outgoing longwave radiation (OLR) data which were used in this study were available on $2.5^O$ x $2.5^O$ latitude/ longitude resolutions. It has been noted that the accuracy of rainfall estimation techniques that use visible and infrared satellite data improve with increasing averaging area (Vonder Haar and Hillger, 1986). Arkin (1979), and Richard and Arkin (1981) found the best estimates of rainfall when rainfall was averaged over $2.5^O$ x $2.5^O$ latitude/ longitude square (about 6 x $10^4$ $km^2$).

In this study both point and areally averaged OLR and rainfall records were used to examine the relationships between OLR and rainfall. The OLR were averaged over the $2.5^O$ x $2.5^O$ latitude/longitude squares. The rainfall records within the respective squares grids were used to obtain areal rainfall values.

It was noted that the OLR grid points were sometimes located over areas with different spatial and temporal rainfall characteristics. An attempt was therefore made to include areal rainfall estimates from the homogeneous climatological zones adopted from (Ogallo, 1989) (figure 2b).

The methods commonly used to estimate areal rainfall include arithmetic mean, Thiessen Polygon, Isohyetal, Isopercentile and Principal Component Analysis (PCA) methods. Most of these methods are laborious especially when

estimating many records. It was noted in section 1.3.2. that a total of 119 stations, evenly distributed over Kenya, was used in this study. The less laborious methods, namely the arithmetic mean and Principal Component Analysis (PCA), were used in this study. The skills of these methods have been discussed by Ogallo (1986, 1989) and Basalirwa (1979). Only a brief account of arithmetic mean and Principal Component Analysis (PCA) methods is included here. The details of the various methods can be obtained in many references including (Basalirwa, 1979; Chow, 1964; Shaw, 1988; WMO, 1965, 1970, 1974; Nemec, 1972; Linsley et al., 1949).

Under the arithmetic mean method, records from locations which are enclosed within the square grid or homogeneous region are areally averaged using arithmetic mean method. The areal rainfall value $(\overline{X}_t)$ may be expressed as

$$\overline{X}_t = \frac{1}{M} \sum_{j=1}^{M} X_{jt} \qquad -------------------(9)$$

Where M is the number of stations, $X_{jt}$ the records from station or grid j during the period t.

In equation 9, each station is given equal weight (1/M) during the averaging. It is, however, known that there are significant differences in the total areal rainfall variability. Many attempts have, therefore, been made to give different weights to individual stations. A good example is the use of Thiessen Polygon method. The weighting functions which have been used in this study were based on

the time coefficients of the dominant PCA modes. This may be expressed as

$$\overline{X}_t = \frac{1}{M} \sum_{j=1}^{M} a_j X_{jt} \quad \text{-----------} \quad (10)$$

Where $X_t$ and $X_{jt}$ are the same as in equation 9, while

the constants $a_1$, $a_2$,......,$a_j$ are the regression weights for the dominant principal component mode over the region. Details of these methods can be obtained from Johnson (1980), Ogallo (1986) among many other references. The basic principles of PCA are, however, discussed later in the text.

The point and areal records were subjected to several analyses in order to examine relationships between OLR and rainfall, incoming radiation, rain-days, cloud cover moisture budget and temperature.

These analyses included correlation and regression analyses. Correlation analysis included the use of Principal Component Analysis (PCA).

## 2.5    CORRELATION ANALYSIS

Correlation coefficient can be used to quantify the degree of relationship between variables. The simplest measure of the degree of relationship between pairs of variables is the simple correlation coefficient (r), which can be expressed as

$$r = \frac{\sum\limits_{t=1}^{N} (X_t - \bar{X})(Y_t - \bar{Y})}{\sqrt{\sum\limits_{t=1}^{N} \{ (X_t - \bar{X})^2 \} \{ \sum\limits_{t=1}^{N} (Y_t - \bar{Y})^2 \}}} \quad \ldots\ldots\ldots (11)$$

Where $X_t$ and $Y_t$ are independent variables at times t, $\bar{X}$ and $\bar{Y}$ arithmetic means of $X_t$ and $Y_t$ at time t, respectively. N is the length of records.

The simple correlations coefficient r is significantly different from Zero when the variables are significantly related. r is positive or negative when the variables are positively or negatively correlated and IrI = 1 when the variables are perfectly correlated. The statistical significance of r may be estimated, using the standard t - test, as indicated in (12).

$$t_{N-2} = r \sqrt{\frac{N-2}{1-r^2}} \quad \ldots\ldots\ldots\ldots\ldots (12)$$

$t_{N-2}$ is the student t - distribution value with N-2 degrees of freedom and N is as defined in equation (11) above. The details of t - test can be obtained in many standard references including (WMO, 1983; Wannacott and Wannacolt, 1985; Battacharyaa and Johnson, 1977).

There is often some time lag in the relationships between many physical variables. Such time lagged relationships are obtained from lagged correlation coefficient ($r_k$) which may be expressed as

$$r_k = \frac{\sum_{t=1}^{N-IkI} (X_t - \bar{X})(Y_{t+K} - \bar{Y})}{\sqrt{\sum_{t=1}^{N} ((X_t - \bar{X})^2) (\sum_{t=1}^{N} (Y_t - \bar{Y})^2)}} \qquad \ldots\ldots\ldots (13)$$

Where K is the time lag and the definitions of the other variables are as in equation (11).

It should be noted from equations (11) and (13) that $r_0$ = r when time lag K = 0.

In this study relationships between satellite derived outgoing longwave radiation (OLR), and rainfall, incoming radiation, moisture budget, cloud cover, rain-days and surface temperature were independently examined by computing the zero lag and lagged correlation coefficients based on point and areal records.

Correlation analyses which were discussed in the previous section examine the relationship between two variables keeping the others constant. This method assumed that the relationships between OLR, rainfall, rain-days, moisture budget, cloud cover, incoming radiation and surface temperature were independent which may not necessarily be true for many physical variables which are often closely related. In the next section an attempt is made to use principal component analysis to examine relationships between several variables and locations.

## 2.6 PRINCIPAL COMPONENT ANALYSIS

The principal component analysis (PCA) and factor analysis (FA) are some of the models that can be derived from the Empirical Orthogonal solutions. The basic principles of

the Empirical Orthogonal analysis are derived from the concept of the variance. A measure of association for the set of variables is first calculated.

This is followed with the construction of a set of orthogonal functions that can represent the measured variables. In factor analysis the orthogonal functions are defined as exact mathematical linear transformation of the original data. The unique variance accounted for by the common set of orthogonal functions (factors) is also considered. Under the principal component analysis (PCA), the unique component of a variable is neglected.

Geometrically the Empirical Orthogonal functions (eigenvectors) are linear projections of the standardized measured variables in the orthogonal vector space. The factor coefficients represent the ordinates of a point representing a variable in this space.

A mathematical model for factor analysis (FA) represented by M common empirical orthogonal functions (factors) and n unique factors can be expressed as:

$$Z_i = a_{i1}F_1 + a_{i2}F_2 + \ldots + a_{im}F_m + d_iU_i$$

$$i = 1, 2, \ldots\ldots\ldots, M \ldots\ldots\ldots\ldots(14)$$

Where $Z_i$ is the variable i in the standardized form, $F_i$ represents the common orthogonal function (factors), $U_i$ the unique factor for variable i, $a_{i1}$ the standard multiple regression coefficient of the variable i on the common factor and $d_i$ is the regression loading of the unique factor, which is often very difficult to estimate for physical variables.

The regression coefficients (loadings) can be obtained from the correlation and covariance matrices of the variables (Harman, 1967; Richman, 1981). The correlation matrix was used in this study to derive the regression weights (loadings). The advantages of correlation matrix include equal weighting of all stations or gridpoints to avoid bias positioning of the synoptic centres. They can also be used to assign perfect position correlation between a variable and itself by setting the diagonal of the input matrix to unity. The loadings derived from the correlation matrix can be regarded as correlation coefficients of the grid points (locations) with a specific orthogonal function (Richman, 1981; Karl et al. 1982; Barnston and Livezy, 1987). Principal Component analysis (PCA) was used in this study since the unique properties of the individual variables/locations are extremely difficult to estimate mathematically. The value of $d_i U_i$ in equation (14) was, therefore, set to zero in this study.

The principal components (factors) are always extracted in the descending order of eigenvalues. This ensures that only a few factors which explain the highest portion of the variance are considered. The first factor explains as much variance as possible followed with the second and so forth.

Under the PCA, variables or locations which are inter-related cluster together onto similar vector spaces(factors). This concept has been used by many authors to examine complex relationships between large numbers of variables (Grimmer, 1963; Ogallo, 1980, 1986, 1989; Barring, 1987; Mungai, 1984;

Gregory, 1975; Wolter, 1989, Janowiak, 1988; Richman, 1981; Dyer, 1975).

The PCA concept was used in this study to study the patterns of the interlocation correlations between rainfall and grid point OLR values.

The unique properties of the PCA and other Empirical Orthogonal functions (factors), which make them powerful tools to study complex relationships between many variables, include:

1.  their reduction of the volume of data by replacing the measured variables and intercorrelated variables by a smaller number of uncorrelated variables (Principal Components),

2.  their capability to reveal the spatial and temporal patterns of the physical processes, depending on the data being analysed. The shape of the map pattern of each principal component may have some resemblance to the patterns for the variable itself,

3.  Principal components (PC's) and their coefficients are orthogonal in time (statistically independent),

4.  the principal components do not require equidistant points of the observations unlike most of the other orthogonal functions (Kutzbach, 1967).

The use of the principal component analysis, however, required the identification of the number of factors which must be included in the solutions. The methods commonly used to determine the number of the PC's to include in the solutions are discussed in the next section.

**2.6.1**   **DETERMINATION OF THE NUMBER OF SIGNIFICANT PRINCIPAL COMPONENTS (FACTORS)**

There are always as many factors (eigenvectors) as the number of variables involved in the analysis. It is, therefore, necessary to determine the number of significant factors that can represent the underlying physical phenomena effectively. The inclusion of very few factors (underfactoring) or very many factors (over factoring) can distort the map patterns obtained from rotated principal components (RPC's). '

The methods commonly used to determine the number of significant factors include Kaiser's criterion (Kaiser, 1960), Scree test (Catell, 1966), the natural logarithm method (LEV) (Craddock and Flood, 1969; Craddock and Flintoff, 1970) and the use of sampling error in the eigenvalues (North et al., 1982). The methods ensure that only a few factors extracting substantial amount of the total variance that may not be considered as noise are retained in the solutions.

The Scree test method plots eigenvalues against the corresponding ordinate eigenvector numbers. The truncation value is near the point where the graph becomes a straight line.

Noting that in Meteorology noise eigenvalues are in geometric progression, Craddock and Flood (1969) suggested a method (LEV) which plots the natural logarithms of the eigenvalues against the ordinate numbers of their principal components. The truncation value is near the point where the graph becomes a straight line.

North, et. al. (1982) among others, suggested the use of sampling errors of the eigenvalues in the determination of the number of significant principal components (factors). The method compares sampling errors for the eigenvalues with separation in the neighbouring eigenvalues. It requires that eigenvalues be separated by at least one or two times the sampling error of the eigenvalue (Barring, 1987). Hence, the sampling error ($\lambda(2/N)^{1/2}$) indicates whether a sample eigenvalue is a faithful representation of the eigenvector (factor). Here, $\lambda$ and N represent the eigenvalue and total number of records, respectively.

Kaiser's criterion retains all eigenvectors with eigenvalues greater than one.

Ogallo (1989) compared the applicability of the four methods in East African rainfall. He found no significant differences in the results obtained from the four methods for the East African rainfall records.

In this study, Kaiser's criterion was used since it was readily available in our computer subroutine.

It has been observed that rotated principal components (RPC's) give better map patterns of the relationships between the physical variables than the direct solutions given in equation (14). This is due to the fact that while the principal components are mathematically orthogonal, the underlying physical processes may not be orthogonal. The rotation does not affect the total variance explained by the eigenvalues. A brief account of the rotation is given in the next section.

## 2.6.2 ROTATION OF PRINCIPAL COMPONENTS (FACTORS)

The two methods commonly used in the rotation of factors are the varimax (orthogonal) (Kaiser, 1959) and oblique rotations. Under the varimax method, all the factors are rotated through ninety degrees ($90^o$) while retaining the orthogonality of the factors.

The oblique rotations include oblimax, oblimin and promax. Under these methods the orthogonality principle discussed under the varimax approach is relaxed and some correlation is allowed between the factors. Although this method is a more powerful approach (Richman, 1981) its application is handicapped by the difficulty in the estimation of the degree of associations between the clustered variables. The varimax solution, which has been widely used by many authors, has been adopted in this study. The study of the rainfall and OLR relationships was based on both unrotated and rotated PCA solutions.

## 2.6.3. PHYSICAL REALITY OF THE PRINCIPAL COMPONENTS (PC'S)

It is always necessary to determine whether the correlation patterns derived from Principal component analysis (PCA) are physically realistic and climatologically stable. The methods commonly used to determine the robustness and consistency of the principal components (PC's) patterns include the use of interstation correlations, PCA for a subgroup of the data, e.g the only locations/variables which have been clustered together, PCA for subperiod of records and vector plotting the variables into the vector space of the dorminant factor(s).

The methods that subject subgroup data to PCA assume that all stations/variables which were clustered together when all stations are subjected to PCA have similar temporal variations. Hence, only one factor would be significant if the subgroup is subjected to PCA.

Under the subperiods methods, the period of study is subdivided into two or more subperiods which are independently subjected to PCA. The PCA map, patterns obtained from the subperiods should be comparable to the ones obtained from complete period if the PC's are physically realistic and stable.

Under the vector plotting, the regression weights on pairs of factors are used to cluster variables into the vector space of the dominant factors. The clusters depict the map patterns of the PC's with variables clustering near the axis of the respective dominant PC.

Inter-station correlation method compares the map patterns obtained from the correlations between the stations and spartial patterns of the dominant PCA modes. The map patterns should be comparable if the PC's are physically realistic.

Details of these methods can be obtained in many references including (North et al., 1982, Richman, 1986; Rinne and Jarvanoja, 1979; Barnston and Livezy, 1987).

In this study, inter-station correlation was used to determine the stability and consistency of the PCA patterns.

## 2.7 REGRESSION ANALYSIS

For any pair of variables which have significant correlation coefficient (r), the next step is generally to determine the nature of the relationship. This is often done by determining the best regression equation governing the relationship.

A linear relationship model which expresses a Meteorological variable ($Y_t$) as a function of OLR ($X_t$) may be expressed as

$$Y_t = a + bX_t \ldots\ldots\ldots\ldots\ldots\ldots\ldots (15)$$

Where a and b are regression constants. The regression constants (a and b) can be estimated from available records.

In this study an attempt was made to determine the functional relationships between various Meteorological variables and OLR at the various locations. The functional relationships (regression equations) were developed only for locations where the correlations coefficients (r) were statistically significant. The statistical significance of the regression constants, together with the variance of rainfall which can be accounted for by OLR were estimated from the Analysis of variance (ANOVA) principals. Details of ANOVA together with other regression principles can be obtained from Wannacott and Wannacott (1985), Battacharyya and Johnson (1977) and Fisher (1958) among other references.

## 3.0 RESULTS AND DISCUSSIONS

In this Chapter, the results obtained from various methods of analysis are discussed. The methods include estimation of missing records, areal rainfall estimation,

quality control tests, correlation, principal component and regression analyses. Also discussed are the spatial patterns of the longterm means of outgoing longwave radiation (OLR). The results from each method are discussed independently in the following sections.

## 3.1 RESULTS OF QUALITY CONTROL TESTS

Figures 3b and 3c give the general patterns of mass curves which were obtained when point and areal records were subjected to mass curve analysis. The results from the mass curves declared all stations and areal records homogeneous.

The fact that all point and areal records were declared homogeneous indicates that the estimated point and areal records were realistic. The homogeneous records formed the base for all further analyses. The results obtained from these analyses are discussed in the following sections.

## 3.2 THE SPATIAL PATTERNS OF MEAN OLR VALUES OVER EAST AFRICA

In this section the spatial patterns of mean OLR values are discussed season by season for the four standard seasons, March-May, June-August, September-November, and December-February.

Figure 4a gives an example of the spatial patterns of the mean OLR values during the March-May (long rainy) season as represented by the peak rainfall month of April. During this season most areas of East Africa receive at least 50mm of rainfall (figure, 4b). The region benefits from the presence of the Intertropical convergence zone (ITCZ) which is located near the equator during this season. From figure

4a it can be seen that the whole region has low OLR values as expected. The lowest values of OLR are observed over parts of the region which are frequented with thunderstorms (WMO, 1953) and receive the highest rainfall amounts during this season. Such areas include Uganda, Western parts of Kenya, and Western and South eastern parts of Tanzania. The arid and semi-arid part of Kenya, which have the lowest thunderstorms cases and receive the lowest rainfall amounts (<200mm) during this season, have relatively higher OLR values.

Figure 5a gives an example of the spatial patterns of mean OLR values during the September-November season which was represented by her peak rainfall month of November. This is another season when most parts of East Africa near the equator receive rainfall (figure , 5b). The region benefits from the presence of ITCZ which passes over it in this season as it retreats to the southern hemisphere. The season is commonly referred to as short-rainy season due to short duration and low magnitudes of rainfall at most locations during this season. Figure 5a shows that OLR values at most locations during this season were relatively higher than those observed during long-rainy season. However, the lowest OLR values were still observed over Western parts of the region which receive the highest rainfall amounts during this season.

Figure 6a gives an example of the spatial patterns of the mean OLR values during the June-August season. The season was represented by her peak rainfall month of July. During this season, all parts of the region, except for

Western Kenya and most parts of Uganda, are generally dry (figure, 6b). The parts of the region near large water bodies also receive rainfall during this season. It is the wettest season at some locations to the north eastern parts of Uganda. Figure 6a indicates that the lowest OLR values were observed over Uganda and Western parts of Kenya which receive the highest rainfall amounts during this season. These wet areas benefit from the lake Victoria circulation and the moist westerly airmass from the Atlantic and Congo/Zaire basins which is locally known as the Congo airmass (EAMD, 1962, Trewartha, 1961).

The Coastal areas are amongst the regions which receive rainfall during this season. The OLR values are, however, relatively high over these areas. The major features in coastal areas during this season are the East African low level jetstream (Findlator, 1968) and land/sea breeze. The sea breeze is very shallow (Asnani and Kinuthia, 1979). Another dominant feature over the region during this season is the Eastern Africa ridge which imposes low level divergence and subsidence over most parts of the region. Such conditions are not favourable for the development of deep convective clouds associated with low OLR values.

Figure 7a gives an example of the spatial patterns of the mean OLR values during December-February season which was represented by her pick rainfall month of January. During this season, the ITCZ is located in the Southern hemisphere. It reaches its furthest southern position over Africa during February. Only southern Tanzania and parts of the region near large water bodies receive substantial rainfall during

Figure 3b: Mass curve of point rainfall for Port Victoria.

Cumulative rainfall (mm) for region 3.
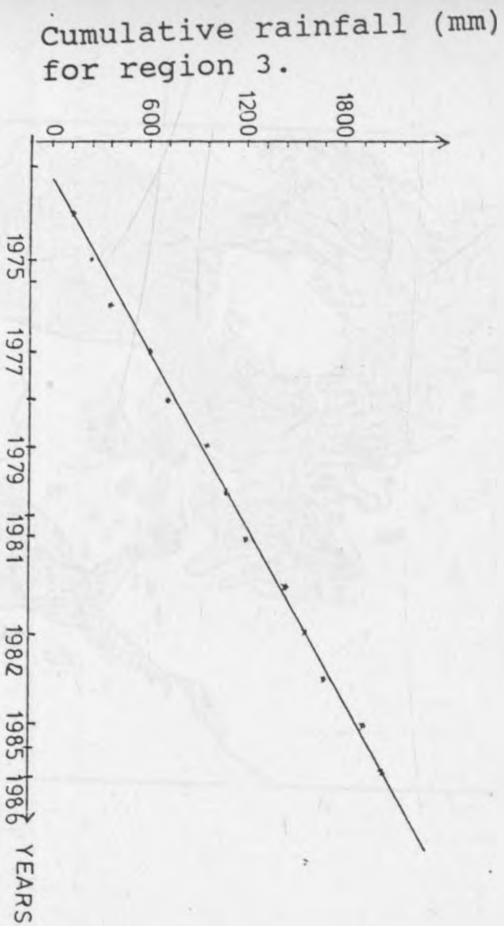
Figure 3c: Mass curve of areal rainfall for region three.

Cumulative rainfall (mm) for Port Vitoria.
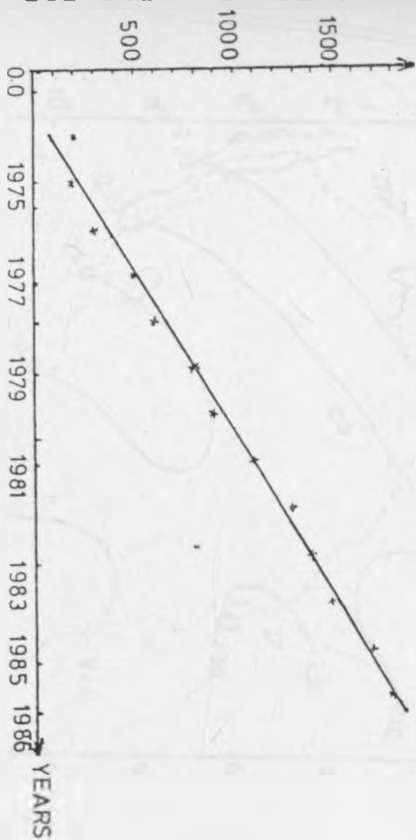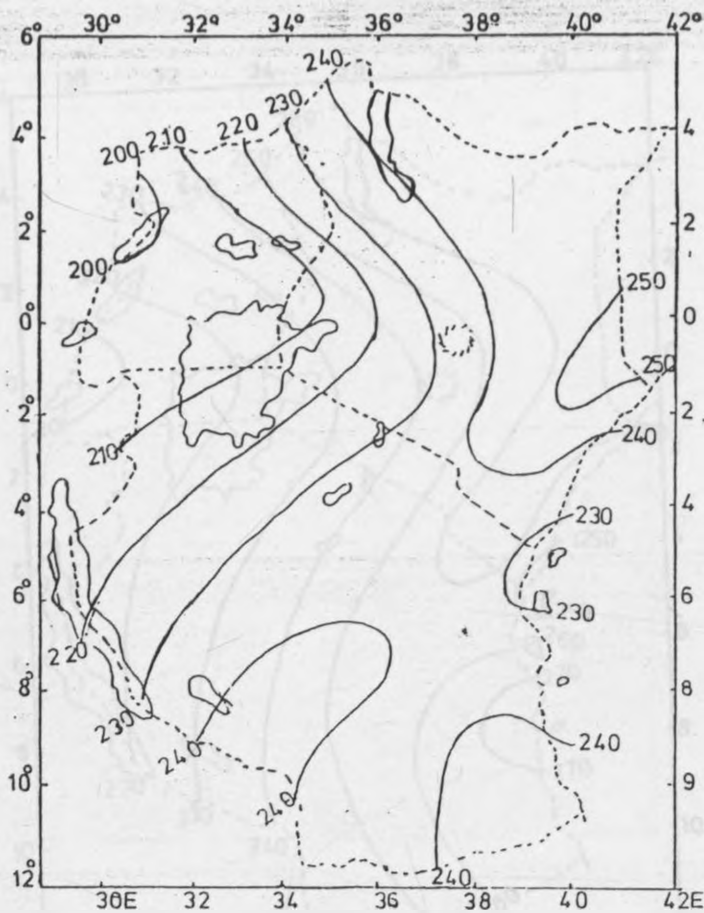
Figure 4a: The spatial patterns of mean OLR values ($Wm^{-2}$) during April.
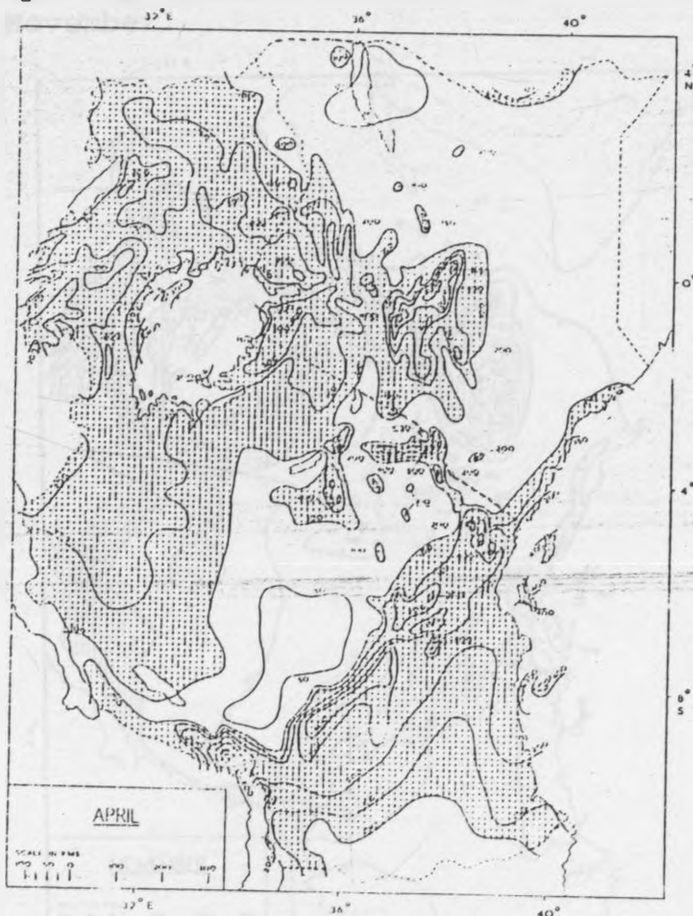


Figure 4b: The spatial patterns of mean rainfall values (mm) during April (adopted from Tomsett, 1969). Shaded area receives over 100mm.
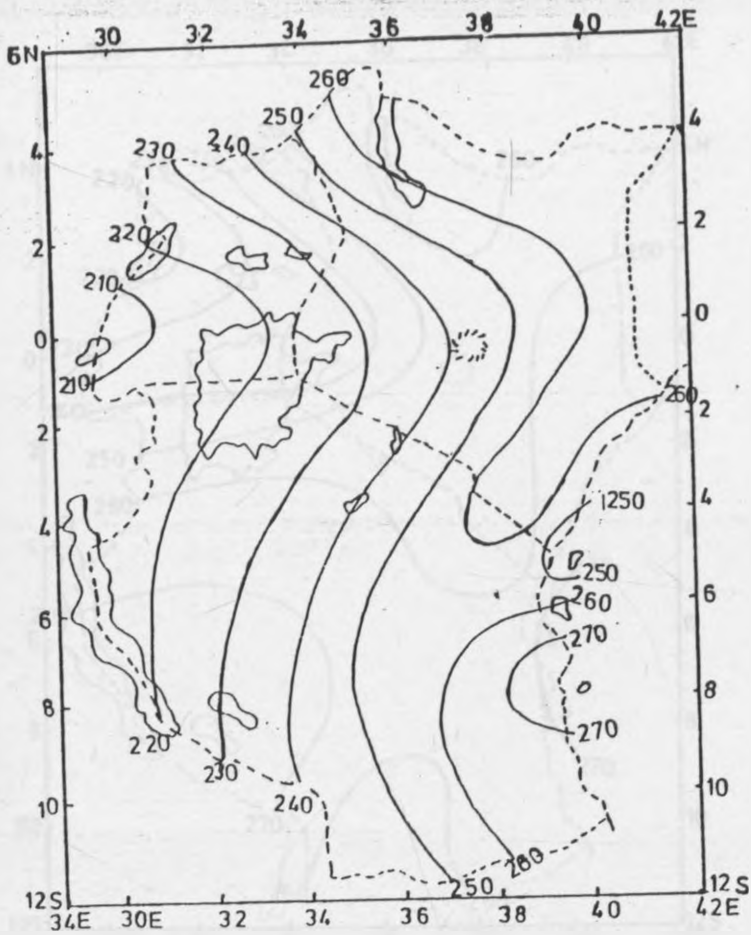
Figure 5a: The spatial patterns of mean OLR values (Wm$^{-2}$) during November.
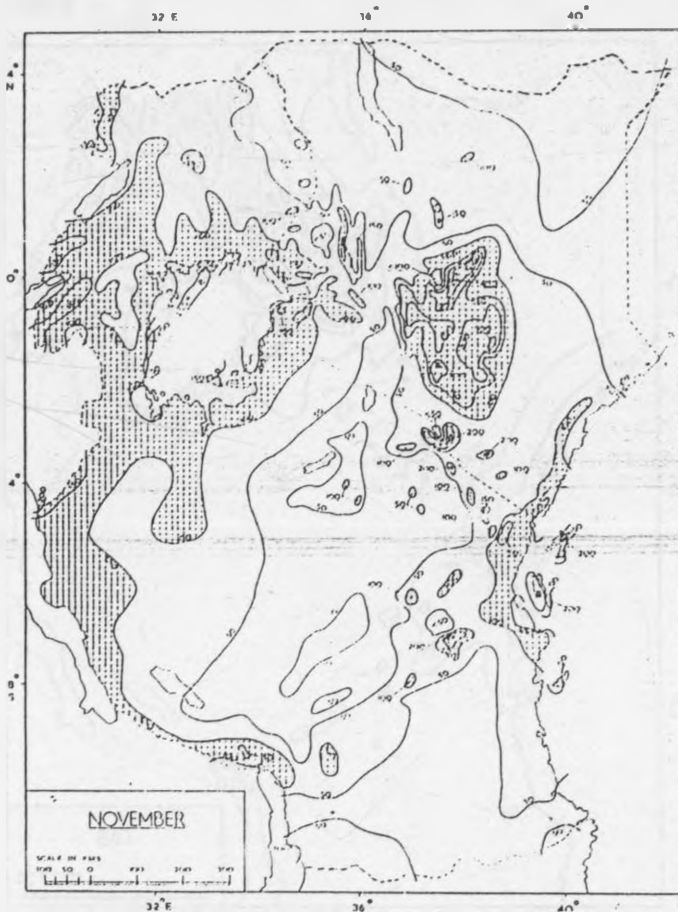


Figure 5b: The spatial patterns of mean rainfall values (mm) during November (Adopted from Tomsett, 1969). Shaded area receives over 100mm.
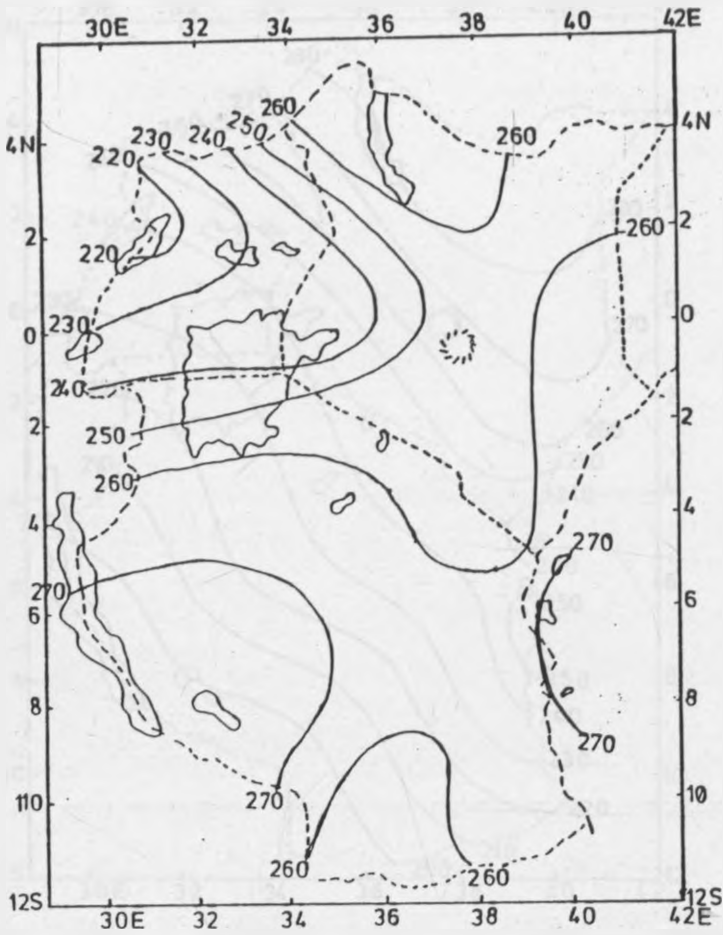
Figure 6a: The spatial patterns of mean OLR values($Wm^{-2}$) during July.



Figure 6b: The spatial patterns of mean rainfall values (mm) during July (Adopted from Tomsett, 1969). Shaded area receives over 100mm.
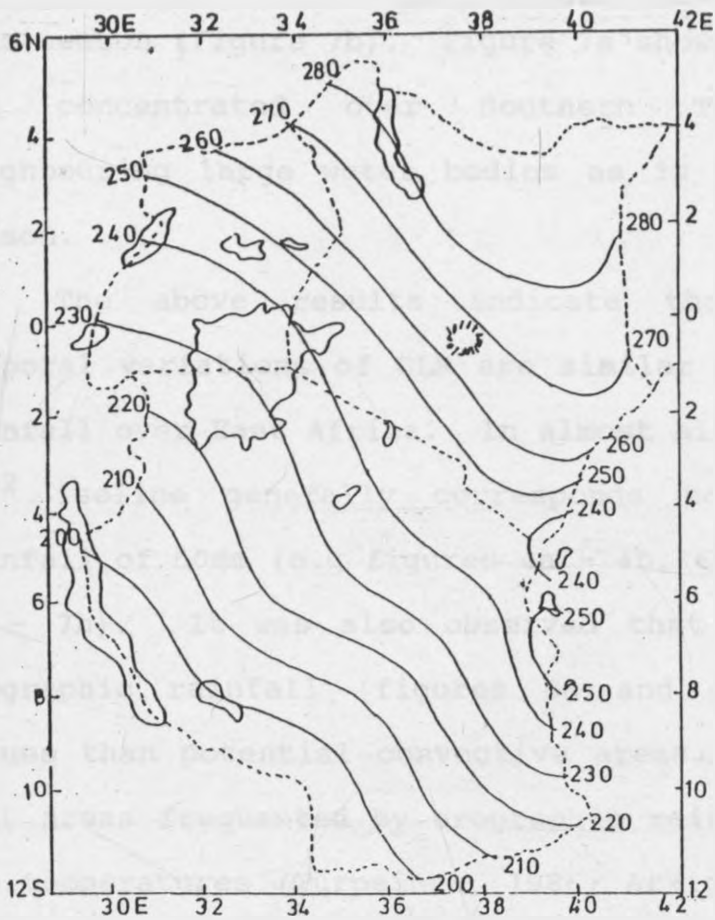
Figure 7a: The spatial patterns of mean OLR values ($Wm^{-2}$) during January.

Figure 7b: The spatial patterns of mean rainfall values (mm) during January (Adopted from Tomsett, 1969). Shaded area receives over 100mm.

this season (Figure 7b). Figure 7a shows that low OLR values are concentrated over Southern Tanzania and areas neighbouring large water bodies as is expected during this season.

The above results indicate that the spatial and temporal variations of OLR are similar to those observed in rainfall over East Africa. In almost all the seasons the 240 $Wm^{-2}$ isoline generally corresponds to the monthly total rainfall of 50mm (e.g figures 4a - 4b, 6a - 6b, together with 7a - 7b). It was also observed that areas frequented by orographic rainfall (figures 5a and 6a) have higher OLR values than potential convective areas. It has been noted that areas frequented by orographic rainfall have high cloud top temperatures (Turpeinen, 1986; Arkin et al., 1988). The eastern parts of Kenya including the coastal areas receive most of their rainfall from layer clouds and have very few thunderstorm cases (WMO, 1953).

Since the spatial patterns of OLR and rainfall were found to be close, an attempt was made to determine the dominant spatial OLR and rainfall modes from the method of principal component analysis (PCA). The results of this analysis are discussed in the next section.

## 3.3. RESULTS FROM PRINCIPAL COMPONENT ANALYSIS (PCA)

In this section the results obtained when OLR and rainfall records were subjected to Principal Component analysis are independently presented under two separate subsections.

## 3.3.1 RESULTS FROM PCA OF OLR

Tables 2 and 3 give the eigenvalues and variances explained by each principal component (factor) for the intermonthly and seasonal OLR records, respectively. It can be seen from table 2 that only the first three factors derived from intermonthly OLR records satisfy Kaiser's criterion (Kaiser, 1960) of significant eigenvectors. The three factors explained about 89% of the OLR variance.

Table 3 shows that for the seasonal records three, four, six and four factors were significant during March-May, September - November, June-August and December-February, respectively. The significant factors accounted for over 86% of OLR variance during all seasons. The significant factors obtained with each OLR record were subjected to Varimax (orthogonal) rotation.

The spatial patterns of the loadings of the three significant rotated factors for the intermonthly records are given in figure 8. Figure 8a gives the spatial patterns of the first rotated principal component (RPC). The figure shows that this RPC was dominant over most of Tanzania. Maximum loadings were concentrated over southern parts of Tanzania which receive maximum rainfall during December - February season (figure 7b).

Figure 8b shows that the second RPC mode was dominant over the coastal areas and to the east of central Highlands. The maximum loadings were concentrated along the coast which benefits from the land/sea breeze associated with the Indian ocean circulation. The third RPC mode was dominant over north western parts of the region (figure 8c). The maximum

loadings were observed over Uganda and Western parts of Kenya which receive substantial rainfall during June-August season (figure 6b) due to the influence of lake Victoria circulation and the moist westerly airmass from the Atlantic and Congo/Zaire basin which is locally known as the Congo airmass (Trewartha, 1961; Tomsett, 1969; Henderson, 1949; Thompson, 1957; EAMD. 1962).

Figure 9 gives the spatial patterns of the dominant RPC modes for March - May seasonal OLR records. It is evident from these figures that the three spatial modes which were dominant in the intermonthly OLR records were still discernible in March-May seasonal records. March-May is generally the major rainfall season for most parts of the region. The rainfall received during this season accounts for the largest proportion of the annual rainfall total at most locations (Tomsett, 1969).

The spatial patterns of the dominant RPC modes which were observed with September-November seasonal records are shown in figure 10. Figure 10a shows that the first RPC mode was dominant over all parts of the region. Maximum values were, however, concentrated to the east of central Highlands. Table 3 indicates that this mode extracted the highest seasonal OLR variance. About 64% of the seasonal OLR variance could be accounted for by the first RPC mode alone during this season. The high degree of the spatial homogeneity in the weather characteristics during the short-rainy season has been discussed by many authors including Ogallo (1989) and Nyenzi (1990). Figures 10b and 10c indicate that the RPC modes which were dominant over the

coast and North western parts of the region with the intermonthly and the march-May seasonal records were still discernible in the September-November OLR records. The fourth RPC, which was unique for the September-November season had maximum loadings over south eastern parts of Tanzania (figure 10d).

Figure 11 gives the spatial patterns of the six significant RPC modes which were obtained with the June-August seasonal records. It is evident from table 3 that the first RPC mode accounted for the least seasonal OLR variance when all the four standard seasons are compared. The season is generally dry apart from the Western parts, which are under the influence of the Congo airmass, and areas near large water bodies. The figure indicates that the dominant RPC modes which were observed with the intermonthly, March-May and September-November records were still appearing in June-August seasonal records. The RPC modes which were unique for the June-August season had maximum loadings over the south eastern, central and western parts of Tanzania (figures 11b, 11e and 11f). Some of these regions are located close to the large south western lakes of Tanzania.

The spatial patterns of the dominant RPC modes which were obtained with December-February seasonal OLR records are given in figure 12. Figure 12a indicates that the first RPC mode was dominant over the southern parts of Tanzania which receive maximum rainfall during this season. The rest of the region is relatively dry during this season apart from areas near large water bodies. The other two RPC modes had spatial patterns similar to those dominant with the intermonthly

records and during the previous seasons (figures 12b and 12d). The fourth RPC mode, which was unique for this season, had maximum loadings over north eastern Kenya, which is generally dry during this season.

It may be concluded from the above analysis that three RPC modes were dominant in the OLR records throughout the year. The dominant modes had maximum loadings centred over the east of the central Highlands including coastal areas, southern Tanzania and north western parts of the region. The results also indicated that some of the RPC modes were uniquely associated with certain seasons and regions. The largest number of unique RPC modes was observed during the June-August season. The largest degree of spatial homogeneity in the rainfall characteristics was however observed during September-November season.

**Table 2: PCA Results of the Intermonthly OLR Records**

| Factor | Eigen-value | Proportion of Variance Explained ( %) | |
|--------|-------------|----------------|------------|
| | | By the Factor | Cumulative |
| 1 | 13.9818 | 48.2 | 48.2 |
| 2 | 9.0465 | 31.2 | 79.4 |
| 3 | 2.6506 | 9.0 | 88.6 |
| 4 | 0.7882 | 2.7 | 91.3 |

**Table 3: PCA Results of the Seasonal OLR Records**

| Season | Factor | Eigen-value | Propotion of Variance Explained (%) | |
|--------|--------|-------------|-----------|------------|
| | | | By factor | Cumulative |
| March-May | 1 | 14.7479 | 52.7 | 52.7 |
| | 2 | 8.5819 | 30.6 | 83.3 |
| | 3 | 1.3144 | 4.7 | 88.0 |
| | 4 | 0.6692 | 2.4 | 90.4 |
| SEPT.-NOV. | 1 | 17.8586 | 63.8 | 63.8 |
| | 2 | 2.9297 | 10.4 | 74.2 |
| | 3 | 2.1335 | 7.7 | 81.9 |
| | 4 | 1.4587 | 5.2 | 87.1 |
| | 5 | 0.7683 | 2.7 | 89.8 |

| | | | | |
|---|---|---|---|---|
| JUNE–AUGUST | 1 | 11.3983 | 40.7 | 40.7 |
| | 2 | 5.5964 | 20.0 | 60.7 |
| | 3 | 3.4376 | 12.3 | 73.0 |
| | 4 | 1.7164 | 6.1 | 79.1 |
| | 5 | 1.2871 | 4.6 | 83.7 |
| | 6 | 1.0096 | 3.6 | 87.3 |
| | 7 | 0.7513 | 2.7 | 90.0 |
| DEC.–FEB. | 1 | 13.5845 | 48.5 | 48.5 |
| | 2 | 6.0130 | 21.5 | 70.0 |
| | 3 | 3.6328 | 13.0 | 83.0 |
| | 4 | 1.0568 | 3.7 | 86.7 |
| | 5 | 0.8298 | 3.0 | 89.7 |
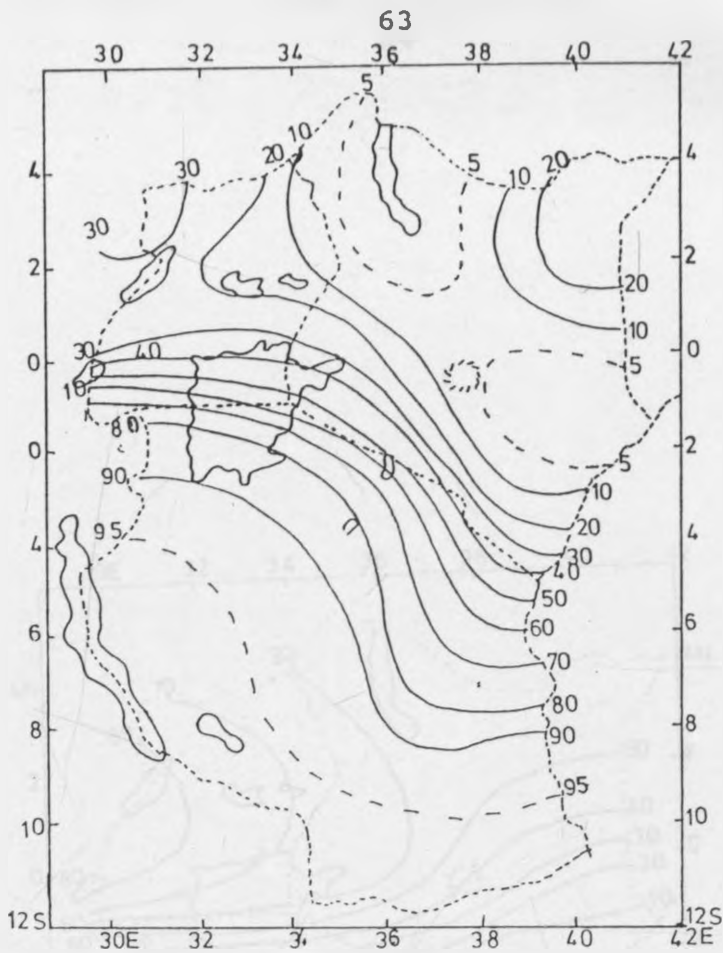
Figure 8a: The spatial patterns of the loadings (X 100) of the first intermonthly OLR RPC.
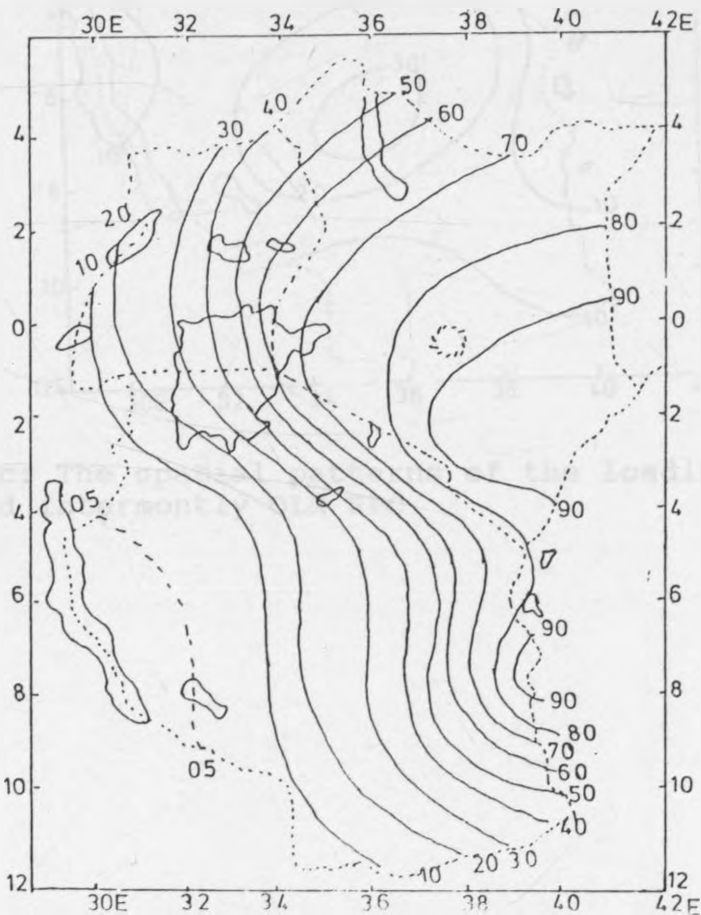


Figure 8b: The spatial patterns of the loadings (X 100) of the Second intermontly OLR RPC.
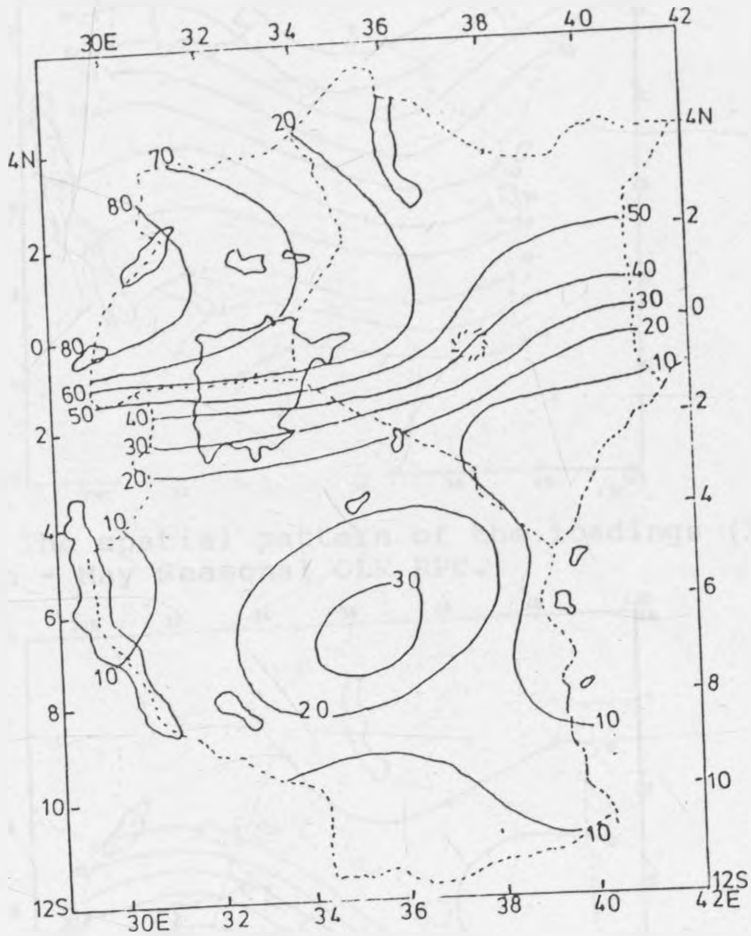
Figure 8c: The spatial patterns of the loadings (X 100) of
the third intermontly OLR RPC
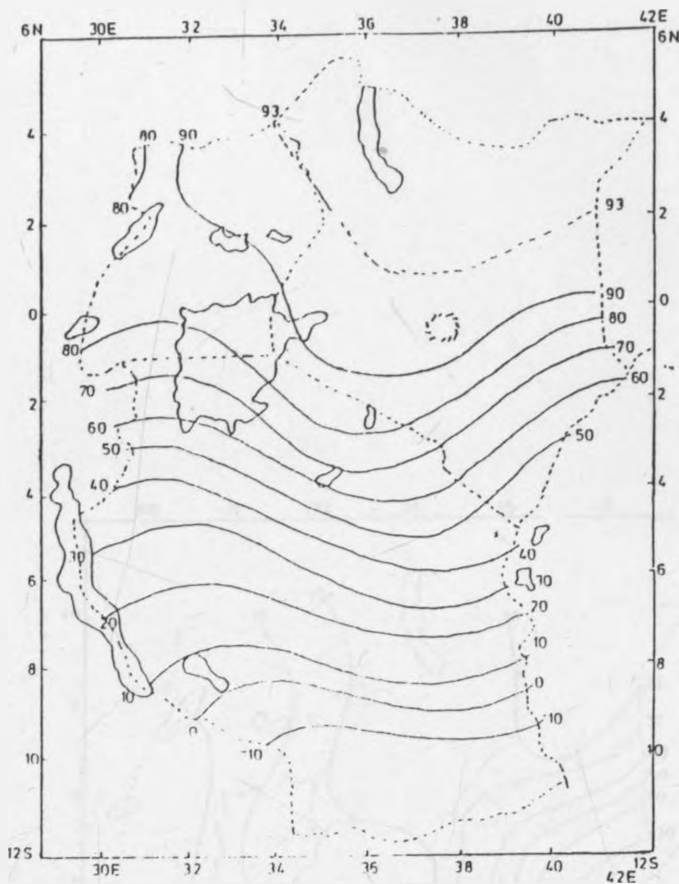
Figure 9a: The spatial pattern of the loadings (X 100) of the
first March - May Seasonal OLR RPC.
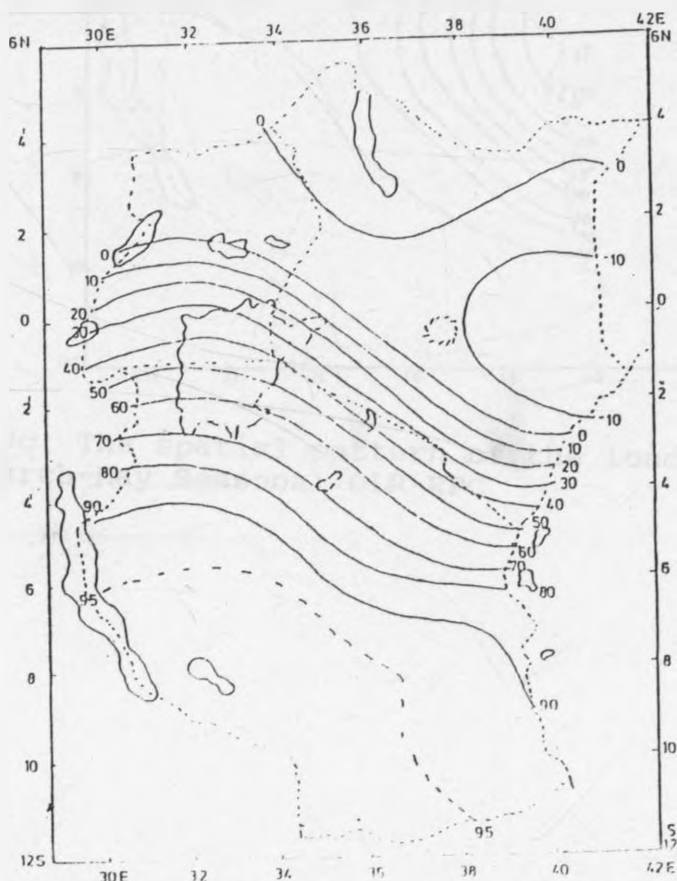


Figure 9b: The spatial pattern of the loadings (X 100) of the
second March-May Seasonal OLR RPC.
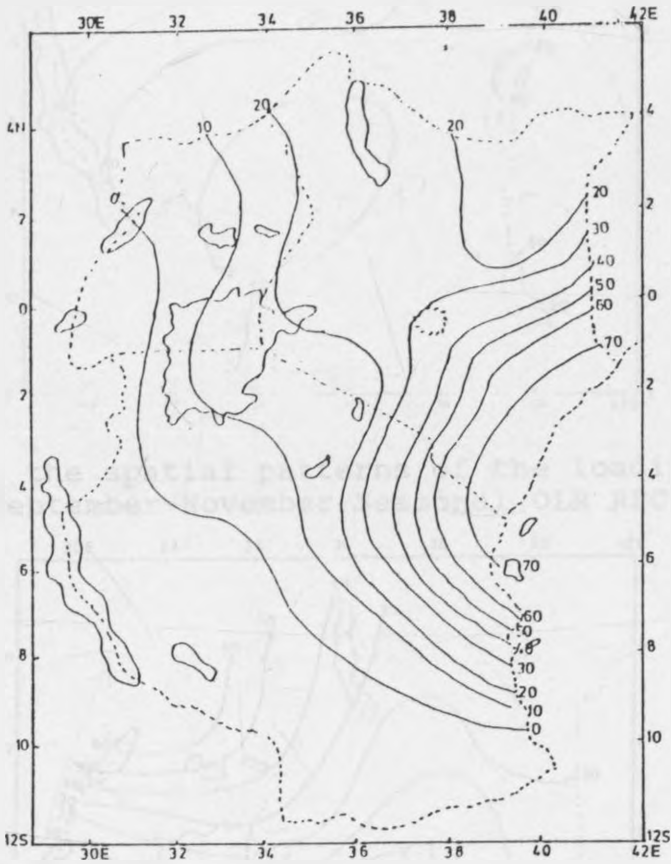
Figure 9c: The spatial pattern of the loadings (X 100) of the third March-May Seasonal OLR RPC
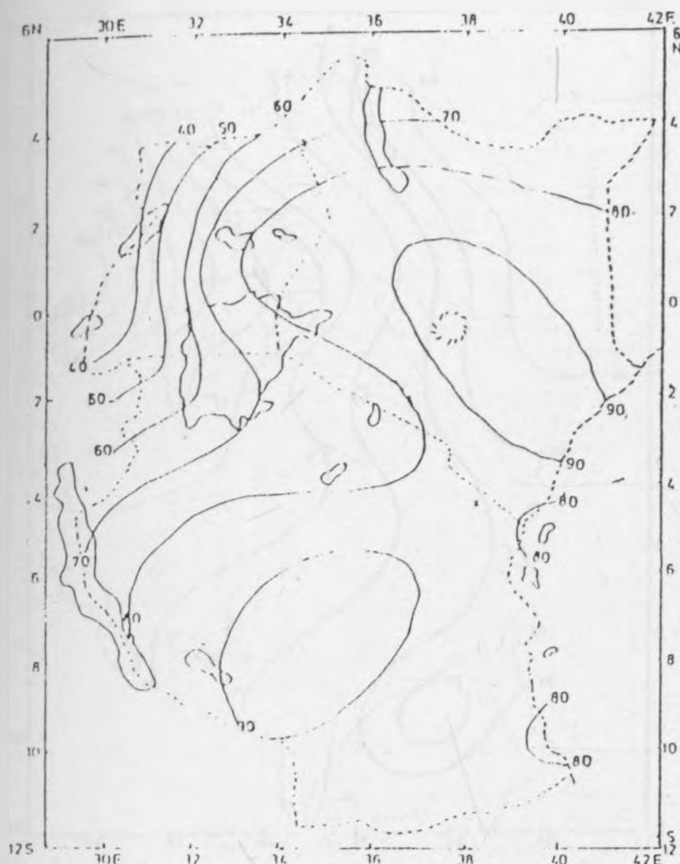
Figure 10a: the spatial patterns of the loadings (X 100) of the first September-November Seasonal OLR RPC.
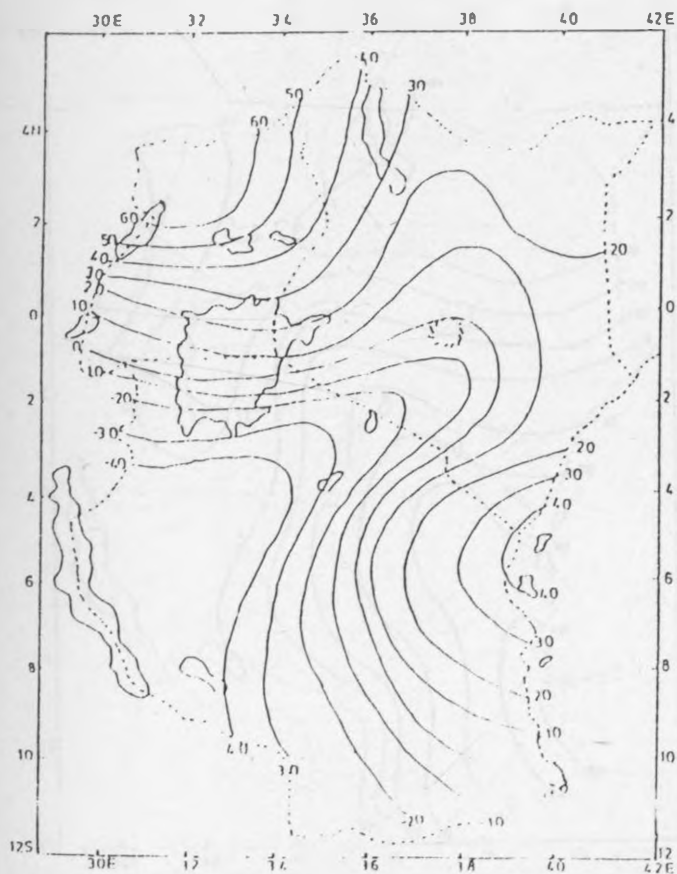


Figure 10b: The spatial patterns of the loadings (X 100) of the second September-November Seasonal OLR RPC.
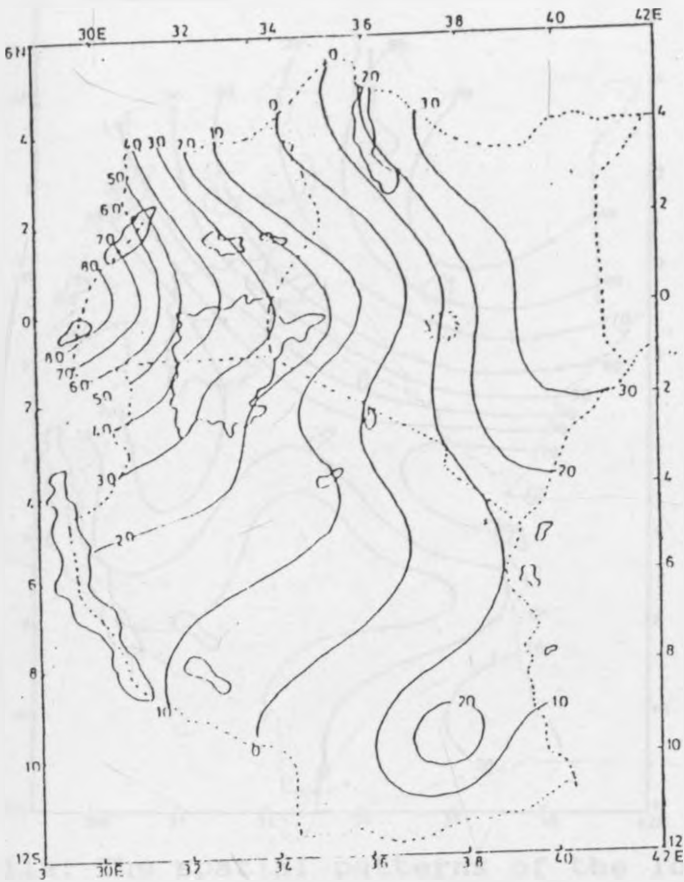
Figure 10c: The spatial patterns of the loadings (X 100) of the third September-November Seasonal OLR RPC.
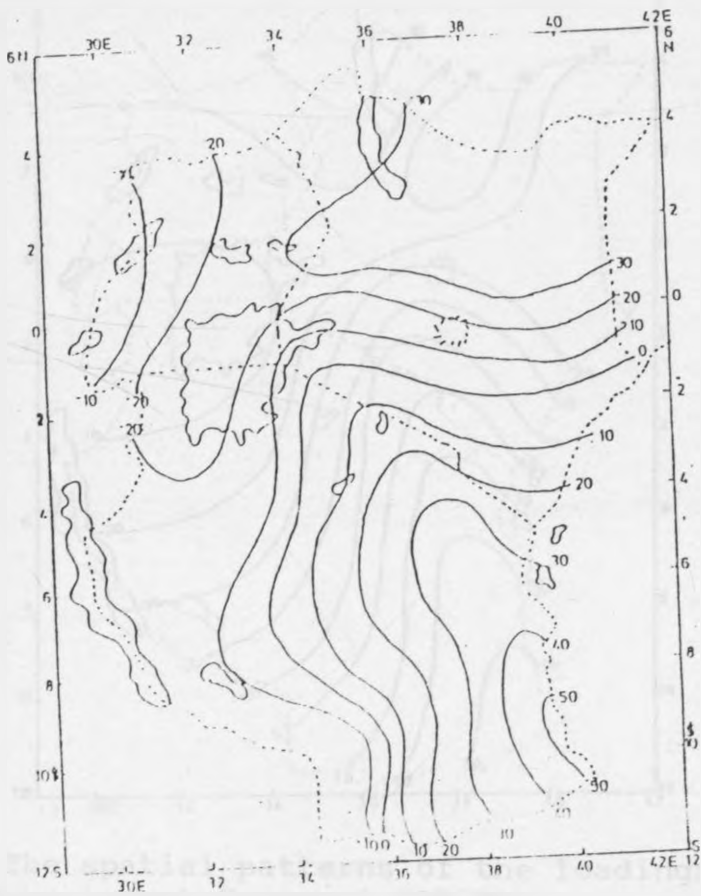


Figure 10d: the spatial patterns of the loadings (X 100) of the fourth September-November Seasonal OLR RPC.
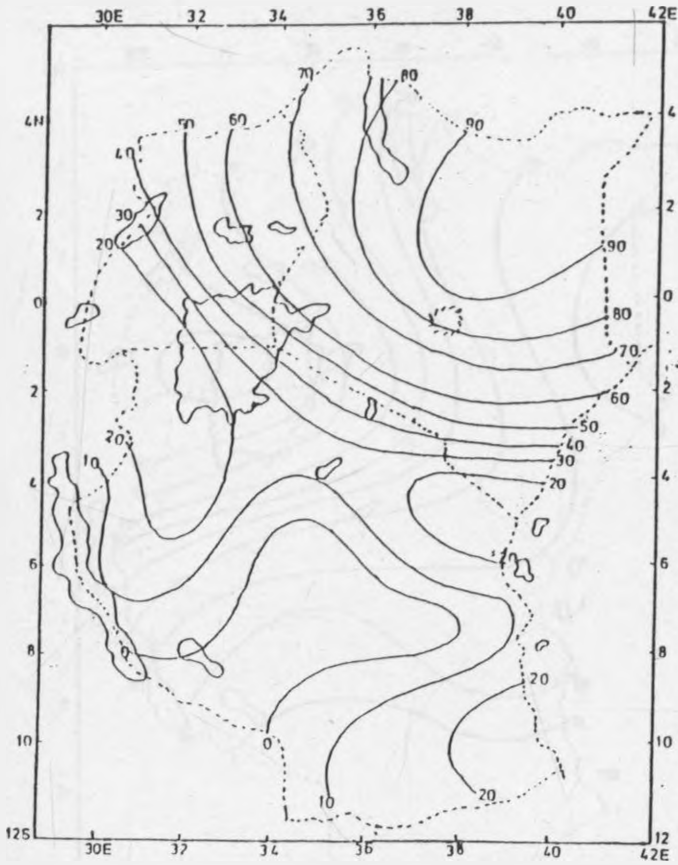
Figure 11a: The spatial patterns of the loadings (X100) of the first June-August Seasonal OLR RPC.
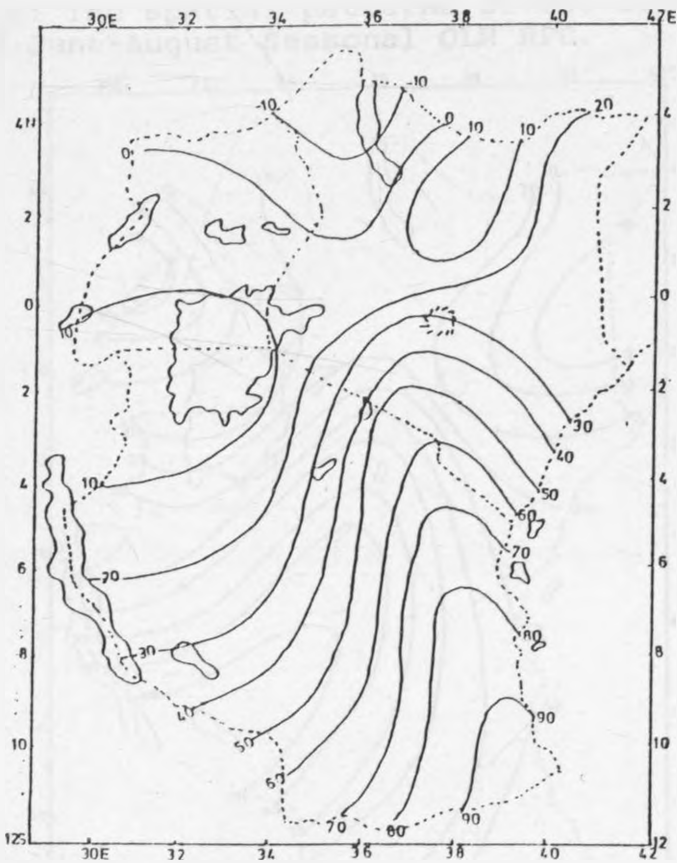


Figure 11b: The spatial patterns of the loadings (X100) of the second June-August Seasonal OLR RPC.
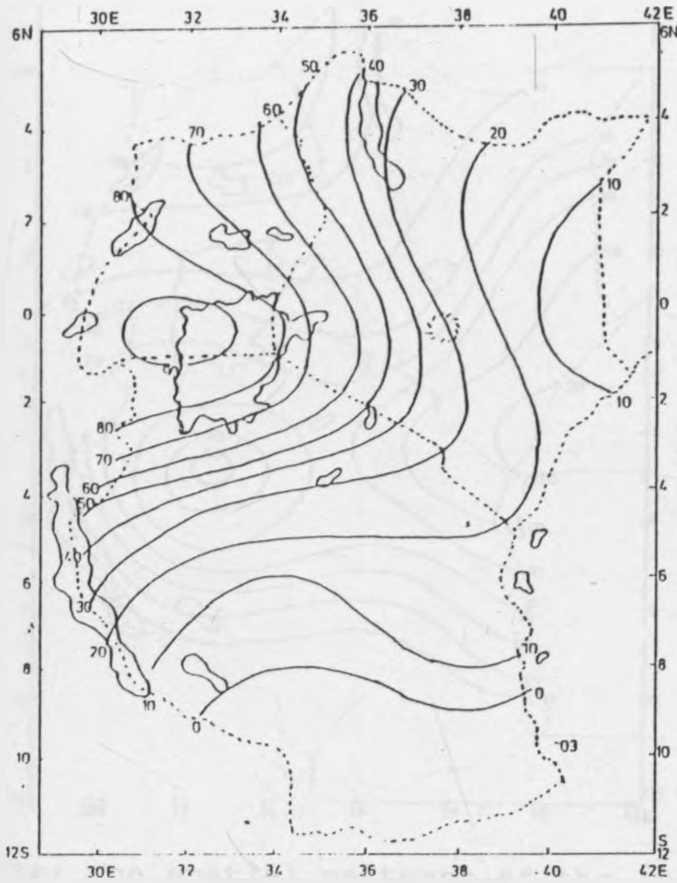
Figure 11c: The spatial patterns of the loadings (X100) of the third June-August Seasonal OLR RPC.
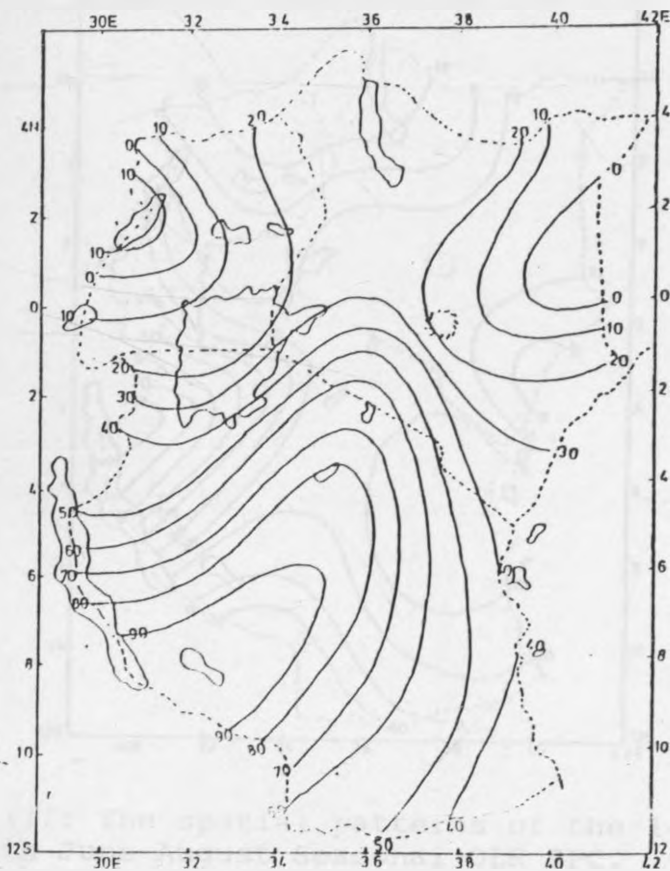


Figure 11d: The spatial patterns of the loadings (X100) of the fourth June- August Seasonal OLR RPC.
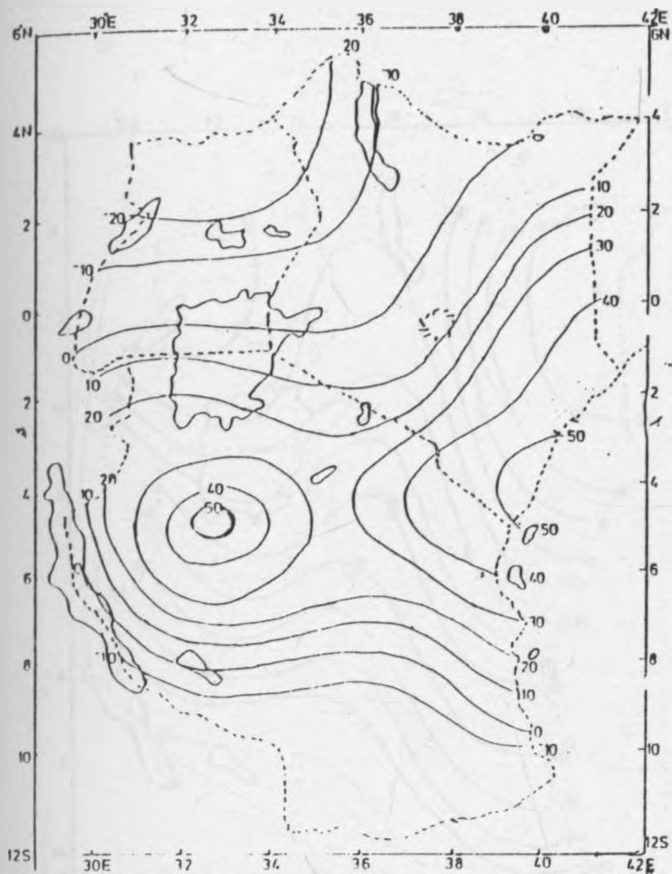
Figure 11e: The spatial patterns of the loadings (X100) of
the fifth June-August Seasonal OLR RPC.
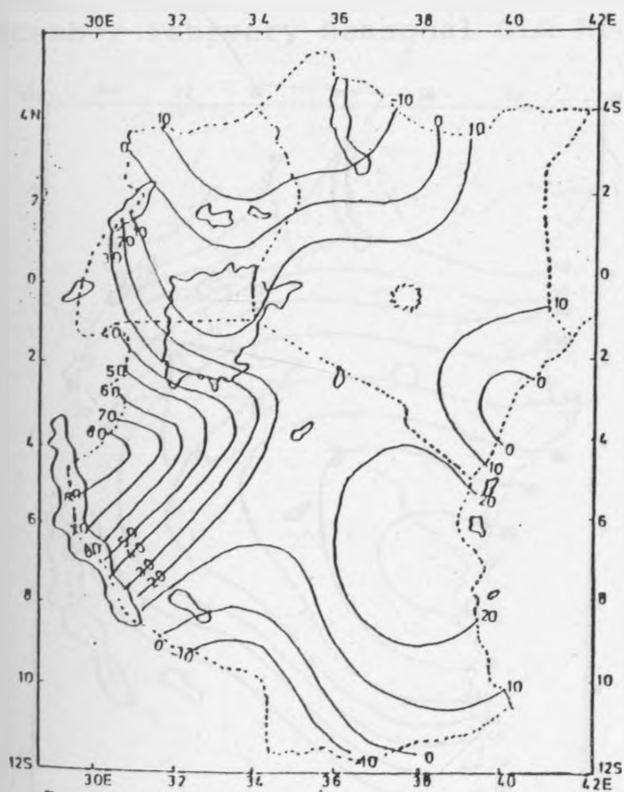


Figure 11f: The spatial patterns of the loadings (X100) of
the sixth June-August Seasonal OLR RPC.
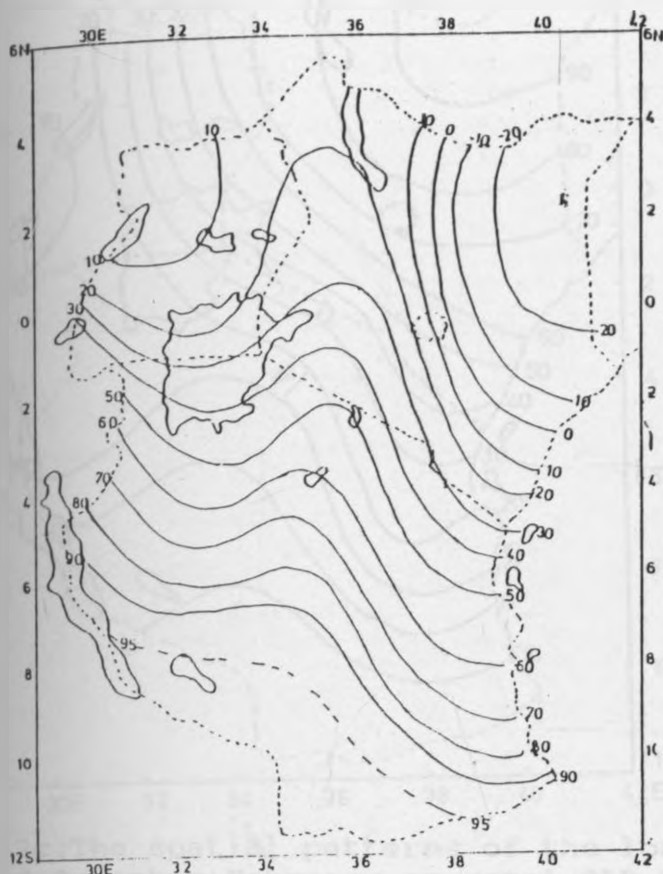
Figure 12a: The spatial patterns of the loadings (X 100) of the first December-February Seasonal OLR RPC.
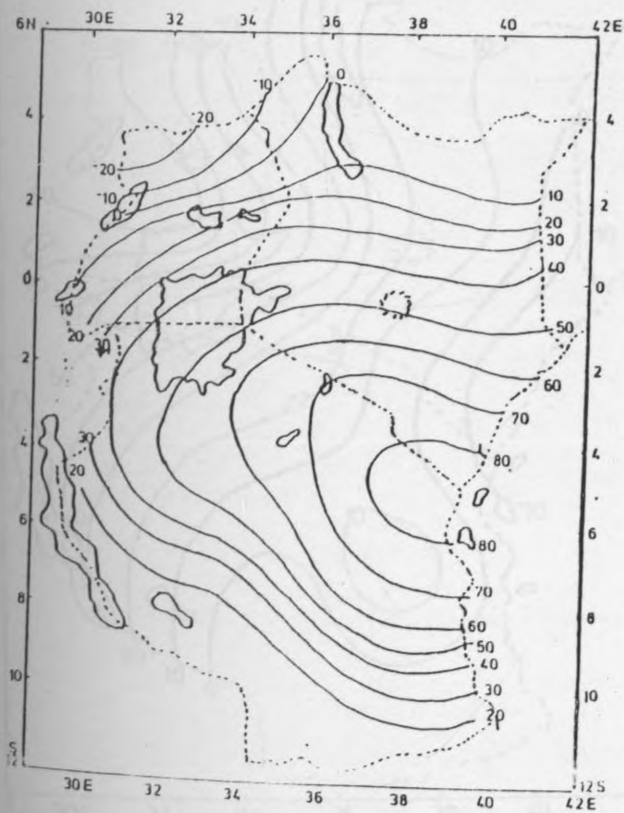


Figure 12b: The spatial patterns of the loadings (X 100) of the Second December-February Seasonal OLR RPC.
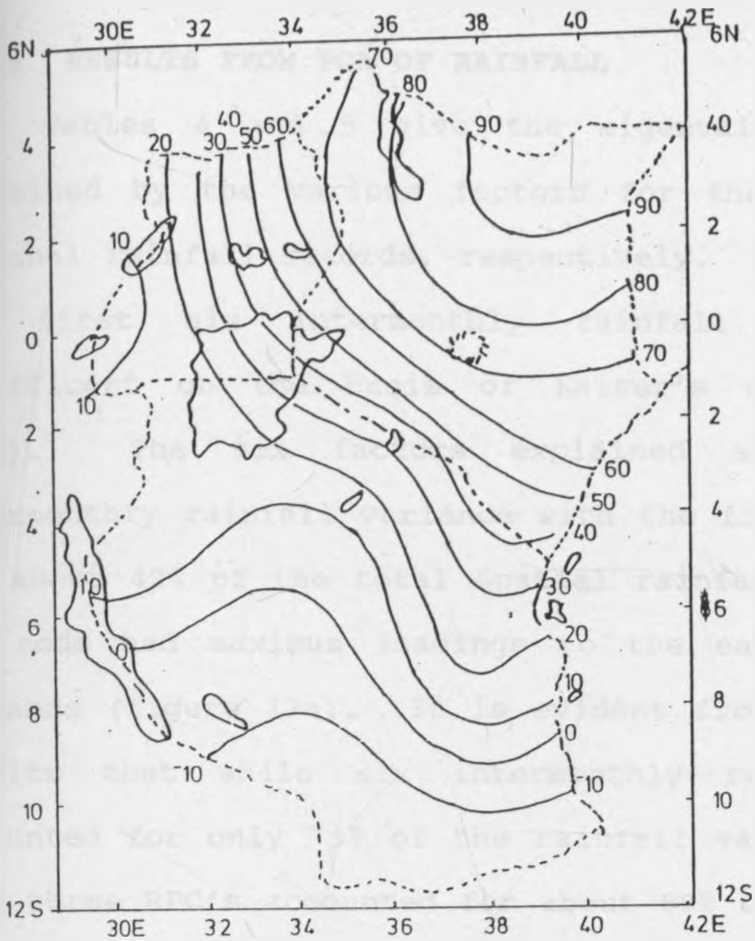
Figure 12c:The spatial patterns of the loadings (X 100) of the third December-February seasonal OLR RPC.
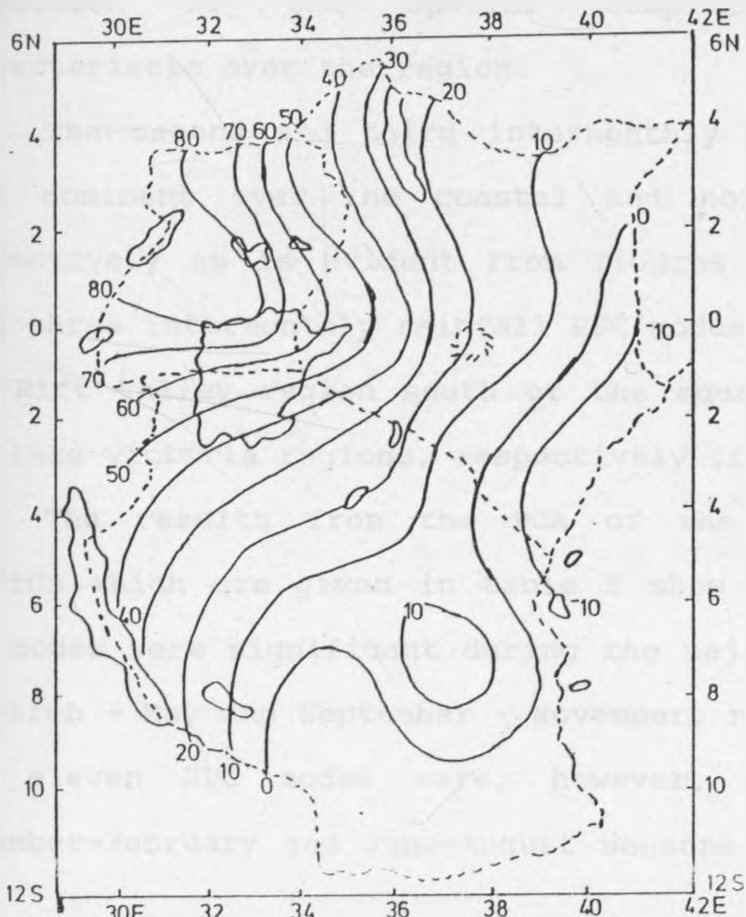


Figure 12d:The spatial patterns of the loadings (X 100) of the fourth December-February Seasonal OLR RPC.

### 3.3.2 RESULTS FROM PCA OF RAINFALL

Tables 4 and 5 give the eigenvalues and variances explained by the various factors for the intermonthly and seasonal rainfall records, respectively. Table 4 shows that the first six intermonthly rainfall RPC modes were significant on the basis of Kaiser's criterion (Kaiser, 1960). The six factors explained about 75% of the intermonthly rainfall variance with the first one accounting for about 42% of the total spatial rainfall variance. This RPC mode had maximum loadings to the east of the central higlands (figure 13a). It is evident from rainfall and OLR results that while six intermonthly rainfall RPC modes accounted for only 75% of the rainfall variance over Kenya, only three RPC's accounted for about 89% of intermonthly OLR variance over the whole of East Africa. This could be a reflection of the spatial complexity of rainfall characteristic over the region.

The second and third intermonthly rainfall RPC modes were dominant over the coastal and north western areas, respectively as is evident from figures 13b and 13c. The last three intermonthly rainfall RPC modes were dominant over the Rift Valley region south of the equator, north eastern and lake victoria regions, respectively (figures 13d-13f).

The results from the PCA of the seasonal rainfall records which are given in table 5 show that seven and six RPC modes were significant during the major rainfall seasons of March - May and September - November, respectively. Eight and eleven RPC modes were, however, significant during December-February and June-August seasons respectively. The

proportions of seasonal rainfall variance explained by the significant factors were about 80, 84, 83 and 84% for the March-May, September-November, June-August and December-February seasons, respectively with the first modes for the respective seasons accounting for about 36, 49, 23 and 43% of the rainfall variance. The spatial patterns of these RPC modes are given in figures 14-17.

It is evident from these figures that the RPC modes which were dominant in the intermonthly rainfall records were still revealed in the RPC patterns of the individual seasons. The March-May, June-August and December-February seasons, however, had some RPC modes which were unique for the respective seasons (figures 14g , 16b, 16i, 16g, 16h, 16k, 17e and 17h). Similar results have been obtained by Ogallo (1989), Nyenzi (1990) and Barring (1987).

It may be concluded from the results from the Principal Component Analysis of OLR and rainfall that the spatial characteristics of OLR are less complex compared to those of rainfall. Six intermonthly rainfall RPC modes, for example, accounted for about 75% of rainfall over Kenya while only three intermonthly OLR RPC modes could extract about 89% of the intermonthly OLR variance over the whole of East Africa. The dominant seasonal weather characteristics were however, discernible from the PCA results of both OLR and rainfall. The OLR, like rainfall, had the maximum spatial relationships during the September-November season. The stability of the observed OLR and rainfall RPC modes are discussed in the next section.

## Table 4:   PCA Results of the Intermonthly Rainfall Records

| Factor | Eigenvalue | Proportion of Variance Explained (%) | |
|--------|-----------|-----------|------------|
| | | By Factor | Cumulative |
| 1 | 15.6742 | 42.4 | 42.2 |
| 2 | 5.1362 | 13.8 | 56.2 |
| 3 | 3.0292 | 8.2 | 64.4 |
| 4 | 1.5988 | 4.4 | 68.8 |
| 5 | 1.3117 | 3.5 | 72.3 |
| 6 | 1.0741 | 2.9 | 75.2 |
| 7 | 0.9275 | 2.5 | 77.7 |

## Table 5: PCA RESULTS OF SEASONAL RAINFALL

| SEASON | FACTOR | EIGENVALUE | Proportion of Variance explained (%) | |
|--------|--------|-----------|-----------|------------|
| | | | By factor | Cumulative |
| Mar-May | 1 | 12.8264 | 35.6 | 35.6 |
| | 2 | 7.1692 | 19.9 | 55.5 |
| | 3 | 2.6624 | 7.4 | 62.9 |
| | 4 | 2.4026 | 6.7 | 69.6 |
| | 5 | 1.3765 | 3.8 | 73.4 |
| | 6 | 1.3056 | 3.7 | 77.1 |
| | 7 | 1.1297 | 3.1 | 80.2 |
| | 8 | 0.8999 | 2.5 | 82.7 |
| Sept-Nov | 1 | 17.7256 | 49.2 | 49.2 |
| | 2 | 4.3881 | 12.2 | 61.4 |
| | 3 | 3.8823 | 10.8 | 72.2 |
| | 4 | 1.6739 | 4.7 | 76.9 |
| | 5 | 1.3249 | 3.6 | 80.5 |
| | 6 | 1.2551 | 3.5 | 84.0 |
| | 7 | 0.8416 | 2.4 | 86.4 |

| | | | | |
|---|---|---|---|---|
| June-Aug. | 1 | 8.1537 | 22.7 | 22.7 |
| | 2 | 4.7616 | 13.2 | 35.9 |
| | 3 | 3.4360 | 9.5 | 45.4 |
| | 4 | 2.7814 | 7.8 | 53.2 |
| | 5 | 2.5894 | 7.1 | 60.3 |
| | 6 | 1.9088 | 5.3 | 65.6 |
| | 7 | 1.5653 | 4.4 | 70.0 |
| | 8 | 1.4145 | 3.9 | 73.9 |
| | 9 | 1.2171 | 3.4 | 77.3 |
| | 10 | 1.1396 | 3.2 | 80.5 |
| | 11 | 1.0603 | 2.9 | 83.4 |
| | 12 | 0.9371 | 2.6 | 86.0 |
| Dec-Feb. | 1 | 15.3320 | 42.6 | 42.6 |
| | 2 | 4.6193 | 12.8 | 55.4 |
| | 3 | 2.4557 | 6.8 | 62.2 |
| | 4 | 1.9485 | 5.5 | 67.7 |
| | 5 | 1.8601 | 5.1 | 72.8 |
| | 6 | 1.7090 | 4.8 | 77.6 |
| | 7 | 1.2263 | 3.4 | 81.0 |
| | 8 | 1.1470 | 3.2 | 84.2 |
| | 9 | 0.8965 | 2.5 | 86.7 |
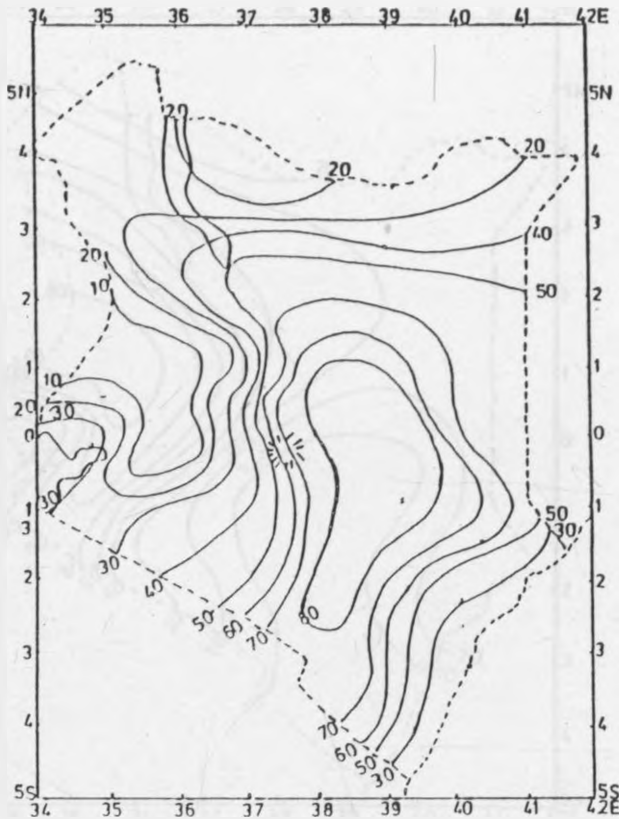
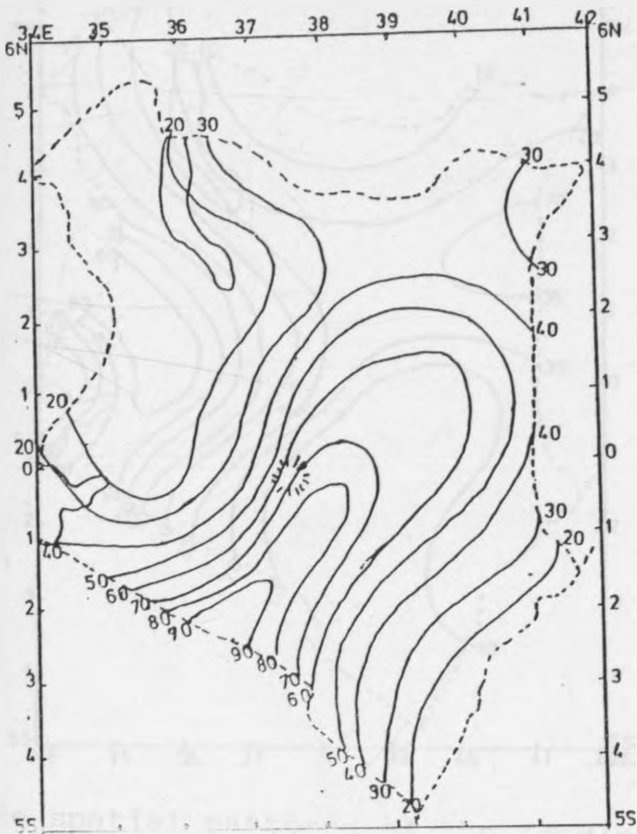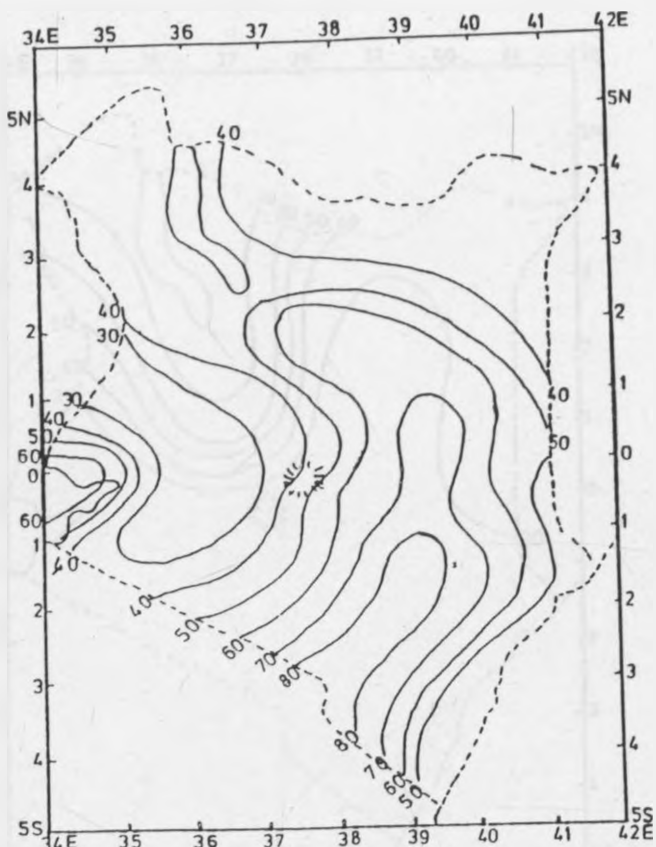Figure 13a:The spatial patterns of the loadings (X 100) of
the first intermonthly rainfall RPC.
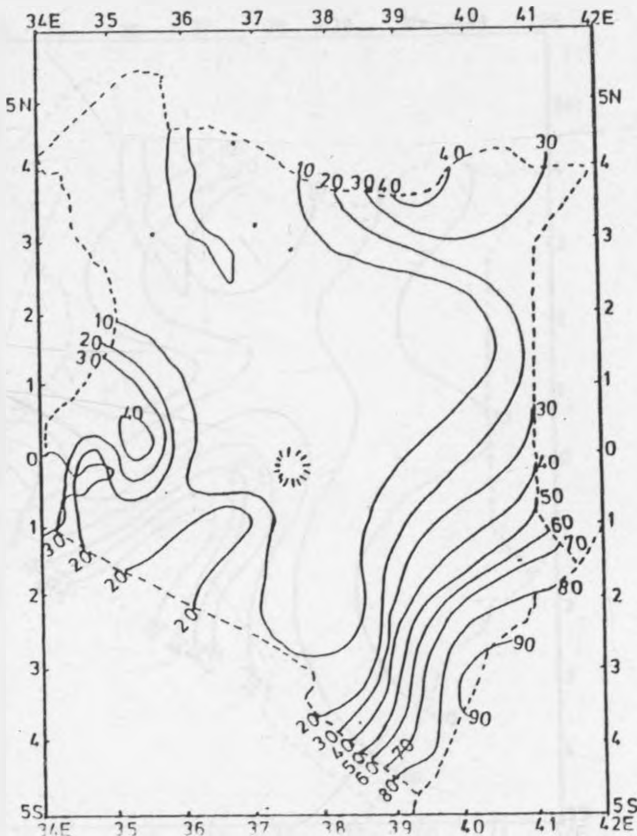


Figure 13b:The spatial patterns of the loadings (X 100) of
the second intermonthly rainfall RPC.
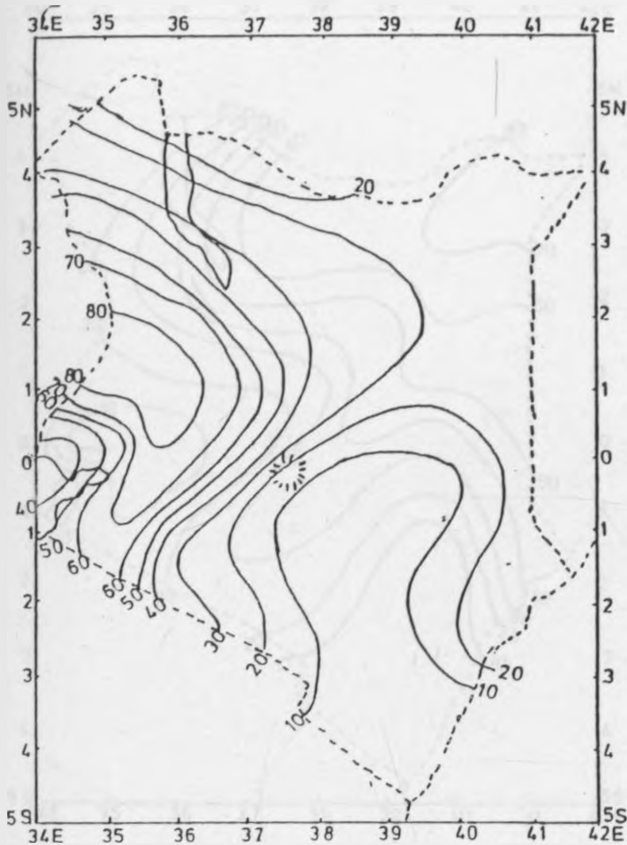
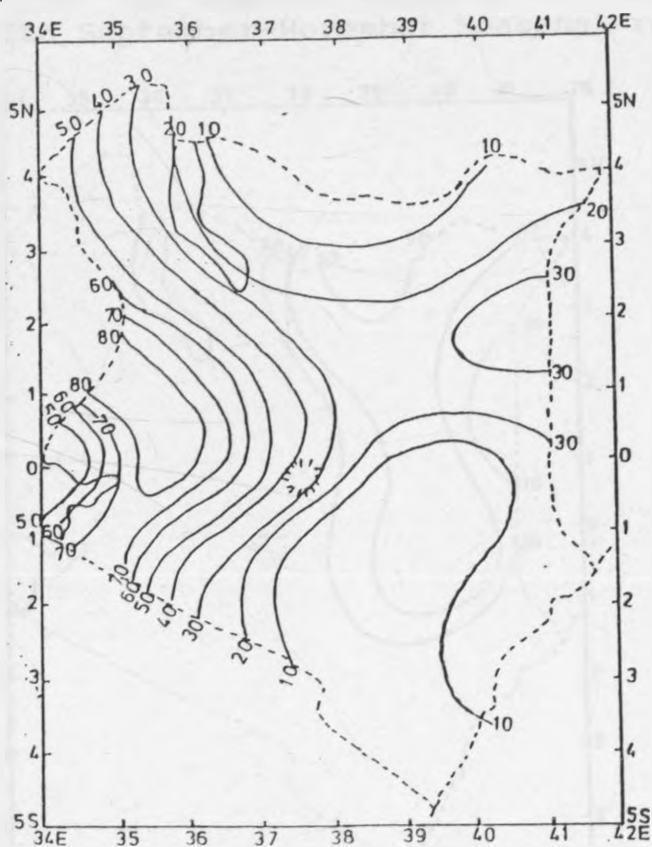Figure 13c:The spatial patterns of the loadings (X 100) of the third intermonthly rainfall RPC.
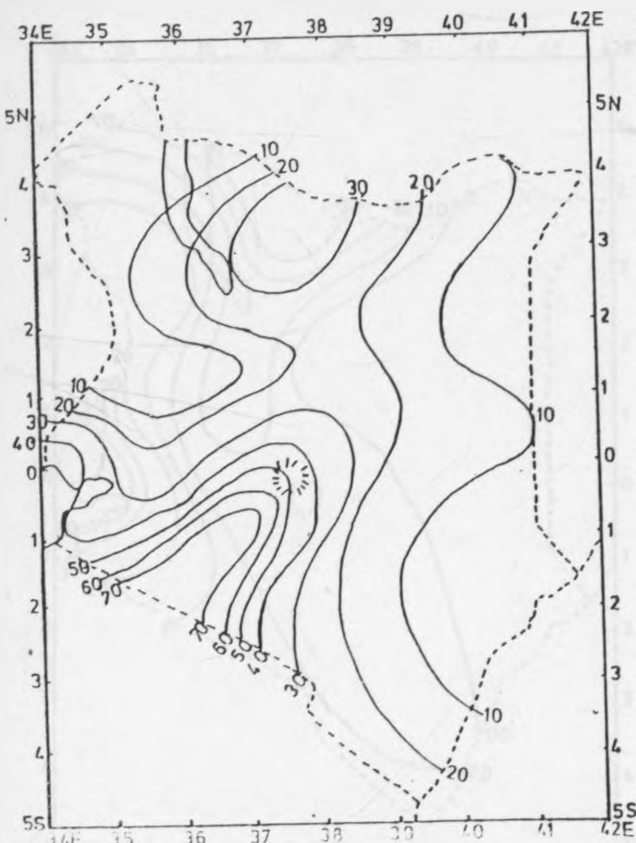


Figure 13d:The spatial patterns of the loadings (X 100) of the fourth intermontly rainfall RPC.
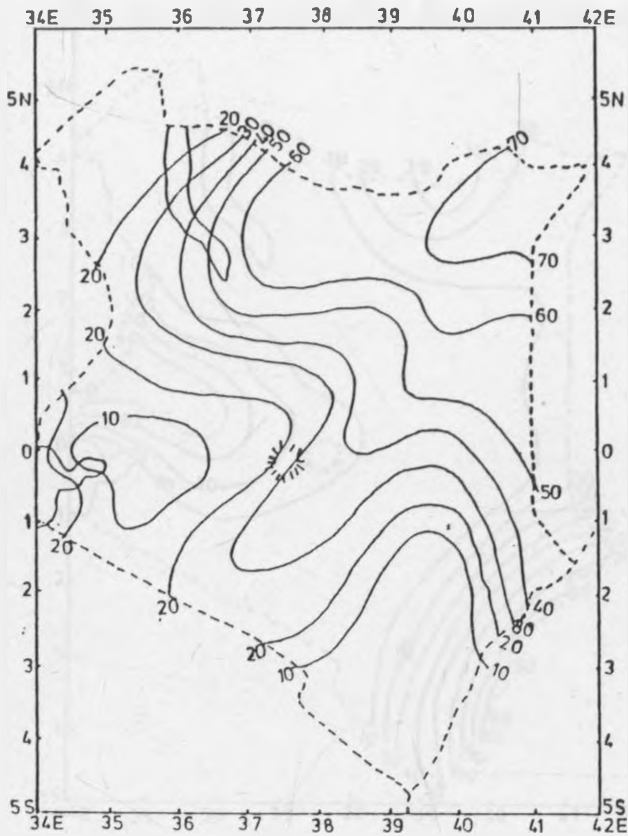
Figure 13e:The spatial patterns of the loadings (X 100) of
the fifth intermonthly rainfall RPC.
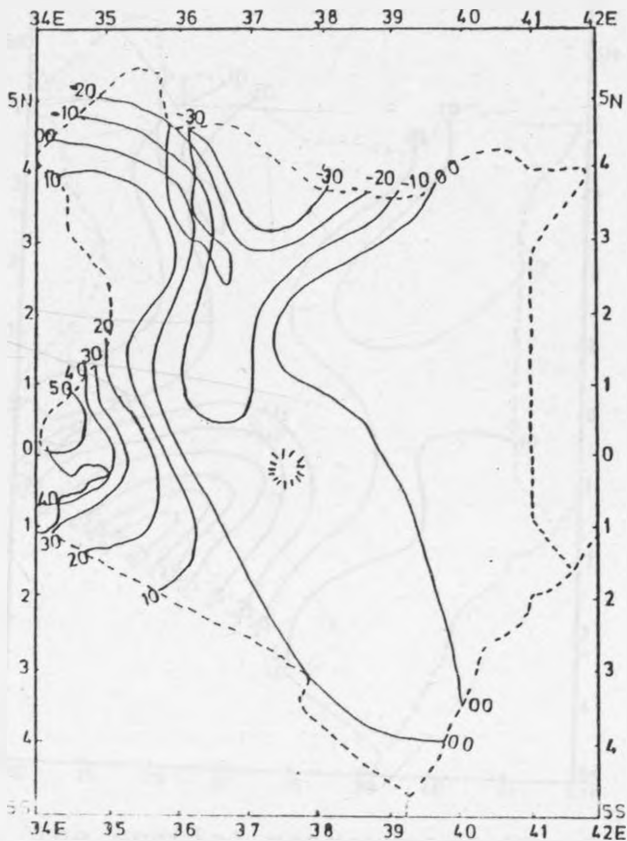


Figure 13f:The spatial patterns of the loadings (X 100) of
the sixth intermontly rainfall RPC.
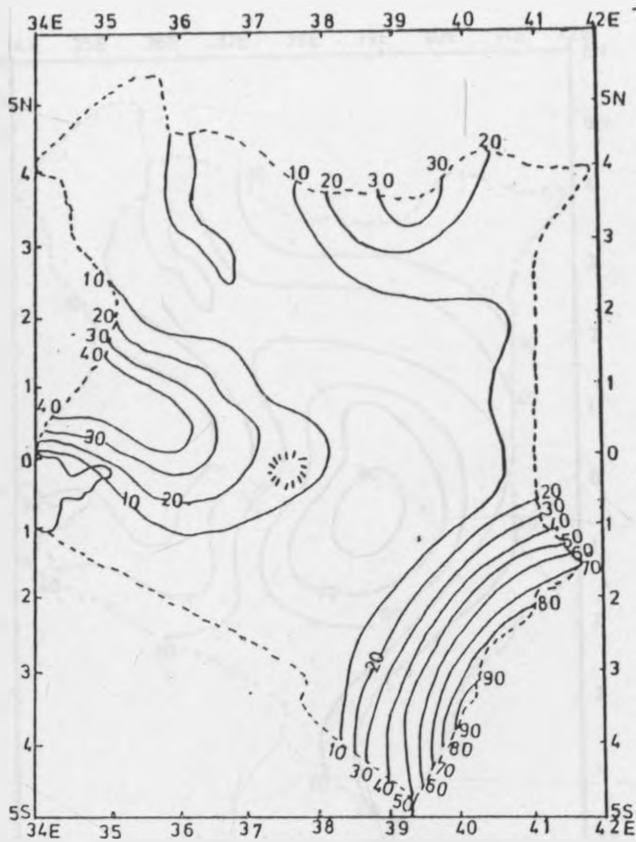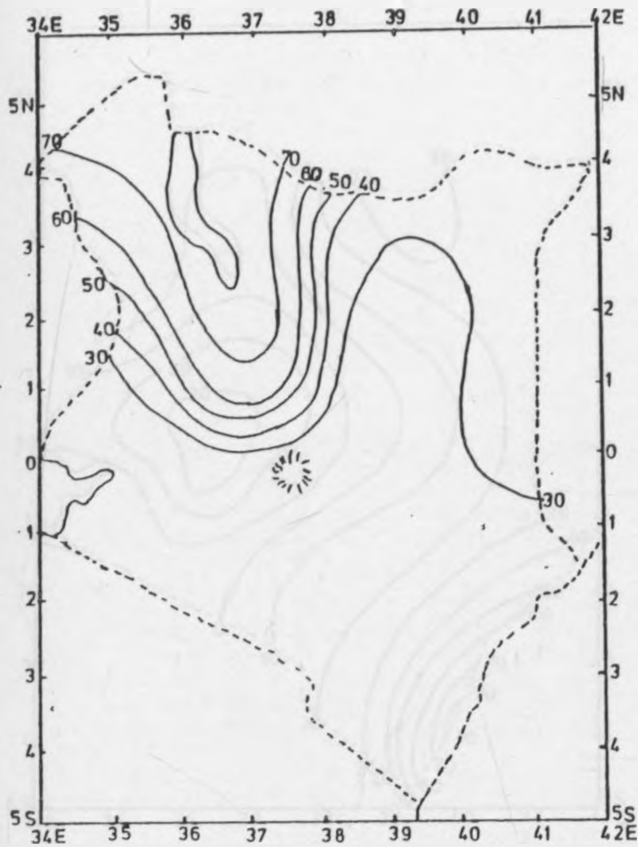
Figure 14a: The spatial patterns of the loadings (X 100) of the first March-May Seasonal rainfall RPC.
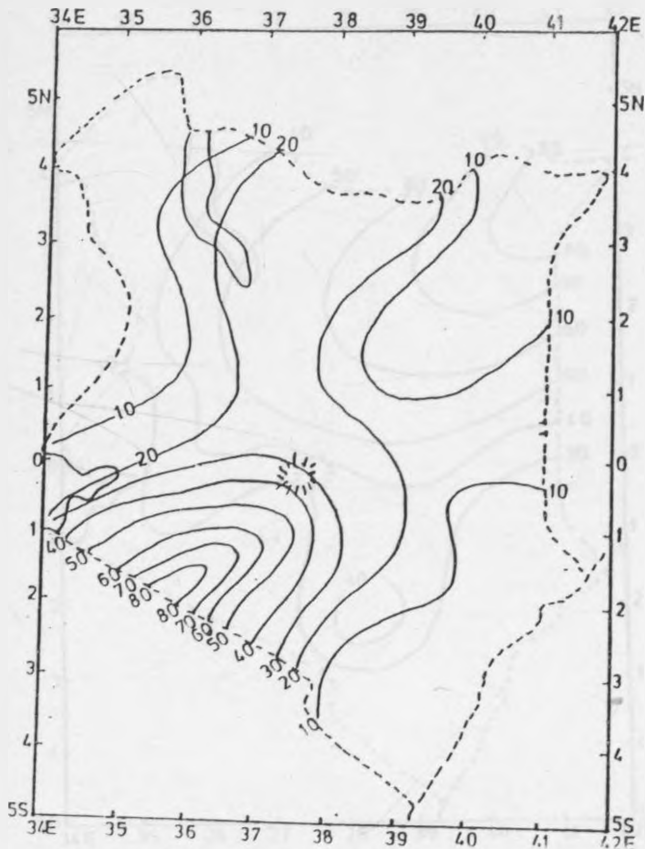


Figure 14b: The spatial patterns of the loadings (X 100) of the second March-May Seasonal rainfall RPC.
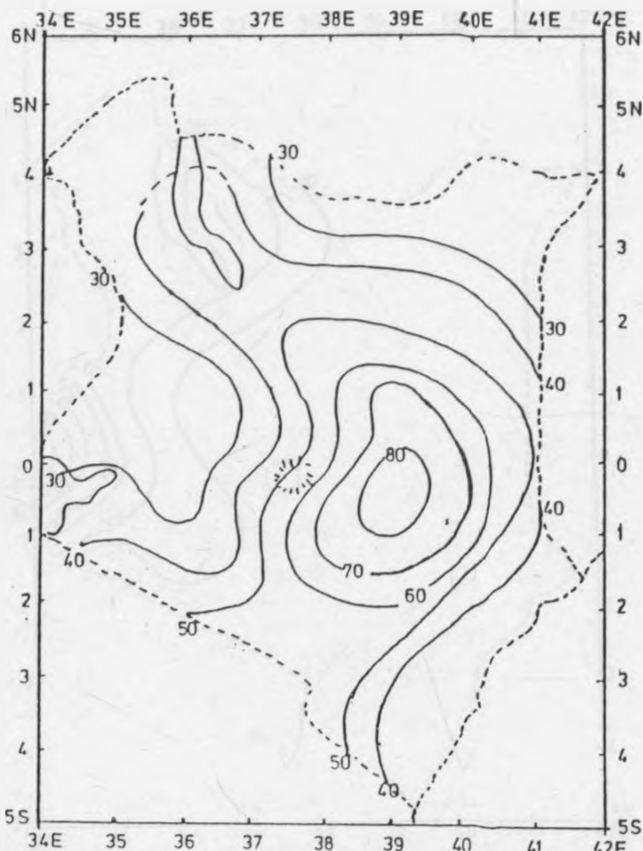
Figure 14c: The spatial patterns of the loadings (X 100) of the third March-May Seasonal rainfall RPC.
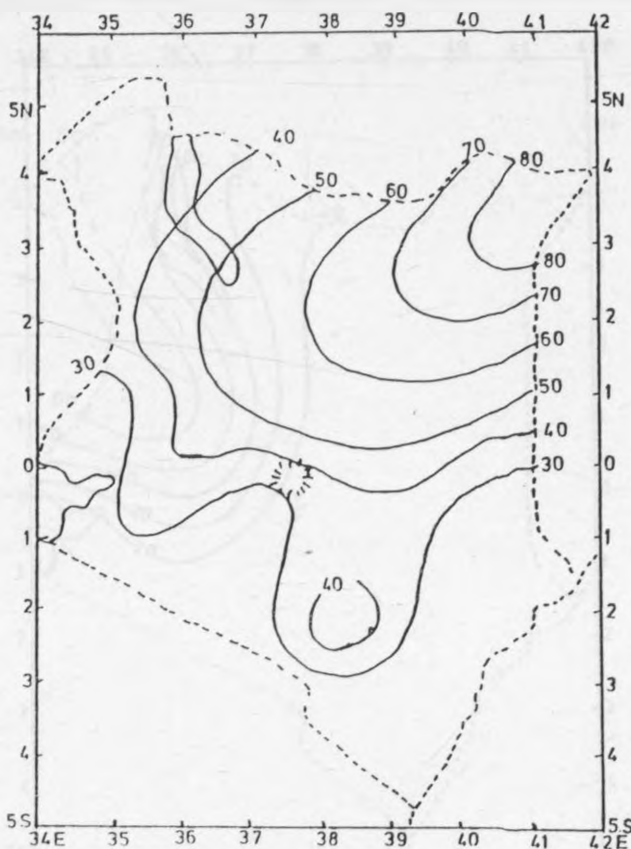


Figure 14d: The spatial patterns of the loadings (X 100) of the fourth March-May Seasonal rainfall RPC.
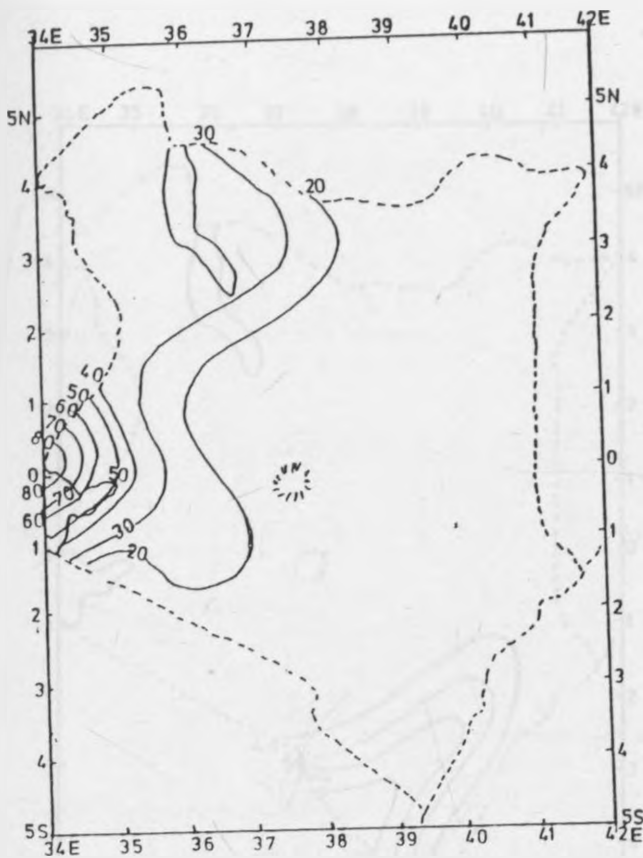
Figure 14e: The spatial patterns of the loadings (X 100) of the fifth March-May Seasonal rainfall RPC.
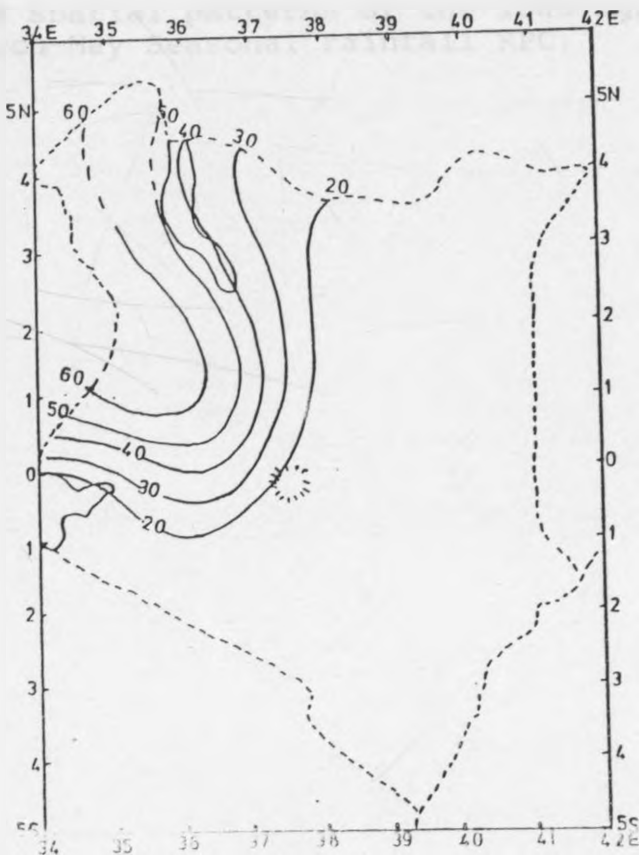


Figure 14f: The spatial patterns of the loadings (X 100) of the sixth March-May Seasonal rainfall RPC.
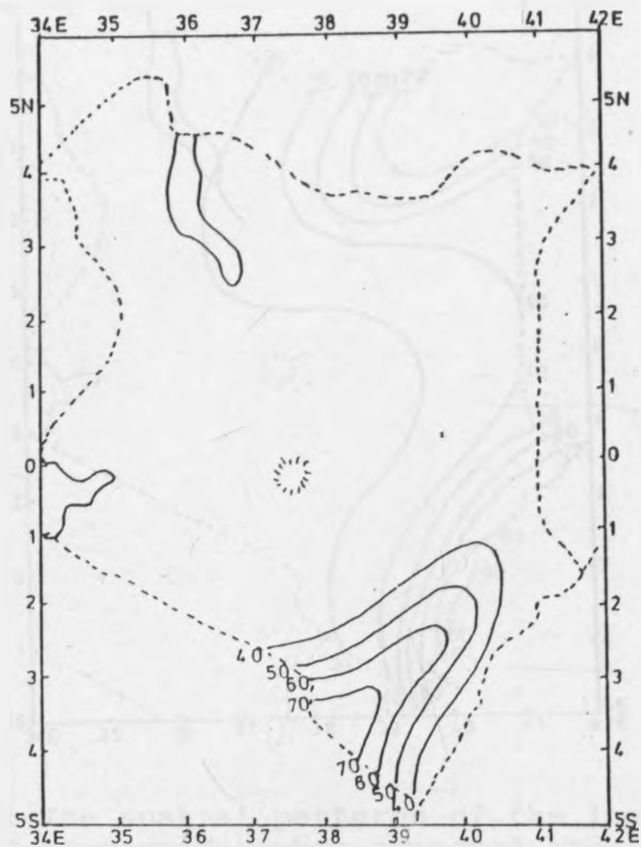
Figure 14g: The spatial patterns of the loadings (X 100) of
the seventh March-May Seasonal rainfall RPC.
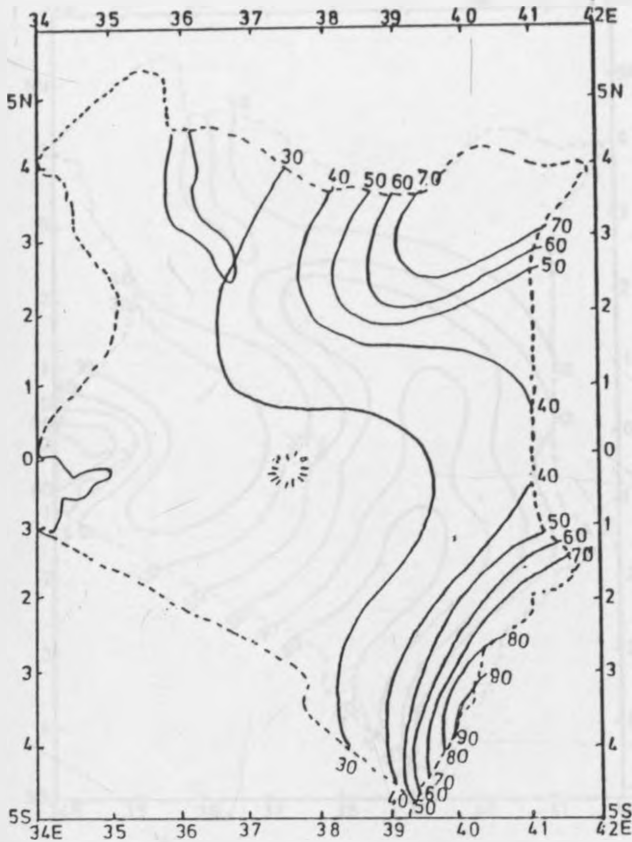
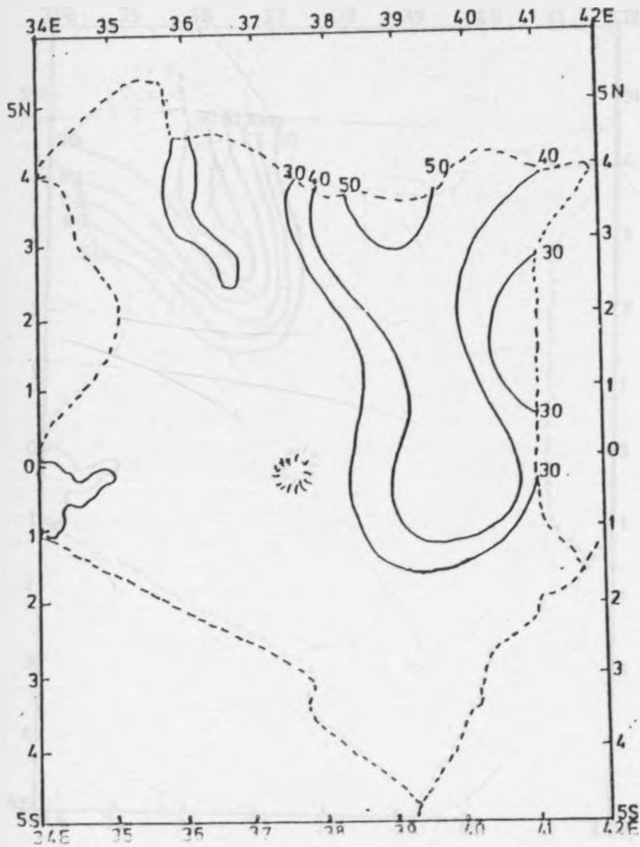Figure 15a: The spatial patterns of the loadings (X 100) of the first September-November seasonal rainfall RPC.



Figure 15b: The spatial patterns of the loadings (X 100) of the second September-November Seasonal rainfall RPC.
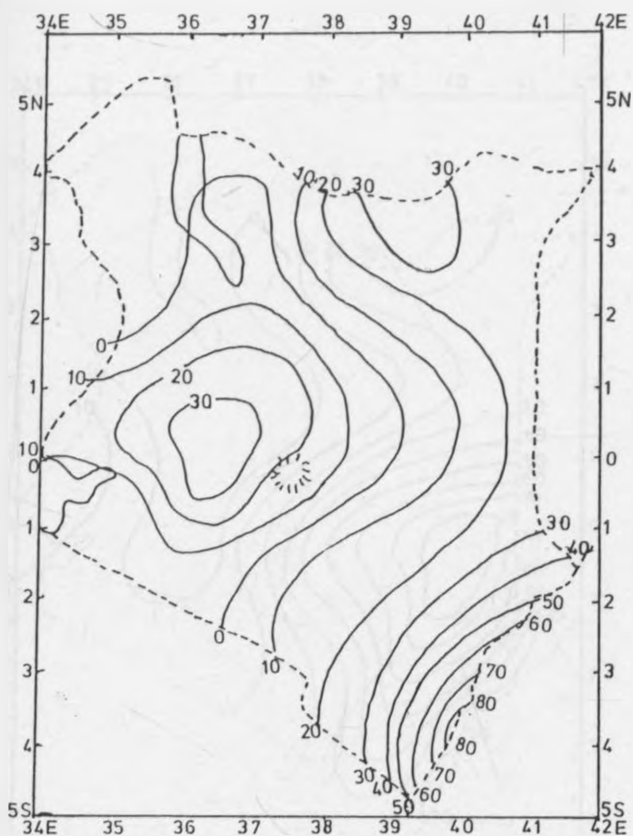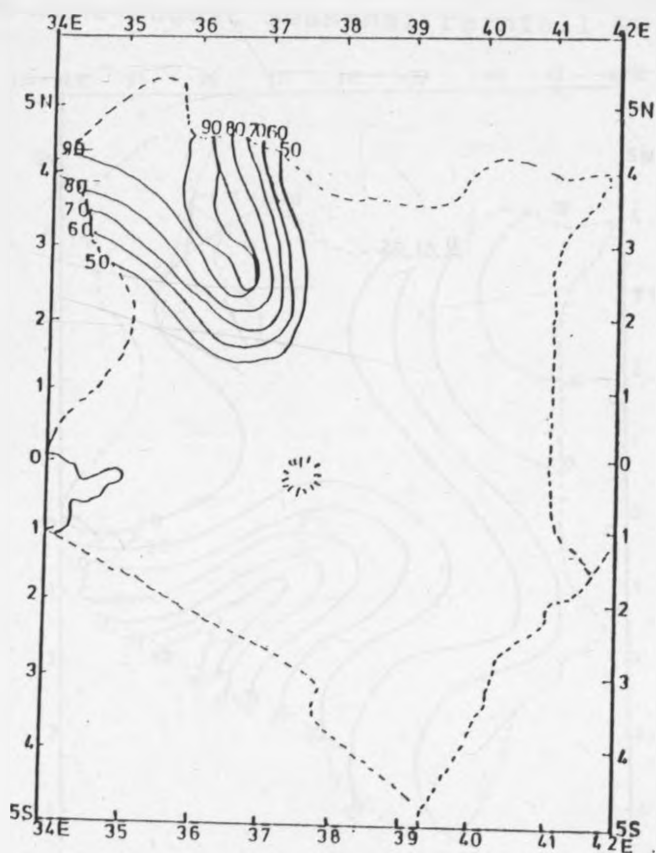
Figure 15c: The spatial patterns of the loadings (X 100) of the third September-November Seasonal rainfall RPC.



Figure 15d: The spatial patterns of the loadings (X 100) of the fourth September-November Seasonal rainfall RPC.

Figure 15e: The spatial patterns of the loadings (X 100) of
the fifth September-November Seasonal rainfall RPC.



Figure 15f: The spatial patterns of the loadings (X 100) of
the sixth September-November Seasonal rainfall RPC.

Figure 16a: The spatial patterns of the loadings (X 100) of the first June-August Seasonal rainfall RPC.



Figure 16b: The spatial patterns of the loadings (X 100) of the second June-August Seasonal rainfall RPC.
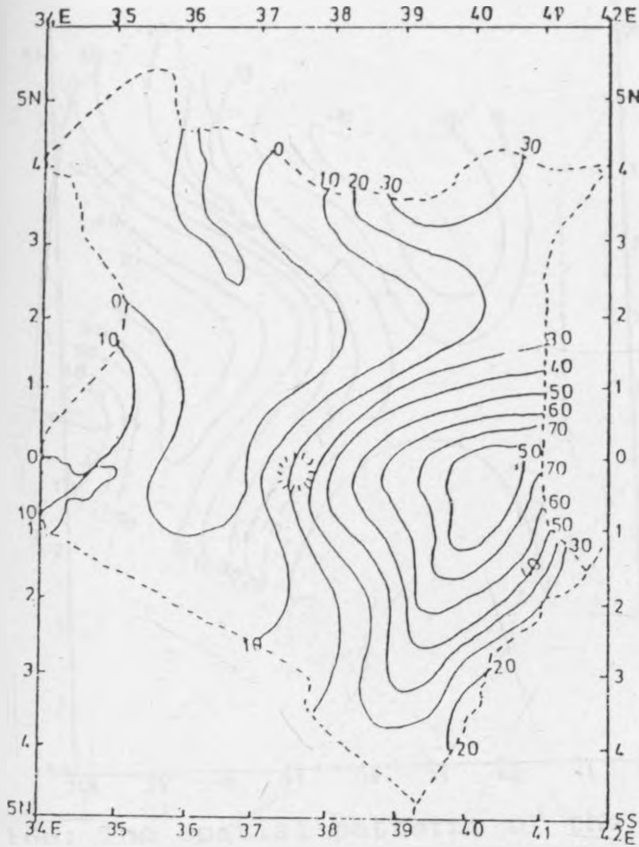
Figure 16c: The spatial patterns of the loadings (X 100) of
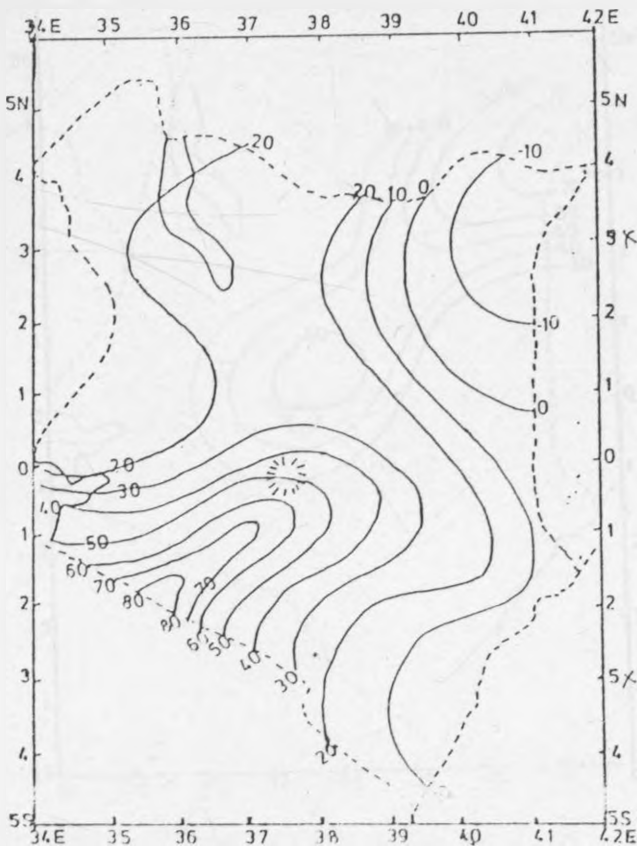The third June-August Seasonal rainfall RPC.



Figure 16d: The spatial patterns of the loadings (X 100) of
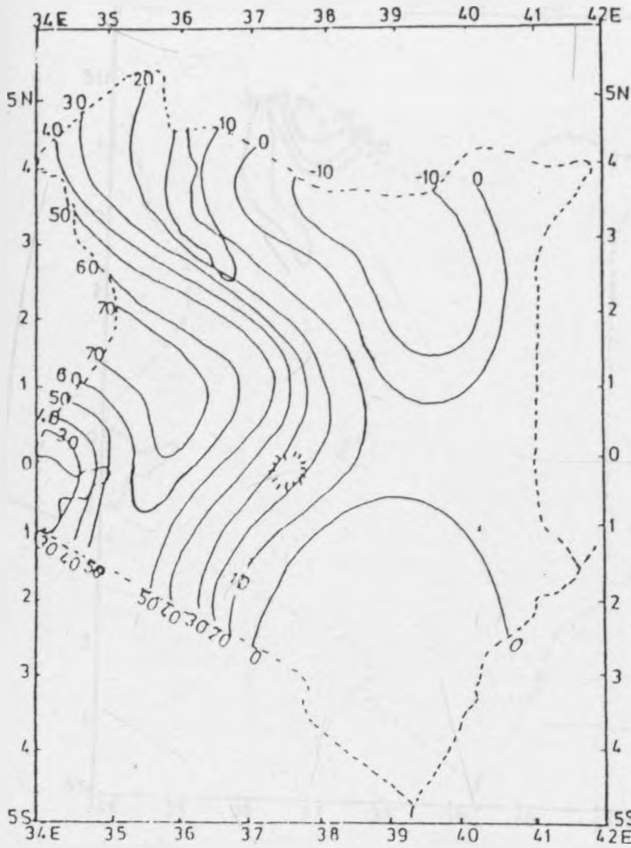the fourth June-August Seasonal rainfall RPC.

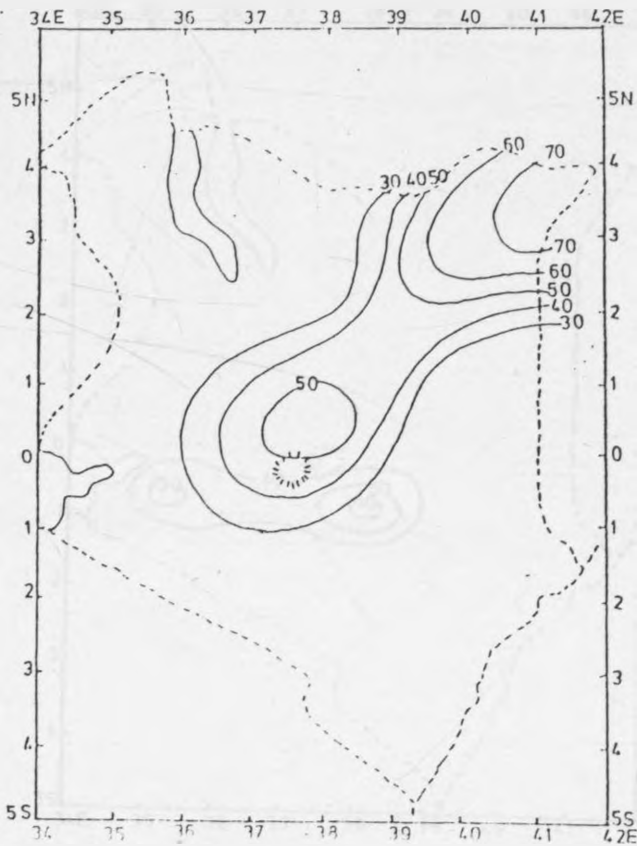Figure 16e: The spatial patterns of the loadings (X 100) of the fifth June-August Seasonal rainfall RPC.



Figure 16f: The spatial patterns of the loadings (X 100) of the sixth June-August seasonal rainfall RPC.
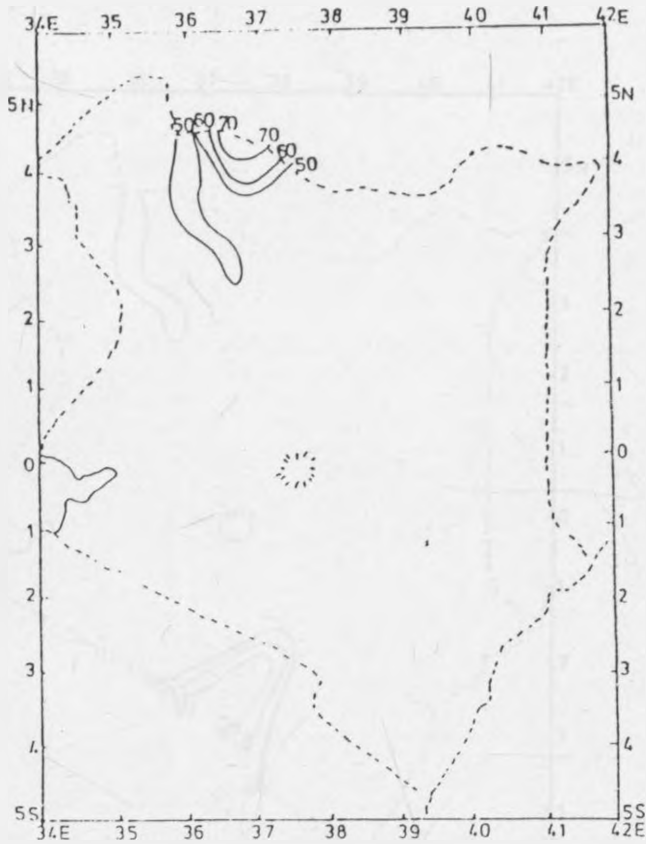
Figure 16g: The spatial patterns of the loadings (X 100) of the seventh June-August Seasonal rainfall RPC.
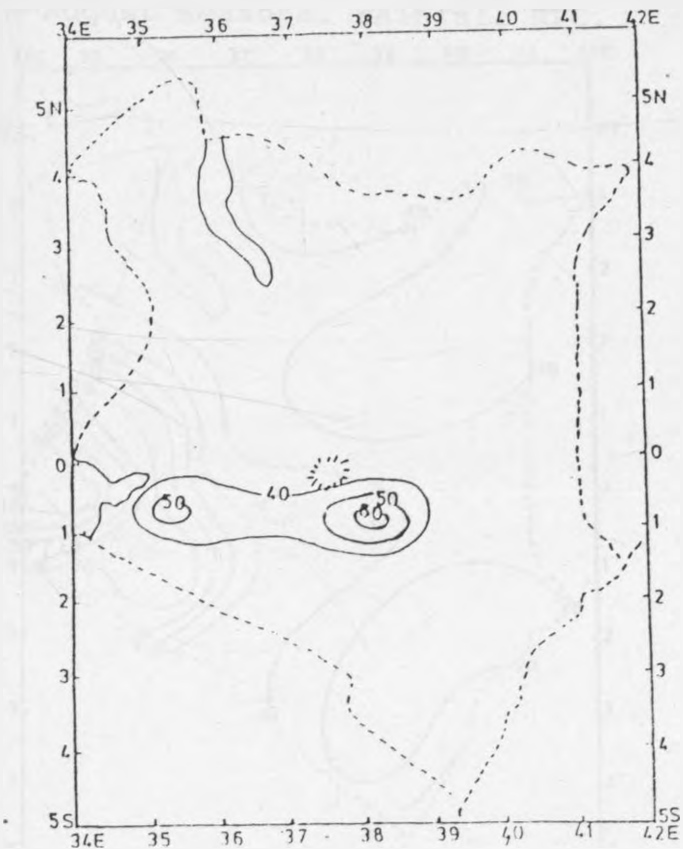


Figure 16h: The spatial patterns of the loadings (X 100) of the eighth June-August Seasonal rainfall RPC.
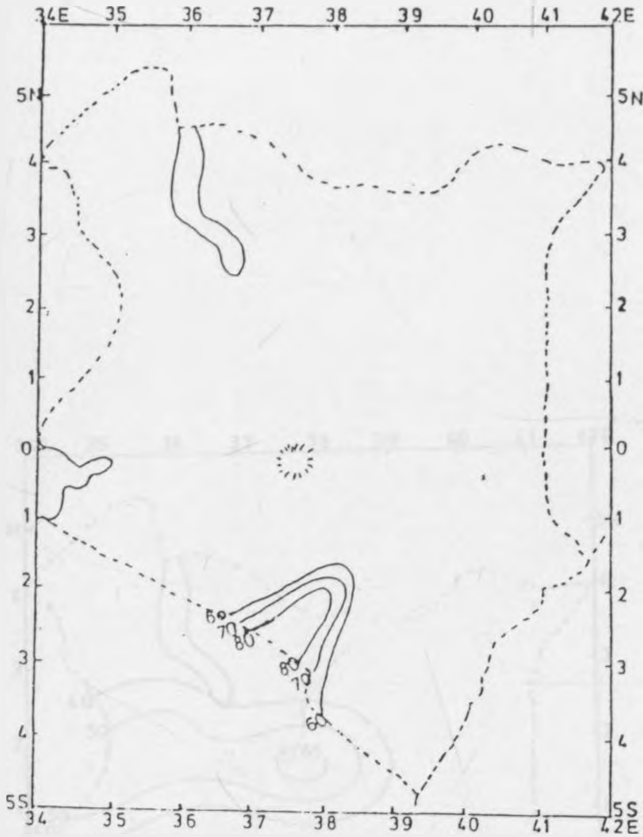
Figure 16i: The spatial patterns of the loadings (X 100) of the ninth June-August Seasonal rainfall RPC.
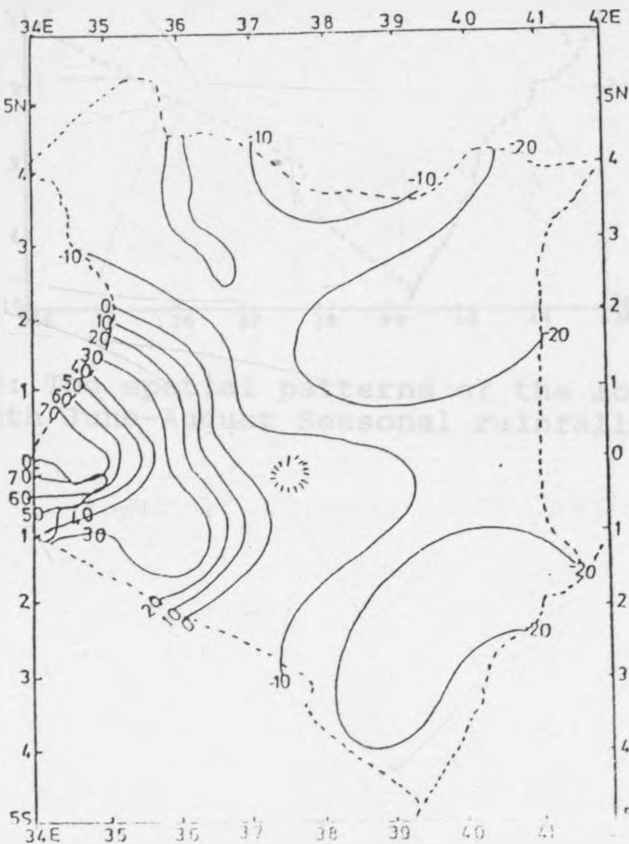


Figure 16j: The spatial patterns of the loadings (X 100) of the tenth June-August seasonal rainfall RPC.
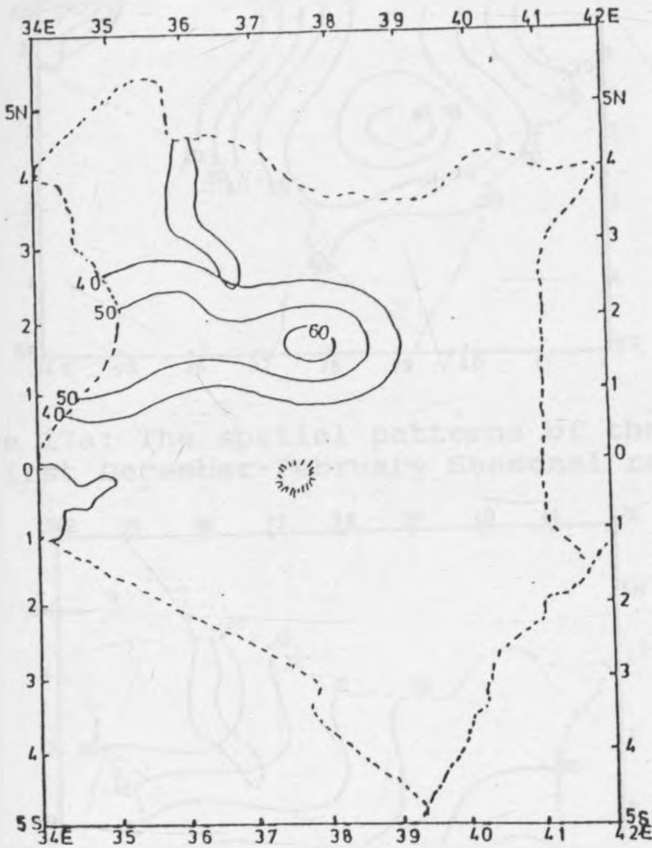
Figure 16k: The spatial patterns of the loadings (X 100) of the eleventh June-August Seasonal rainfall RPC.

Figure 17a: The spatial patterns of the loadings (X 100) of the first December-February Seasonal rainfall RPC.



Figure 17b: The spatial patterns of the loadings (X 100) of the second December-February seasonal rainfall RPC.

Figure 17c: The spatial patterns of the loadings (X 100) of the third December-February Seasonal rainfall RPC.



Figure 17d: The spatial patterns of the loadings (X 100) of the fourth December-February seasonal rainfall RPC.

Figure 17e: The spatial patterns of the loadings (X 100) of the fifth December-February seasonal rainfall RPC.



Figure 17f: The spatial patterns of the loadings (X 100) of the Sixth December-February Seasonal rainfall RPC.
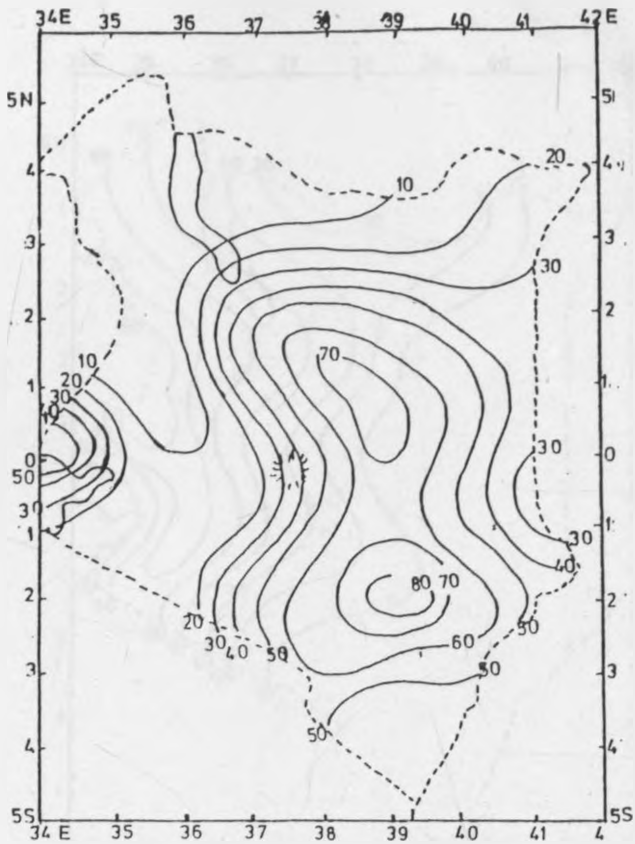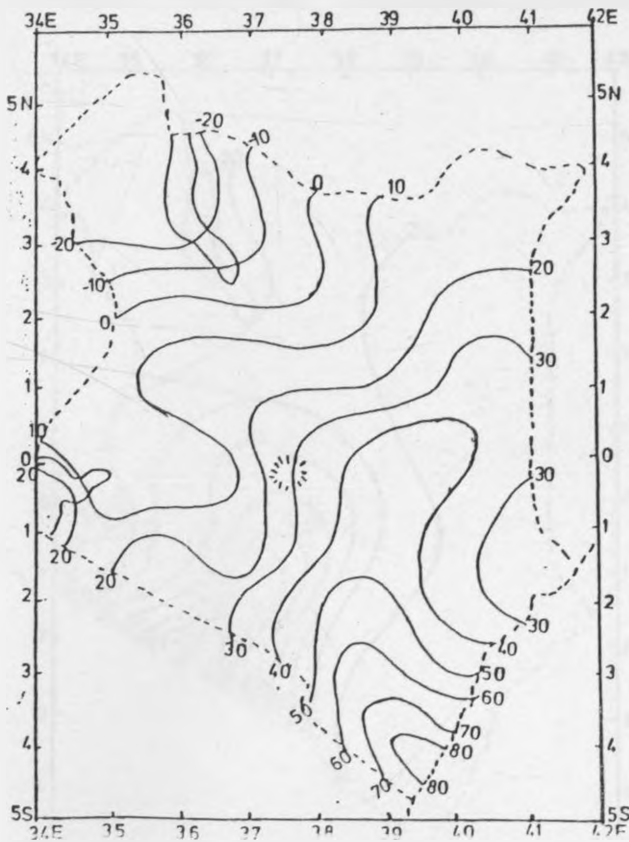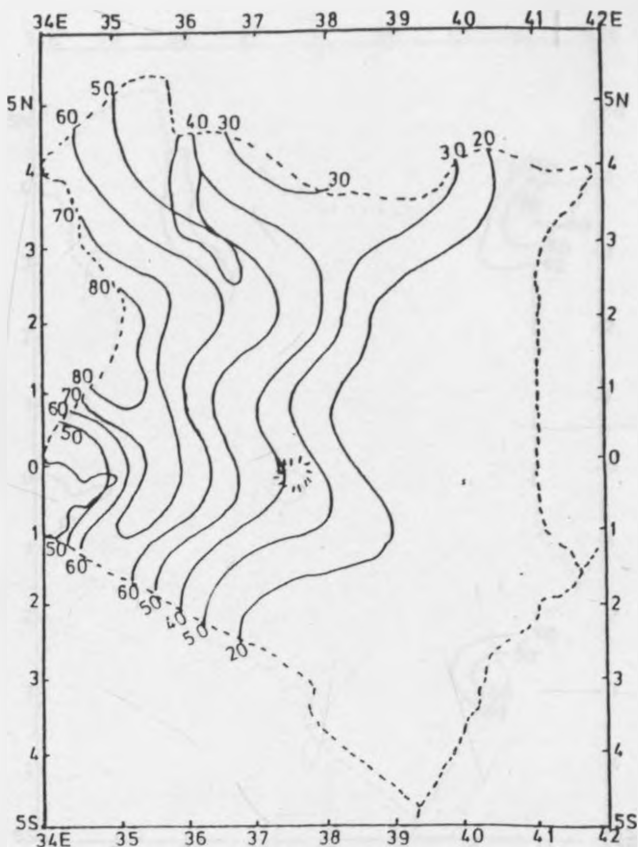
Figure 17g: The spatial patterns of the loadings (X 100) of
the Seventh December-February Seasonal rainfall RPC.
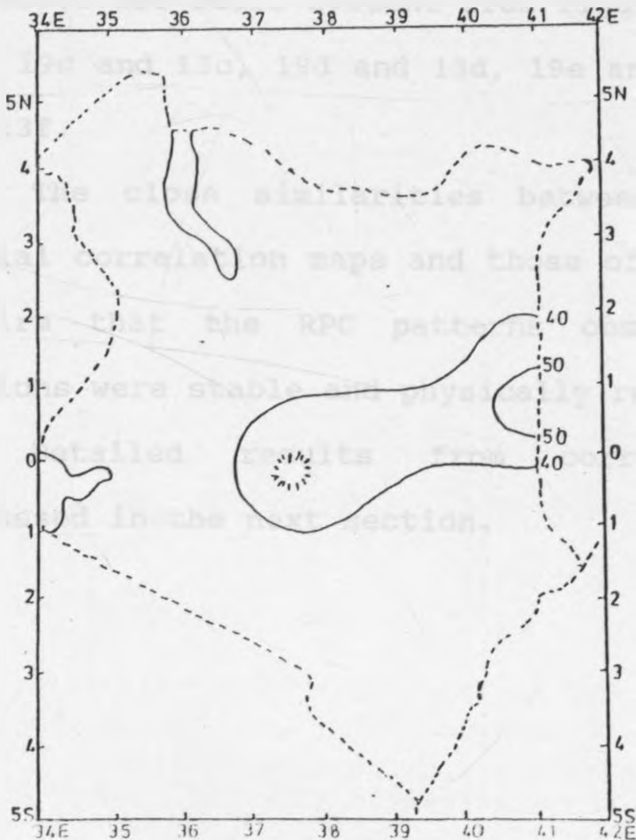


Figure 17h: The spatial patterns of the loadings (X 100) of
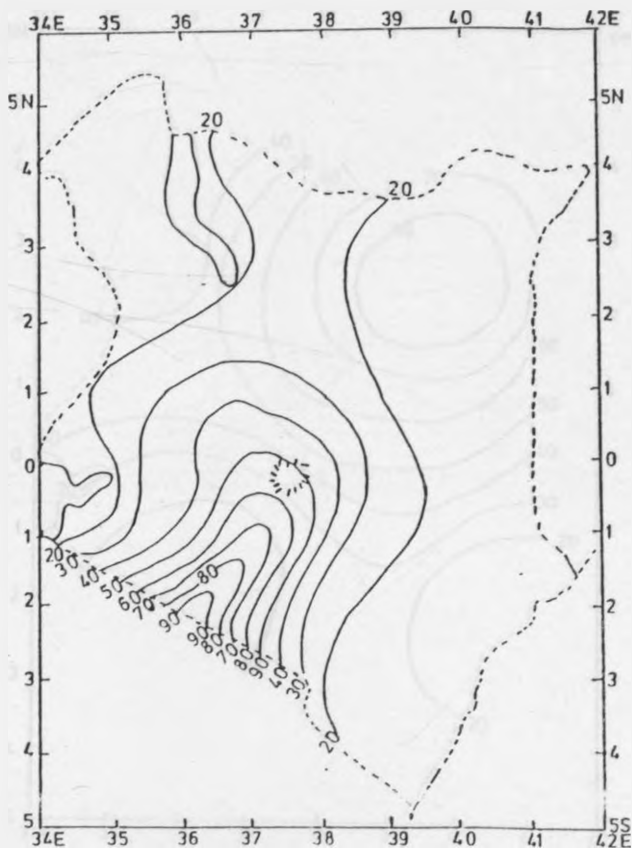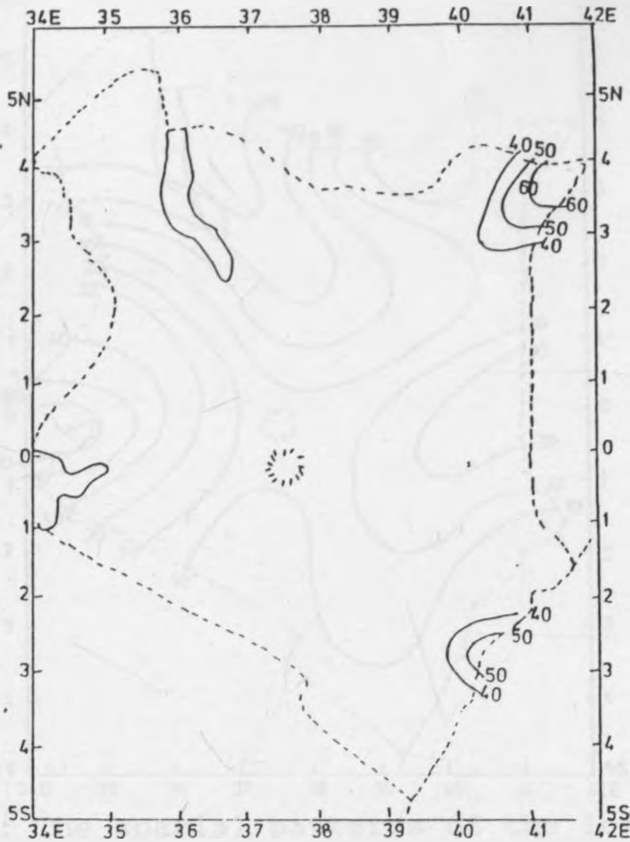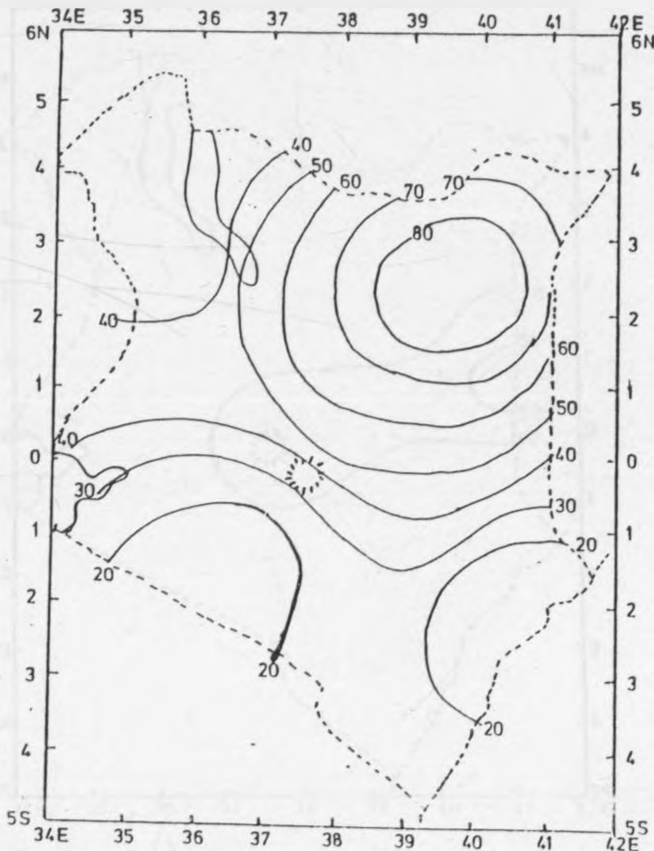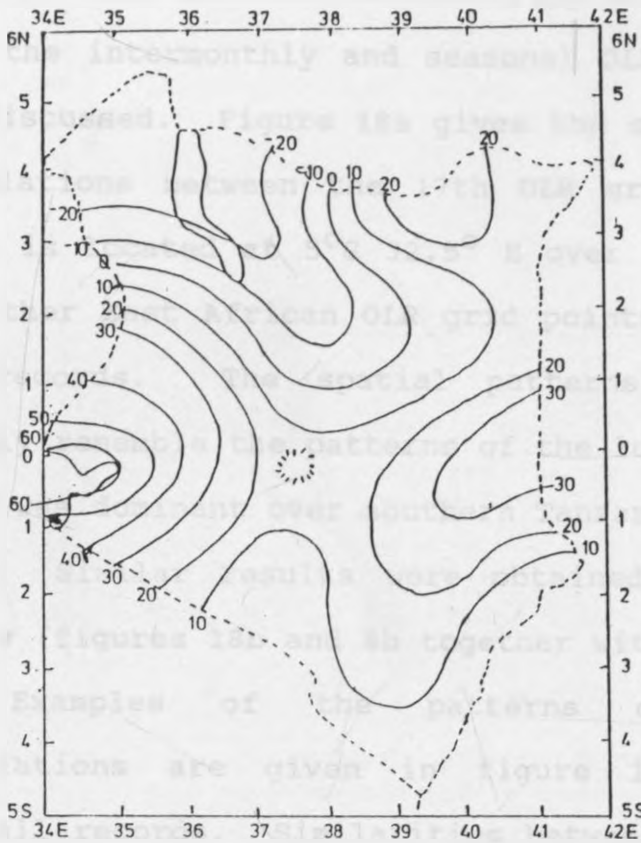the eighth December-February seasonal rainfall RPC.

## 3.4 STABILITY OF THE DERIVED RPC PATTERNS

In this section the stability of the RPC modes derived from the intermonthly and seasonal OLR and rainfall records are discussed. Figure 18a gives the spatial patterns of the correlations between the 17th OLR gridpoint (figure 1a), which is located at $5^{O}S$ $32.5^{O}$ E over Southern Tanzania, and the other East African OLR grid points for the intermonthly OLR records. The spatial patterns of the correlations closely resemble the patterns of the loadings of the RPC mode which was dominant over southern Tanzania (figures 8a, 9b and 12a). Similar results were obtained with the other grid points (figures 18b and 8b together with 18c and 8c).

Examples of the patterns of the interstation correlations are given in figure 19 using intermonthly rainfall records. Similarities between the spatial patterns of interstation correlations and the corresponding rainfall RPC modes are still evident from figures 19a and 13a, 19b and 13b, 19c and 13c, 19d and 13d, 19e and 13e together with 19f and 13f.

The close similarities between the patterns of the spatial correlation maps and those of the dominant RPC modes confirm that the RPC patterns observed in the previous sections were stable and physically realistic.

Detailed results from correlation analysis are discussed in the next section.
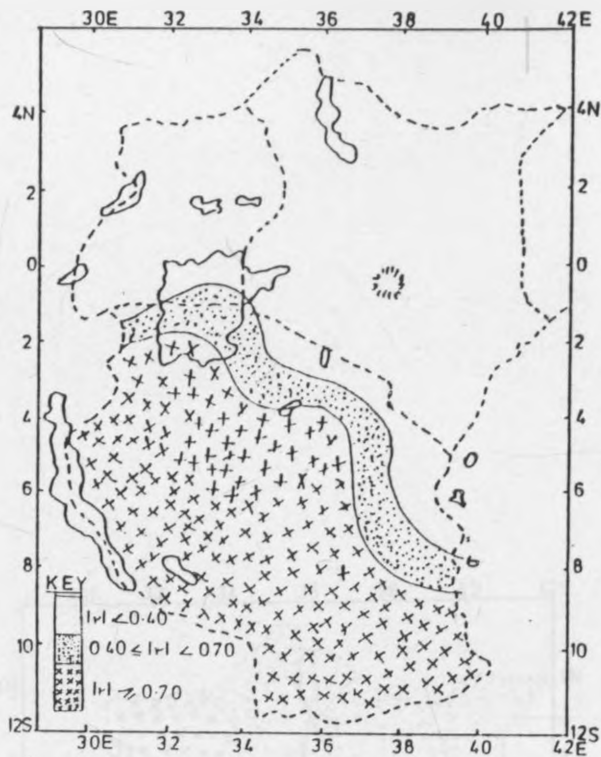
Figure 18a: OLR intergrid point correlations between the other grid points and the seventeenth grid point.
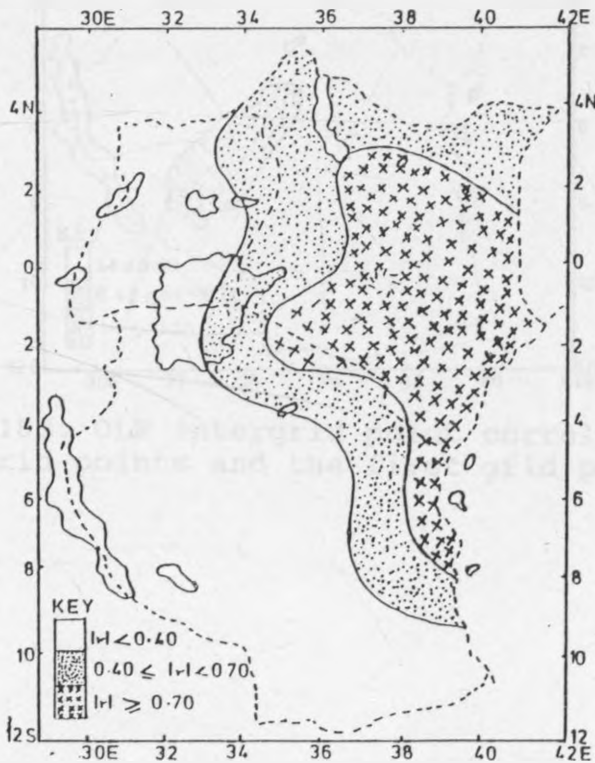
Figure 18b: OLR intergrid point correlations between the other grid points and the fifteenth grid point.
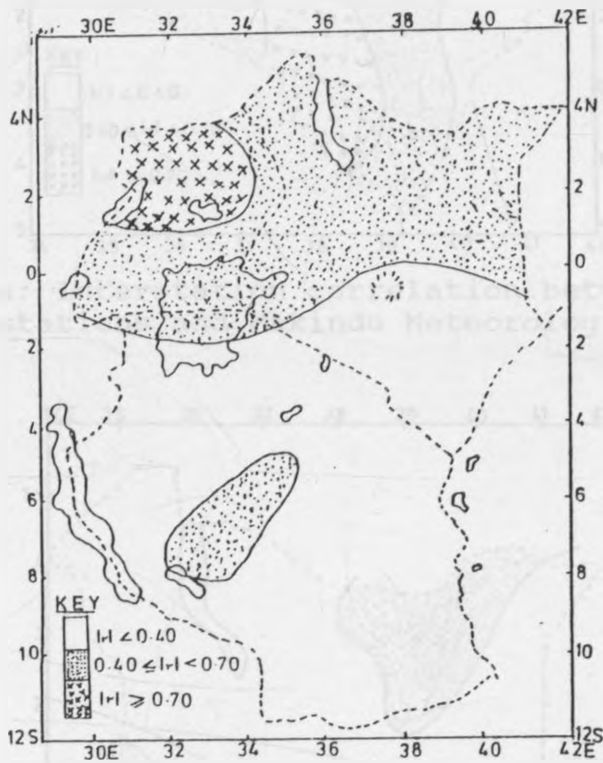
Figure 18c: OLR intergrid point correlations between the other grid points and the first grid point.

Figure 19a: Interstation correlation between the other
rainfall stations and Makindu Meteorological Station.
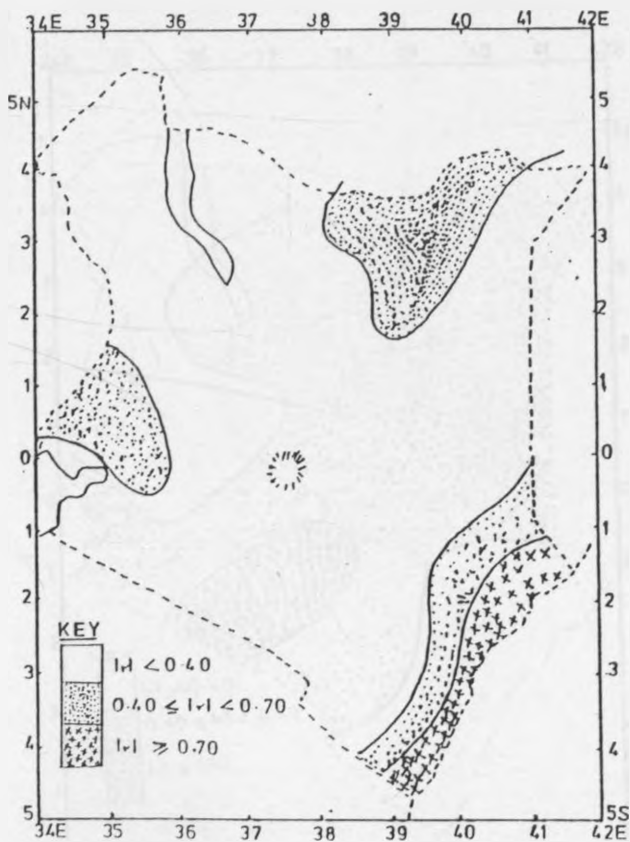


Figure 19b: Interstation correlation between the other
rainfall stations and Malindi Meteorological Station.
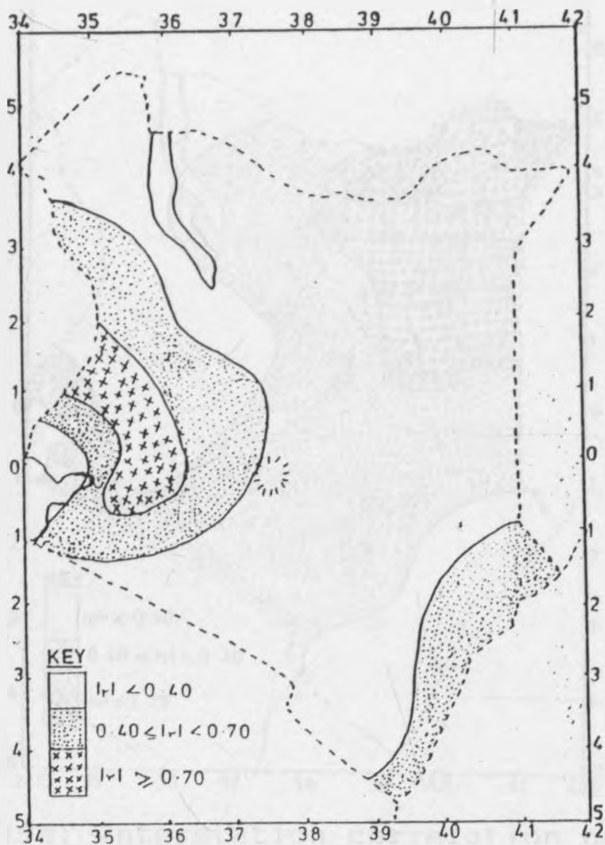
Figure 19c: Interstation correlation between the other rainfall stations and Kitale Meteorological Station.
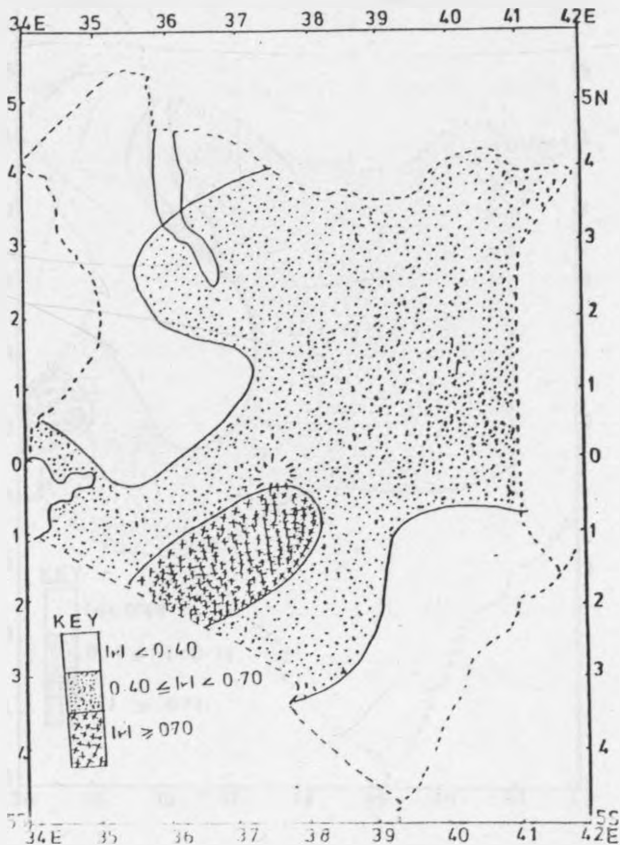


Figure 19d: Interstation correlation between the other rainfall stations and Nairobi Water Station.
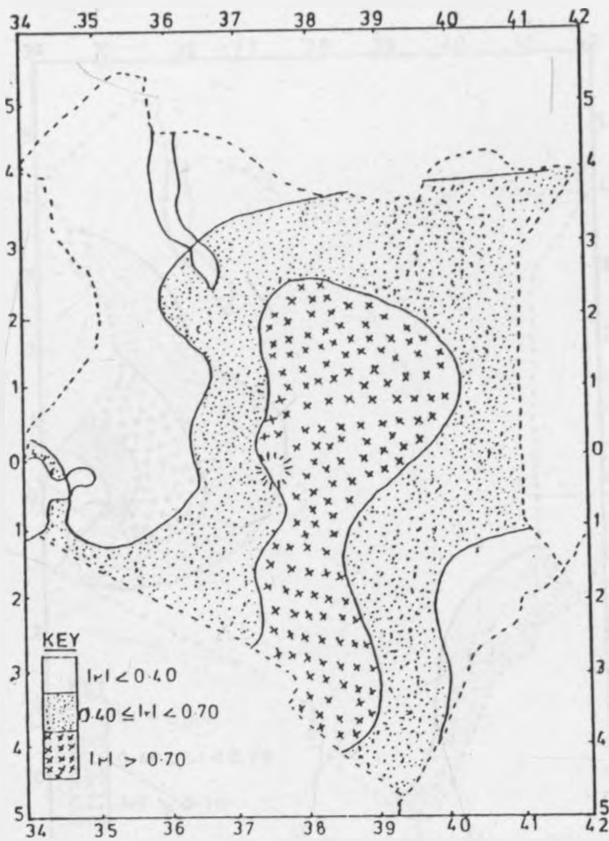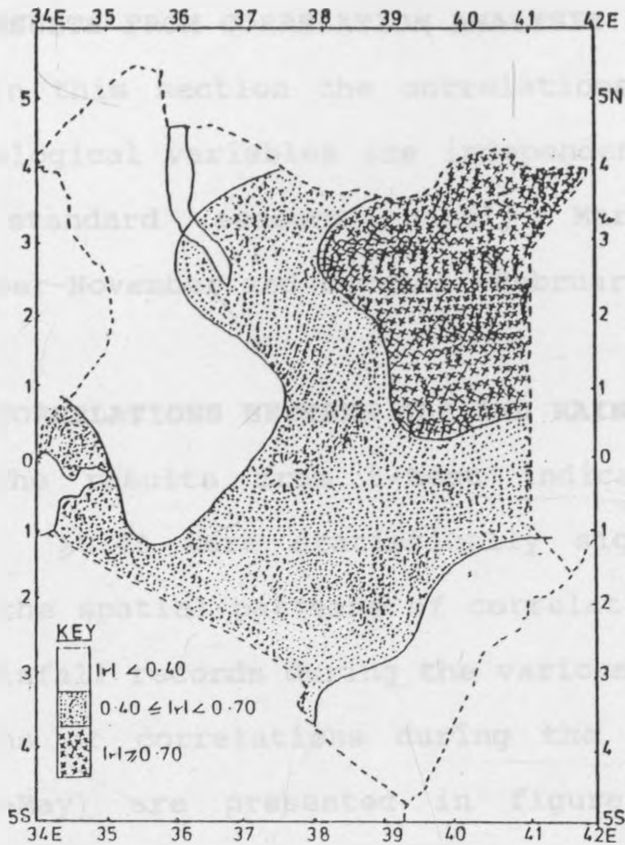
Figure 19e: Interstation correlation between the other rainfall stations and Mandera Meteorological Station.
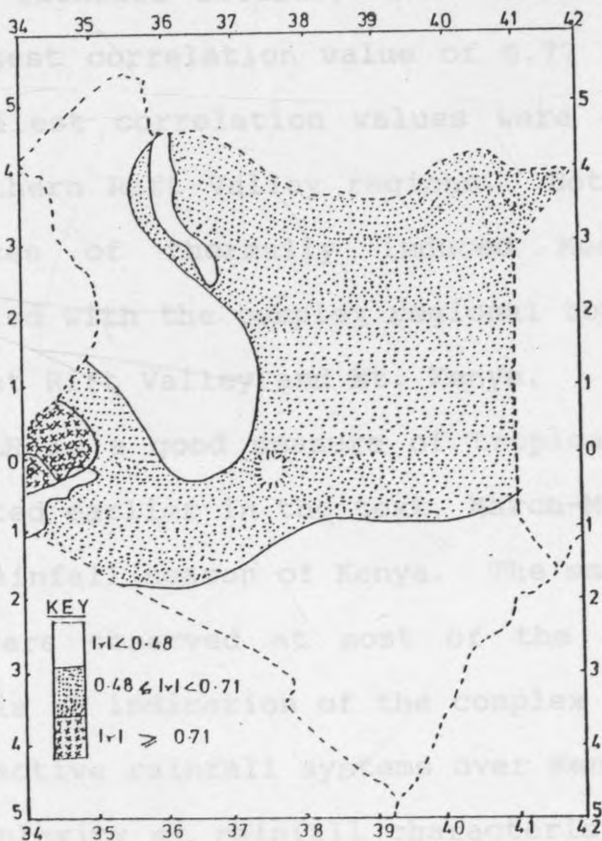


Figure 19f: Interstation correlation between the other rainfall stations and Port Victoria Rainfall Station.

## 3.5  RESULTS FROM CORRELATION ANALYSIS

In this section the correlations between OLR and the Meteorological variables are independently discussed for the four standard seasons namely March-May, June-August, September-November and December-February.

### 3.5.1 CORRELATIONS BETWEEN OLR AND RAINFALL

The results from t-test indicated that correlation values ⩾0.48 were statistically significant. Figure 20 gives the spatial patterns of correlations between point OLR and rainfall records during the various seasons. The spatial patterns of correlations during the major rainfall season (March-May) are presented in figure 20a using the peak rainfall month of April. It is evident from figure 20a that although there were significant correlations between point OLR and rainfall records, the values were generally small. The largest correlation value of 0.77 was observed at Lamu. The smallest correlation values were observed over Central and Northern Rift Valley regions. Both regions have strong influences of thermally induced Meso-scale circulations associated with the complex regional topography which include the Great Rift Valley and Mt. Kenya.

OLR is a good measure of tropical convection. As has been noted earlier in the text, March-May (long-rainy) is the major rainfall season of Kenya. The small correlation values which were observed at most of the locations during this season is an indication of the complex nature of the patterns of convective rainfall systems over Kenya during this season. The complexity of rainfall characteristics during the season

have been observed by many authors including Ogallo (1989).
The regional systems like topography, land/sea breezes and
other thermally induced Meso-scale systems have significant
modifications on the large scale monsoonal wind systems.
Such small scale convective phenomena may also not be
represented effectively by twice daily NOAA polar Orbiting
Satellite Observations.

Figures 21, 22 and 23 give the spatial patterns of
correlations between the various OLR grid points (figure 1b)
and rainfall areally averaged over the various homogeneous
climatological regions during the various seasons. Figure 21
indicates that the magnitudes of correlations were generally
larger when compared with the point correlation values. The
largest correlation values for the various regions ranged
between 0.55 and 0.90. The largest correlation value of 0.90
was observed in climatological region 2 (figure 21a) It is
also evident from figure 21 that rainfall from some
climatological regions were strongly correlated with OLR
records while others, especially those located in the
neighbourhood of large water bodies and with complex
topography, had relatively small correlation values.

Examples of the patterns of correlations which were
obtained when both OLR and rainfall records were areally
averaged are given in figure 24 for the various seasons.
Both OLR and rainfall records were averaged over $2.5^{\circ}$ x $2.5^{\circ}$
latitude/longitude squares located over Kenya as shown in
figure 1b. It can be seen from figure 24a that the values of

correlations during long-rainy season ranged between 0.38 and 0.89. The largest correlation values are still observed over the eastern and north eastern Kenya.

A general comparison of figures 20a, 21 and 24a indicates that the values of correlations obtained with areal records were generally larger than those obtained with point records. The improvement in the relationships between infrared satellite data and rainfall with increasing spatial and temporal averaging scales has been noted by Richards and Arkin (1981).

Areal averaging is capable of minimizing the effects of errors which may exist in the records and localized factors which introduce spatial differences in the patterns of correlations.

The results for the OLR and rainfall correlations during September-November (short-rainy) season are given in figures 20b, 22 and 24b as represented by the month of November. The rainfall for this season is centred around the month of November. It is evident from these figures that the correlation values for short-rainy season were generally larger when compared to the values which were obtained for long-rainy season. Better correlations between rainfall and synoptic systems during short-rainy season have also been observed by Ogallo (1989) and Nyenzi (1990). The largest correlation values for both point and areally averaged records ranged between 0.86 and 0.97.

The spatial patterns of correlations between OLR and rainfall during June-August season as represented by the month of July are shown in figures 20c, 23 and 24c. This

season is generally dry except for Western Kenya, Lake Victoria regions and parts of the coastal areas. The Western parts of Kenya are under the influence of the moist Congo airmass during this season. The figures show that correlation values were generally small for both point and areally averaged records. The largest correlation values were centred around the northern coastal areas where Lamu had a peak value of 0.60.

The relatively small values of correlations which were observed over western and coastal areas during June-August season can be attributed to the complex patterns of regional systems during this season. Unlike the long-and short-rainy seasons when the country is under the influence of the ITCZ, rainfall during this season is generally associated with large water bodies whose land/sea breeze may not be represented effectively by twice daily NOAA polar orbiting satellite measurements. The other dominant regional systems during this season are the East African low level jetstream (along the coast) (Findlator, 1968) and Congo/Zaire airmass over Western Kenya (EAMD, 1962; Trewartha, 1961; Henderson, 1949). The convergence in the southerly winds course substantial rainfall over the coastal areas during this season (EAMD, 1962).

During December-February season, most parts of the country are dry. Only areas near Lake Victoria and the Indian Ocean receive substantial rainfall. Correlation values observed over the relatively wet areas were generally small for both point and areally averaged records. The
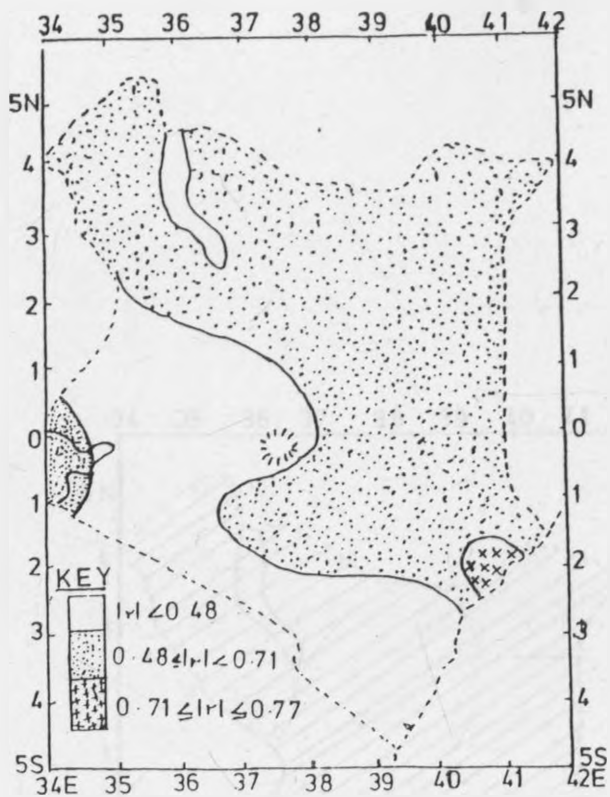
Figure 20a: Correlations between point OLR and rainfall during April.
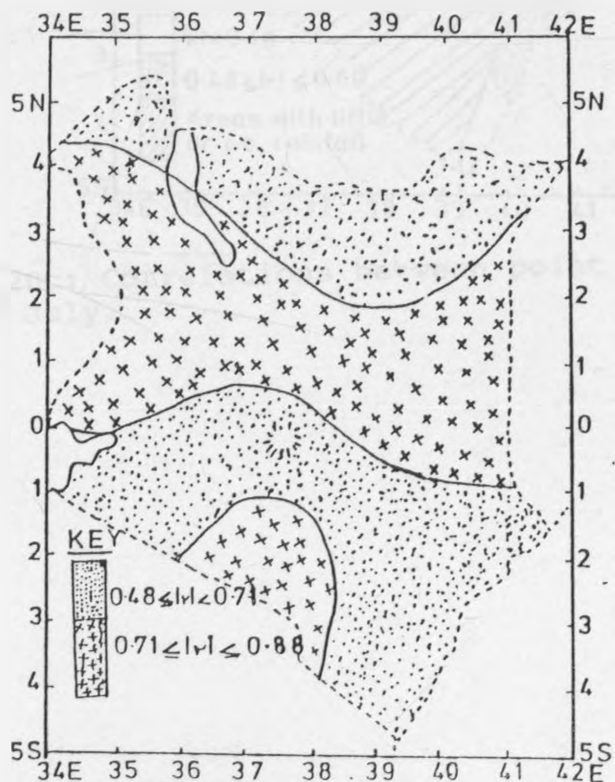


Figure 20b: Correlations between point OLR and rainfall during November.
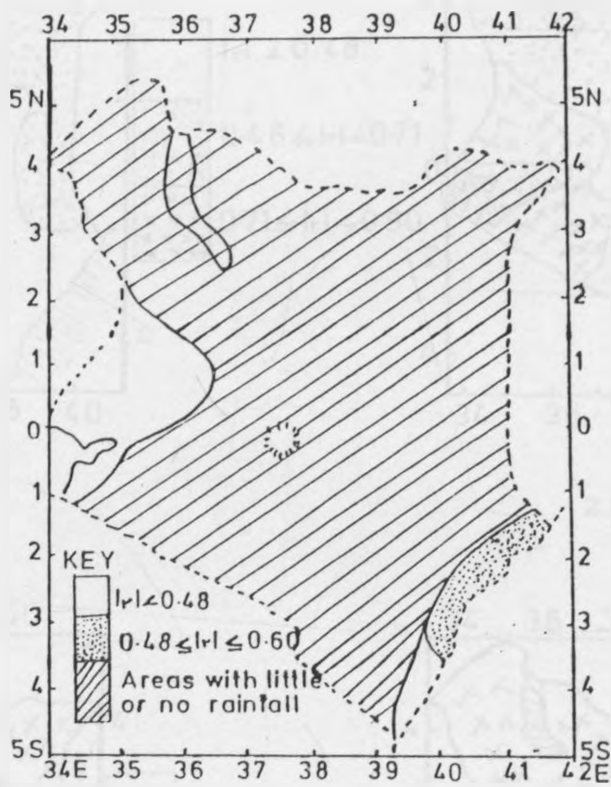
Figure 20c: Correlations between point OLR and rainfall during: July.
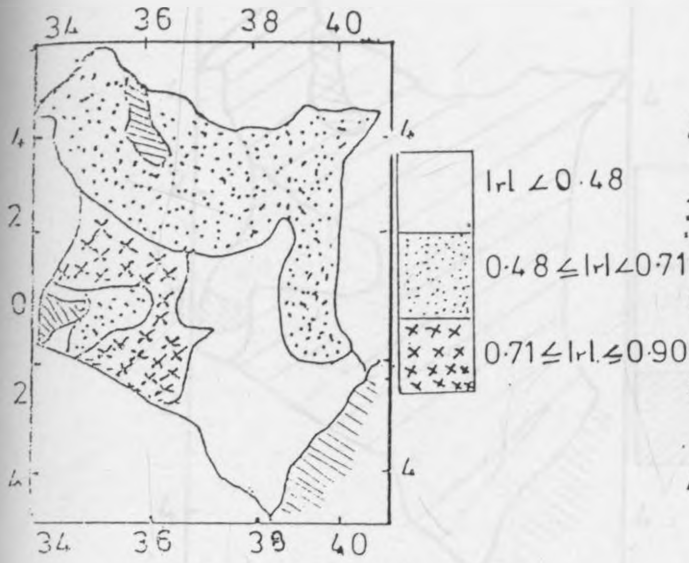
21a:
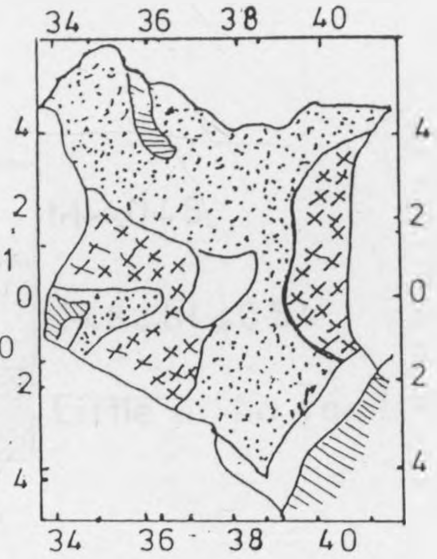
21b:
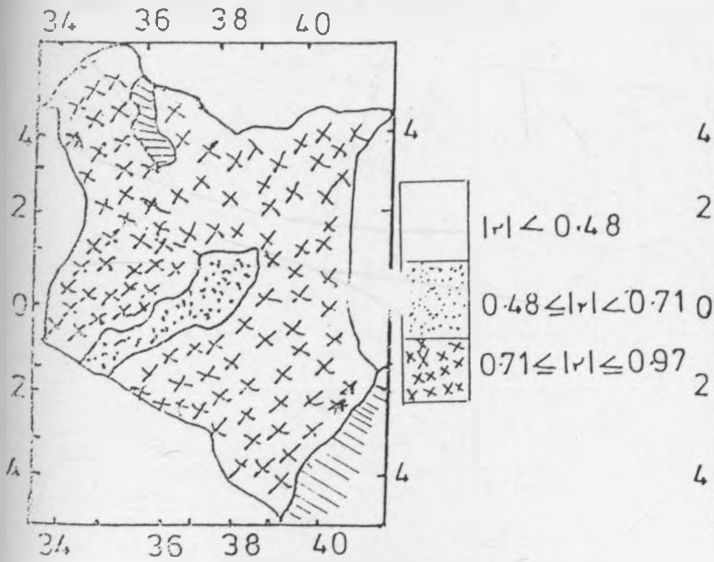


22a:

22b:

Figure 21: Correlations between regional areal rainfall during April and OLR at: (21a) grid point 3 (21b) grid point 4.

Figure 22:Correlations between regional areal rainfall during November and OLR at (22a) grid point 3 (21b) grid point 4.
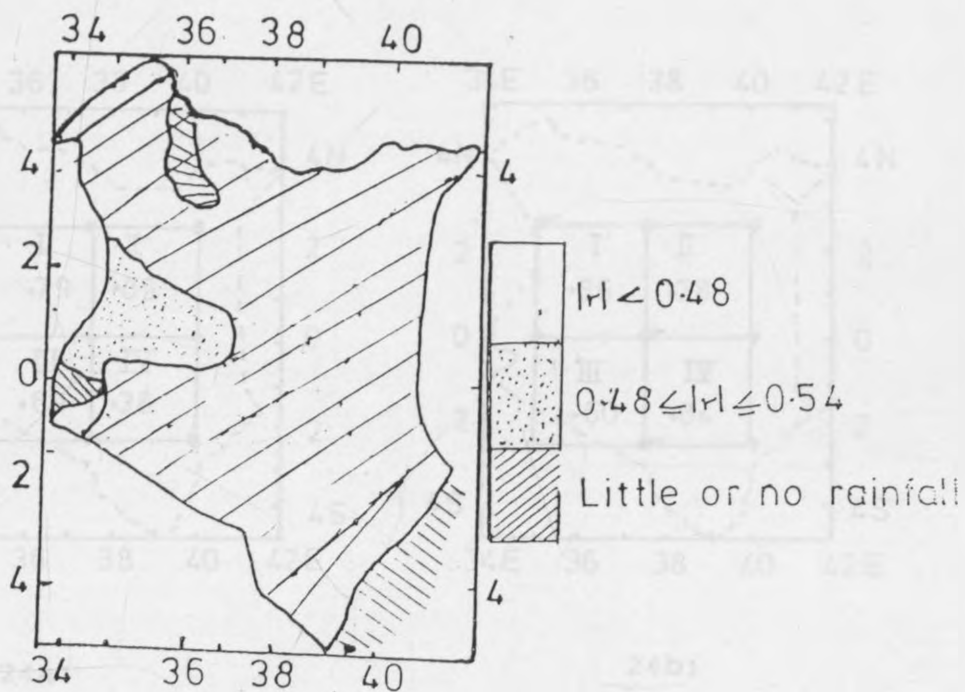
Figure 23: Correlation between regional areal rainfall during July and OLR at grid point 13.
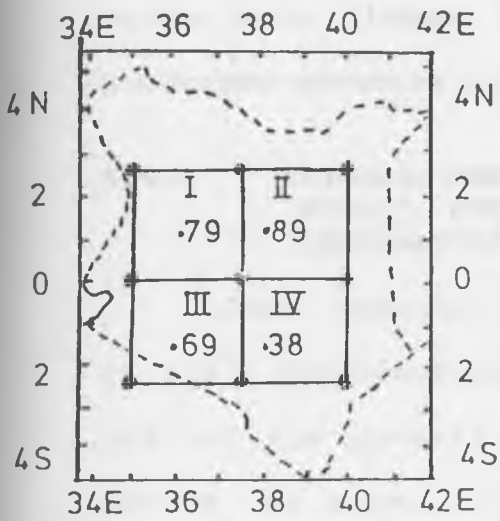
24a:
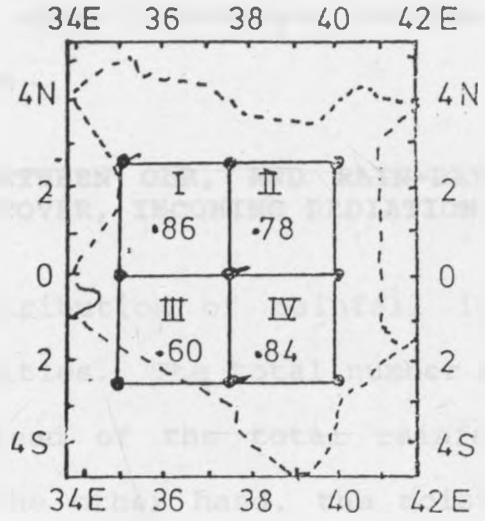


24b:
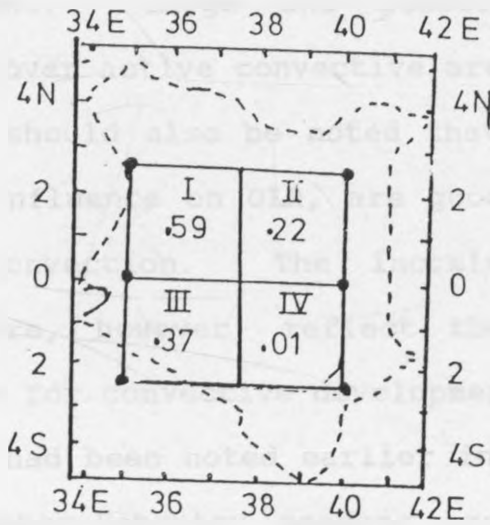


24c:

Figure 24: Correlations between 2.5° x 2.5°latitude/Longitude
square areal OLR and rainfall records during (24a) April,
(24b) November (24c) July.

largest correlation values were observed in the coastal areas.

It may be concluded from these results that correlations between OLR and rainfall were statistically significant in some seasons and locations. The correlation values were highest for areally averaged records and during September-November season.

**3.5.2    CORRELATIONS BETWEEN OLR, AND RAIN-DAYS, MOISTURE BUDGET, CLOUD COVER, INCOMING RADIATION AND SURFACE TEMPERATURE**

Good temporal distribution of rainfall is vital for rainfall dependent activities. The total number of rain-days reflect the general spread of the total rainfall received during the month. On the other hand, the moisture budget, expressed as the difference between rainfall and evaporation, gives an indication of the moisture available for convective development. Large and positive moisture budgets are expected over active convective areas (Morrissey, 1986).

It should also be noted that the clouds, which have a maximum influence on OLR, are good indicators of centres of active convection. The incoming radiation and surface temperature, however, reflect the amount of solar energy available for convective developments.

It had been noted earlier in the text that June-August and December-February seasons are generally dry over most parts of Kenya except for areas near large water bodies. More emphasis will, therefore, be put on the relationships during the major rainfall seasons, March-May and September-November.

The results from t-test indicated that correlation values $\geq 0.48$ were statistically significant. Figures 25 -29 give the spatial patterns of correlations between OLR, and rain-days, moisture budget, cloud cover, incoming radiation and surface temperature, respectively, during the various seasons.

It is evident from figure 25a that the values of correlations obtained with the number of rain-days during long-rainy season, which was represented by the peak rainfall month of April, were generally small especially over the highly convective western parts and coastal areas which normally have large numbers of rain-days. These areas have strong diurnal cycle in convection which may not be effectively represented by twice daily OLR satellite observations. The local satellite crossing times (which have varied between 2.00 and 9.00 am/pm for morning/ afternoon observations respectively (Janowiak et. al, 1985)) may not be able to represent accurately the strong diurnal cycle in convection over these areas. Significant correlations were, however, observed over most of the dry areas.

During short-rainy season, whose rainfall is centred around the month of November, significant correlations were observed over most parts of the country (figure 25b). The largest correlation values were observed over the western parts. The largest correlation values of 0.84 and 0.89 were observed at Dagorretti and Kitale for long-and short-rainy seasons, respectively.

Correlations between OLR and moisture budget records are given in figure 26 for the two major rainfall seasons.

The relatively small correlation values over the highly convective western parts during long-rainy season are quite evident from figure 26a. Relatively small correlation values were also observed over the coastal area. Large correlation values were again centred over the relatively dry areas where moisture availability and large-scale convergence are dependent on the convergence of South easterly and north easterly monsoonal wind systems associated with the regional location of the ITCZ. It should also be noted that clouds over dry areas have stronger longlived updrafts which lead to higher maximum rain rates and steeper drops in brightness temperatures than in moist areas (Simpson et al., 1988).

Over the western and coastal areas, sea lake/land breeze, Katabatic/Anabatic winds, westerly incursions of moist air from the Atlantic and Congo/Zaire basin and other thermally induced meso-scale systems interact to produce strong but complex spatial and temporal variations in regional convective patterns. Such complex variations and the associated strong diurnal cycle in convection may not be effectively represented by twice daily NOAA polar orbiting satellite observations. It can, however, be seen from figure 26b that relatively large correlation values were observed at most locations during the short-rainy season as in the case of the number of rain-days. The largest correlation value of 0.89 was observed at Voi during the short-rainy season.

Figure 27 gives the spatial patterns of correlations obtained with cloud cover during the various seasons. The figure shows that the correlation values were still generally small especially over the highly convective western parts and coastal areas during all the seasons. Relatively large correlation values were again observed over the relatively dry areas. The largest correlation value of 0.84 was observed at Narok during short-rainy season (figure 27b). The small correlation values over the western and coastal areas may be attributed to the limitations of polar orbiting satellite observations to effectively represent the strong diurnal cycles in convection over these areas.

The spatial patterns of the correlations obtained with the incoming radiation during various seasons are given in figure 28. The patterns are generally similar to those which were obtained with the previous variables. The western parts and coastal areas are still having relatively small correlation values. These areas are frequented with cloudness which greatly influence the incoming radiation (Trewartha, 1968).

Figure 29 gives the spatial patterns of correlations obtained with the surface temperature during March-May and September-November seasons. The figure shows that the values of correlations were small at most locations. The largest correlation value of 0.72 was observed at KARI Muguga during the long-rainy season (figure 29a). All the correlation values during June-August and December-February seasons were insignificant.
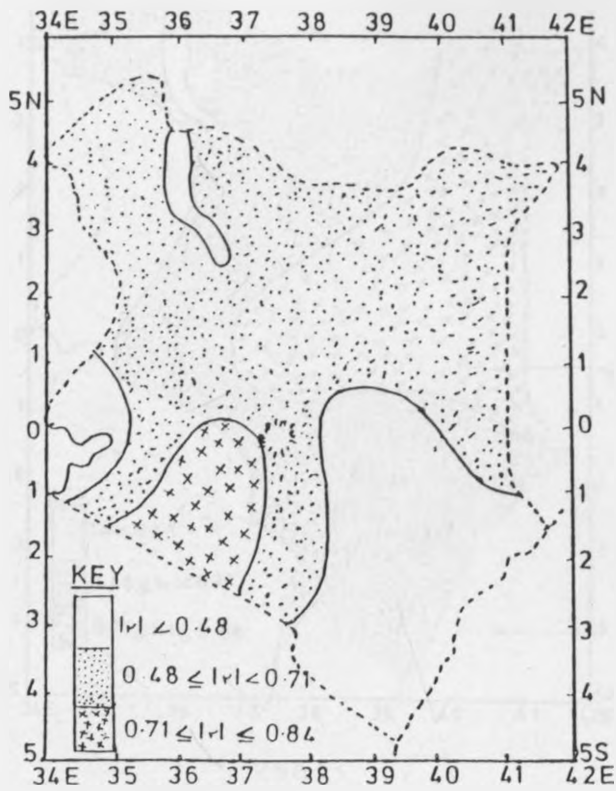
25a:
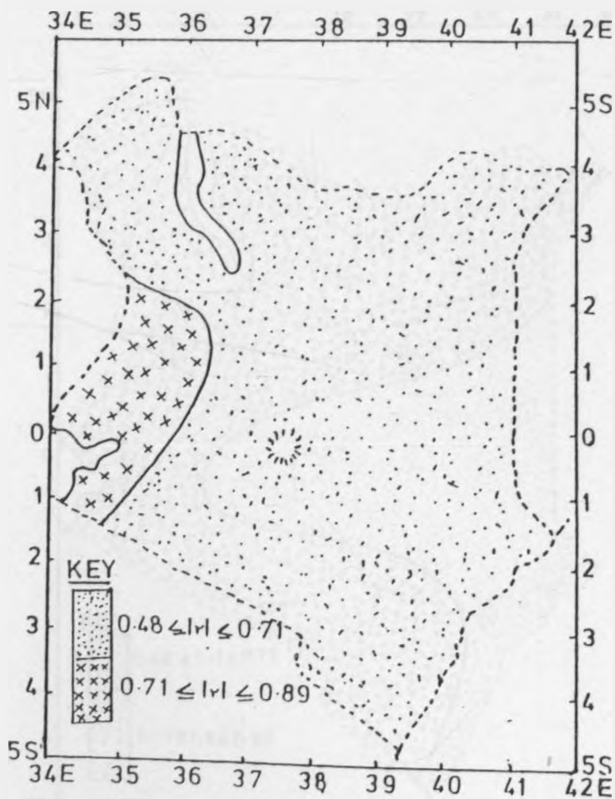


25b:

Figure 25: Correlations between point-OLR and raindays during (25a,) April (25b,) November.
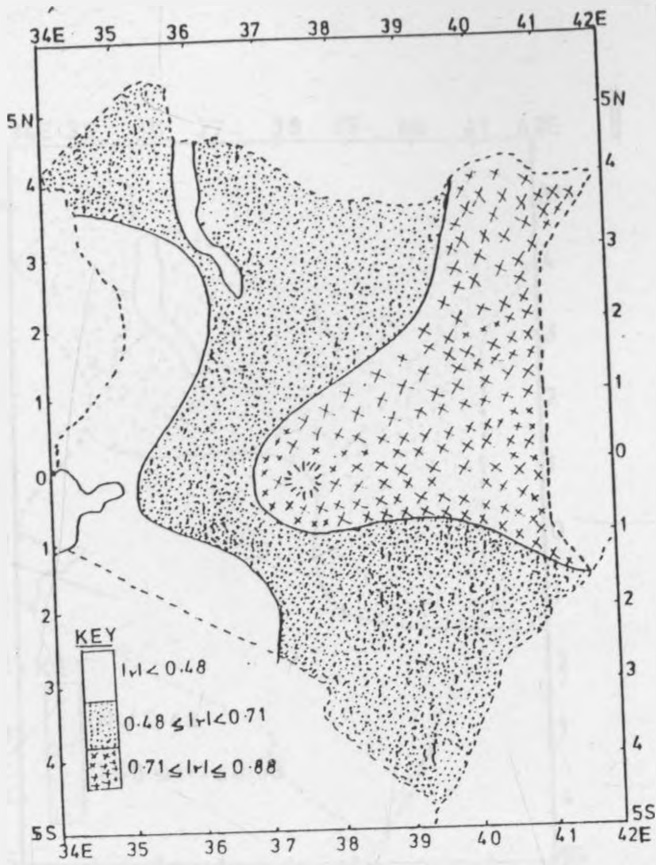
26a:
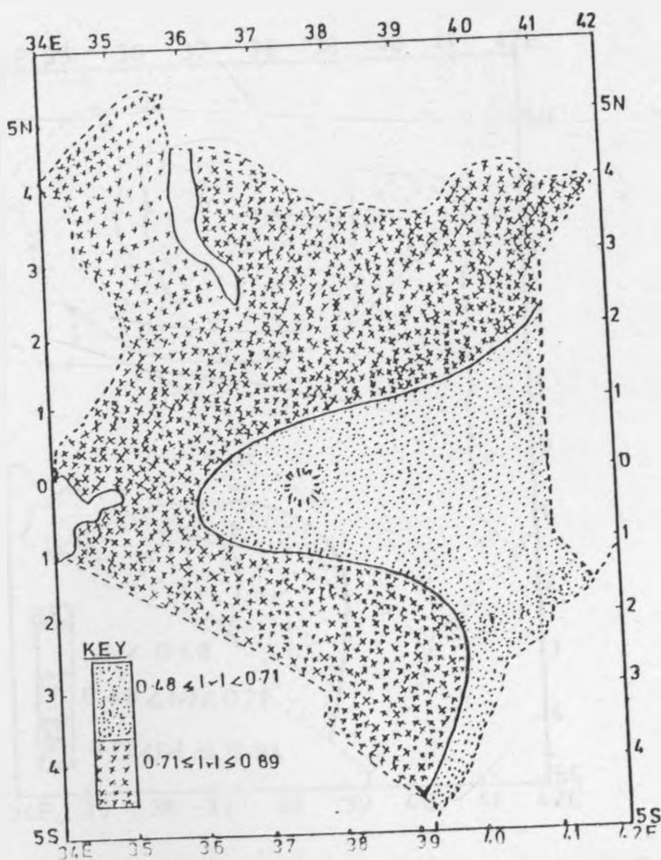


26b:

Figure 26: Correlations between point OLR and moisture budget during (26a) April (26b) November.
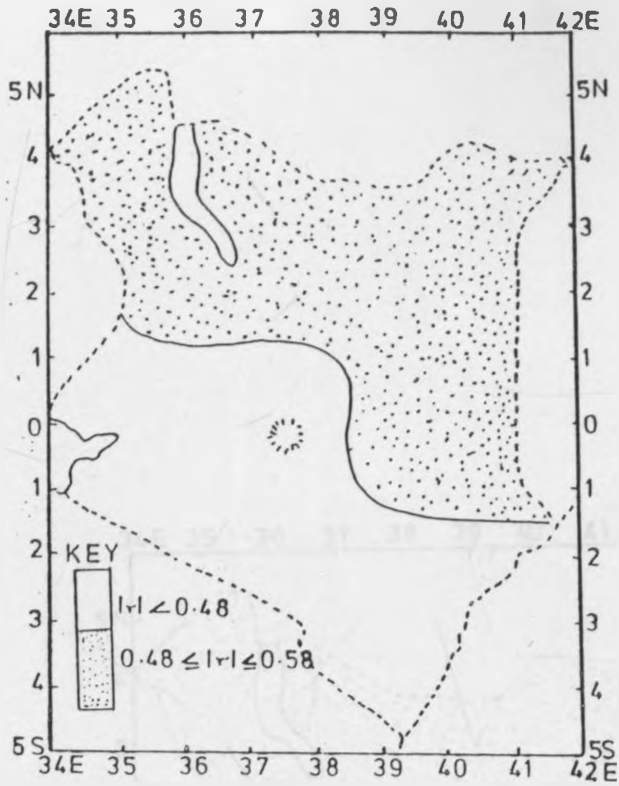
Figure 27a: Correlations between point OLR and cloud cover during April.
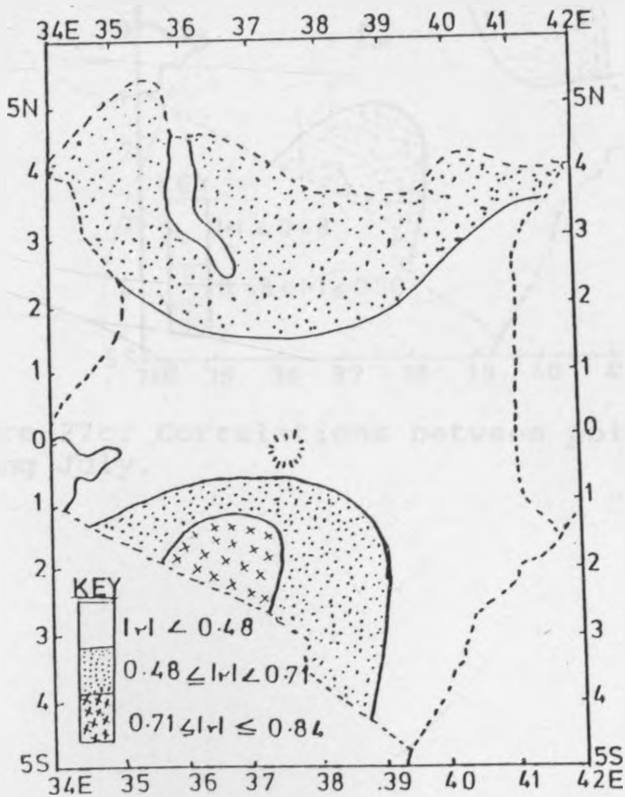


Figure 27b: Correlations between point OLR and cloud cover during November.
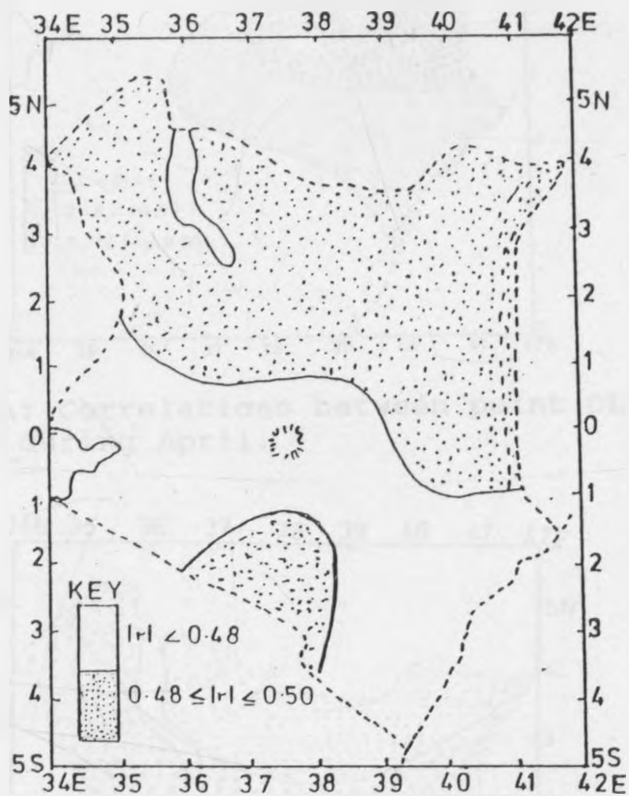
Figure 27c: Correlations between point OLR and cloud cover
during July.
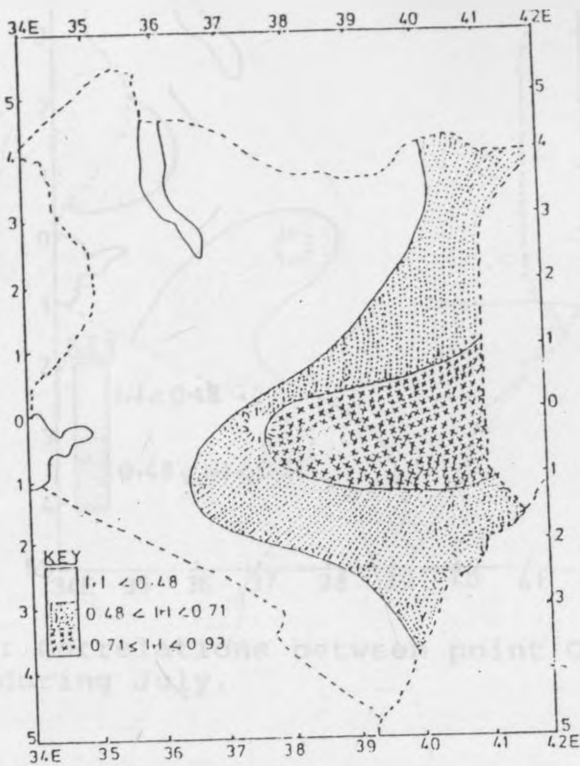
Figure 28a: Correlations between point OLR and the incoming
radiation during April.
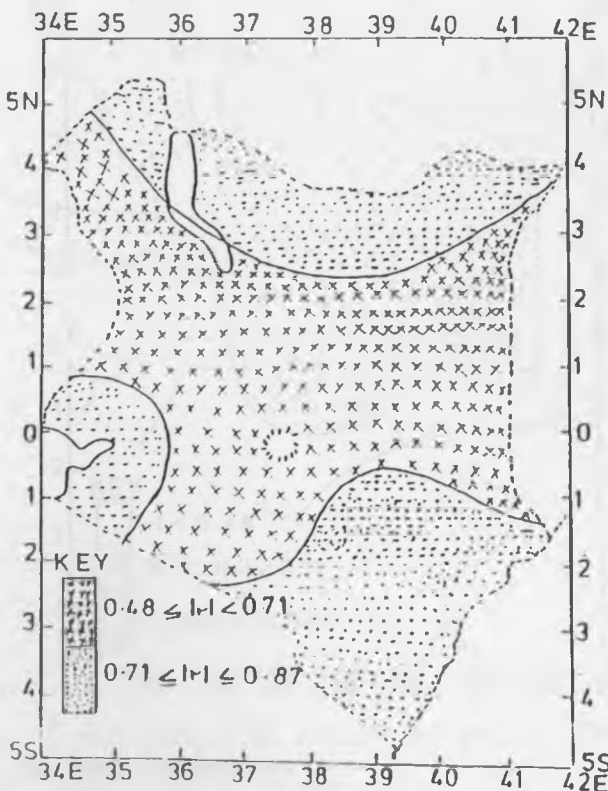


Figure 28b: Correlations between point OLR and the incoming
radiation during November.
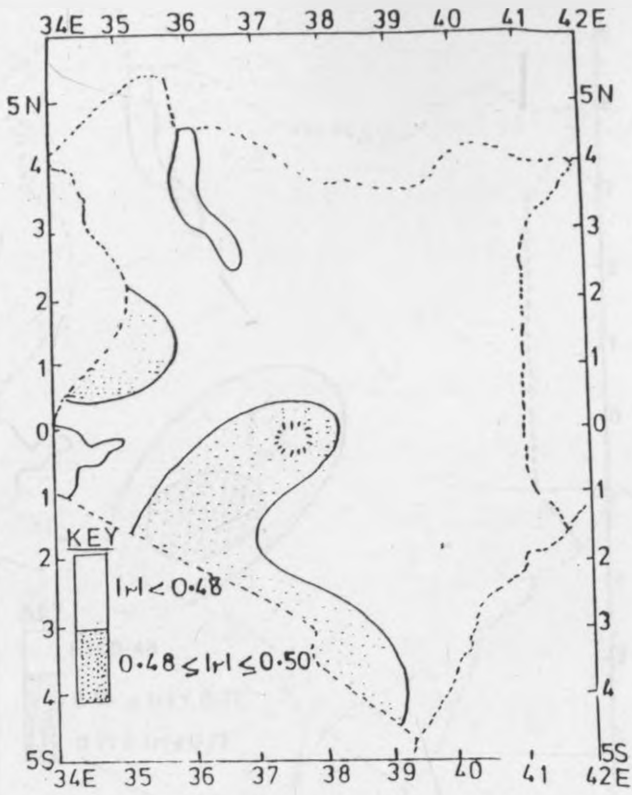
Figure 28c: Correlations between point OLR and the incoming radiation during July.
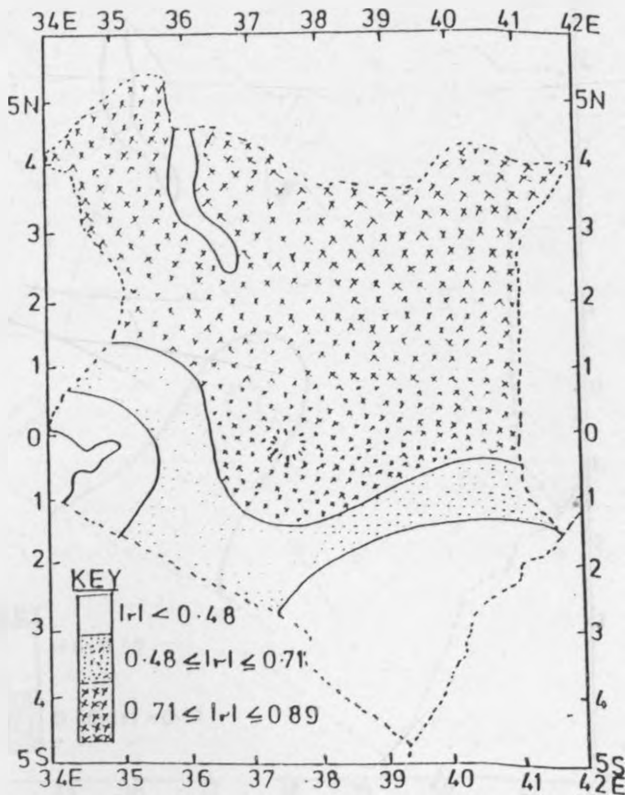


Figure 28d: Correlations between point OLR and the incoming radiation during January.
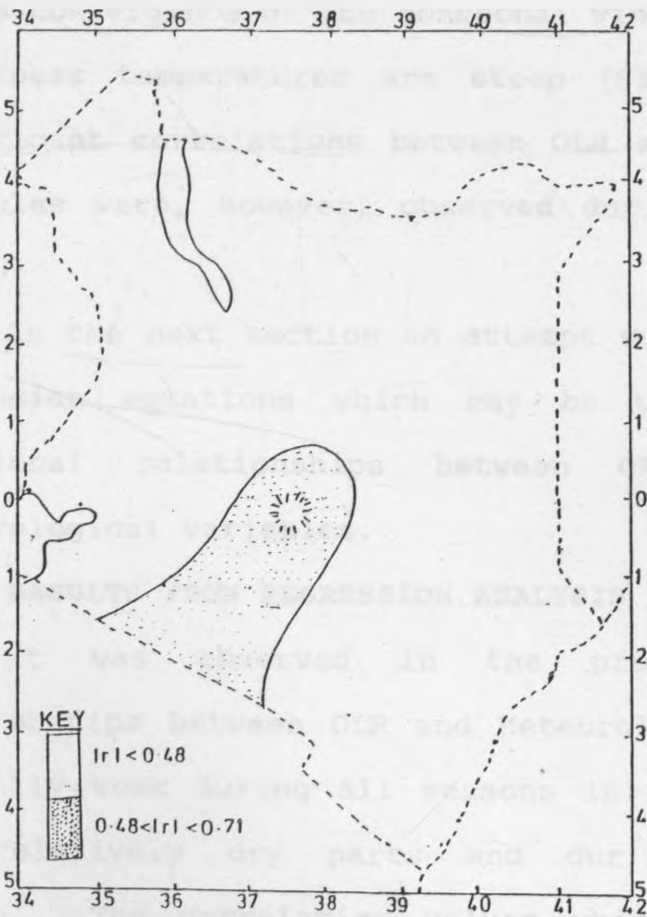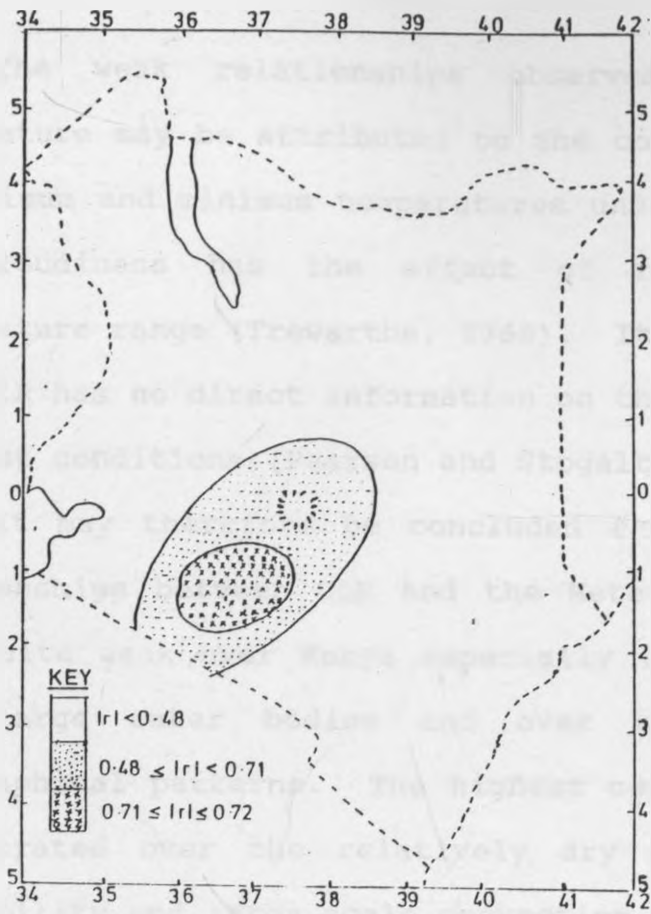
Figure 29: Correlations between point OLR and surface temperature during (29a) April (29b) November.

The weak relationships observed with the surface temperature may be attributed to the complex characteristics of maximum and minimum temperatures under cloudy conditions. The cloudiness has the effect of reducing the diurnal temperature range (Trewartha, 1968). It should also be noted that OLR has no direct information on the earth surface under overcast conditions (Pearson and Stogaitis, 1989).

It may therefore be concluded from this section that relationships between OLR and the Meteorological parameters were quite weak over Kenya especially in the western parts, near large water bodies and over regions with complex topographical patterns. The highest correlation values were concentrated over the relatively dry parts where moisture availability and large scale convection are totally dependent on the convergence of the monsoonal winds, and drops in cloud brightness temperatures are steep (Simpson et al., 1988). Significant correlations between OLR and the Meteorological variables were, however, observed during September-November season.

In the next section an attempt will be made to develop regression equations which may be used to describe the functional relationships between OLR and the various Meteorological variables.

## 3.6 RESULTS FROM REGRESSION ANALYSIS

It was observed in the previous sections that relationships between OLR and Meteorological variables were generally weak during all seasons in most areas apart from the relatively dry parts and during September-November season. The correlation values which were observed over

western and coastal areas during long-rainy season were less than 0.48. This indicates that OLR accounted for less than 25% of the variance of most of the meteorological variables used in the study. It was further observed that the correlation values were generally larger when areal records were used. The regression equations discussed in this study will, therefore, be limited to seasons which had significant correlation values between OLR and meteorological variables.

The regression equations obtained with the various meteorological variables are given in tables 6 and 7. It can be seen that the constants (a) had confidence levels above 95% in all cases apart from two cases involving the incoming radiation. The results from the analysis of variance (ANOVA) indicated that all values of the slopes (b) were significant above 95% confidence levels. The tables also show that only the incoming radiation, which is positively correlated to OLR, had positive slopes.

Table 6:   Regression Equations obtained with Rainfall during
various seasons

| SEASON | Averaging Area | Constant (a)+ve | | Slope (b) -ve | | VR |
|---|---|---|---|---|---|---|
| | | VALUE | C.L | VALUE | C.L | % |
| SEPTEMBER- | REGION | | | | | |
| NOVEMBER | 1 | 515 | >99 | 1.85 | >99 | 53 |
| | 2 | 1126 | >99 | 4.09 | >99 | 74 |
| | 3 | 2018 | >99 | 7.29 | >99 | 81 |
| | 4 | 1588 | >99 | 5.81 | >99 | 74 |
| | 5 | 1740 | >99 | 6.33 | >99 | 76 |
| | 6 | 920 | >99 | 3.21 | >99 | 66 |
| | 7 | 1870 | >99 | 6.20 | >99 | 42 |
| | 8 | 2087 | >99 | 7.28 | >99 | 94 |
| | 9 | 1733 | >99 | 6.30 | >99 | 77 |
| | 10 | 1107 | >99 | 4.01 | >99 | 79 |
| | 11 | 1024 | >99 | 3.90 | >99 | 71 |
| | 12 | 1132 | >99 | 3.97 | >99 | 83 |
| | SQUARE | | | | | |
| | I | 1129 | >99 | 4.18 | >99 | 74 |
| | II | 1272 | >99 | 4.56 | >99 | 61 |
| | IV | 1574 | >99 | 5.83 | >99 | 71 |
| MARCH-MAY | REGION | | | | | |
| | 1 | 789 | >99 | 2.97 | >95 | 36 |
| | 2 | 1102 | >99 | 4.15 | >99 | 81 |
| | 4 | 780 | >99 | 2.20 | >95 | 55 |
| | 5 | 789 | >99 | 2.77 | >99 | 49 |
| | 6 | 751 | >99 | 2.56 | >99 | 61 |
| | 8 | 1210 | >99 | 4.10 | >99 | 59 |
| | 9 | 1304 | >99 | 4.78 | >99 | 61 |
| | 10 | 657 | >99 | 2.43 | >99 | 67 |
| | SQUARE | | | | | |
| | I | 749 | >99 | 2.61 | >99 | 62 |
| | II | 827 | >99 | 2.91 | >99 | 79 |
| | III | 1220 | >99 | 4.52 | >99 | 48 |
| JUNE-AUGUST | REGION | | | | | |
| | 3 | 271 | >99 | 0.92 | >99 | 49 |
| | SQUARE | | | | | |
| | I | 975 | >99 | 5.53 | >95 | 35 |

Key:  C.L : - Confidence level

   V R : - Maximum variance which can be explained

      by the regression equation

Table 7 : Regression Equations obtained with the other
Meteorological variables.

| SEASON | STATION | VARIABLE | CONSTANT (a) | | COEFFICIENT(b) | | VR |
|---|---|---|---|---|---|---|---|
| | | | VALUE | C.L | VALUE | C.L | % |
| SEPTEMBER- | 9037016 | RN | 91.5 | >99 | -0.30 | 98 | 38 |
| NOVEMBER | 9136158 | RN | 66.6 | >99 | -0.23 | 98 | 42 |
| | 8935181 | RN | 102.0 | >99 | -0.39 | 98 | 46 |
| | 8739000 | RN | 58.1 | >99 | -0.20 | >99 | 44 |
| | 8834098 | RN | 84.3 | >99 | -0.32 | >99 | 79 |
| | 9034025 | MB | 1369 | >99 | -6.08 | >99 | 52 |
| | 9135001 | MB | 935 | >99 | -4.34 | >99 | 55 |
| | 9237000 | MB | 3129 | >99 | -12.5 | >99 | 69 |
| | 9338001 | MB | 1901 | >99 | -7.84 | >99 | 79 |
| | 8840000 | MB | 1475 | >99 | -6.07 | >99 | 77 |
| | 9338001 | CC | 13.1 | >99 | -0.03 | 98 | 44 |
| | 8737000 | CC | 19.2 | >99 | -0.05 | >99 | 48 |
| | 9135001 | CC | 19.2 | >99 | -0.06 | >99 | 71 |
| | 9136164 | RD | -255 | 90 | +2.80 | >99 | 53 |
| | 9135001 | RD | -620 | 95 | +4.43 | >99 | 66 |
| | 8937065 | RD | -470 | 90 | 3.59 | >97 | 50 |
| MARCH-MAY | 9136158 | RN | 55.5 | >99 | -0.18 | >99 | 53 |
| | 9136164 | RN | 71.1 | >99 | -0.26 | >99 | 71 |
| | 9237000 | RN | 62.2 | >99 | -0.22 | >99 | 45 |
| | 9137000 | RN | 93.5 | >99 | -0.32 | >99 | 67 |
| | 9035279 | MB | 699 | >99 | -2.98 | >99 | 49 |
| | 8937000 | MB | 1358 | >99 | -5.98 | >99 | 53 |
| | 9237000 | MB | 1144 | 98 | -4.98 | 98 | 42 |
| | 9338001 | MB | 687 | 98 | -3.30 | 98 | 45 |
| | 8840000 | MB | 1345 | >99 | -6.03 | >99 | 59 |
| | 9136164 | RD | -163 | 75 | +2.54 | 98 | 44 |
| | 8937065 | RD | -797 | >99 | +5.28 | >99 | 86 |
| DEC-FEB. | 8937065 | RD | -1131 | >99.5 | +6.81 | >99 | 79 |
| | 8639000 | RD | -633 | 95.0 | +3.96 | >99 | 64 |

KEY:

RN: Rain - Days, MB:- Moisture  Budget, CC: Cloud Cover

RD: Incoming radiation

CL: Confidence level

VR: Maximum variance which can be explained by the
regression equation.

Table 6 further shows that during the short-rainy season OLR regression equations accounted for more than 60% of rainfall variance at all locations with exceptions of regions 1 and 7.   It was observed in the previous section that correlations value for regions 1 and 7 were approximately 0.73 and 0.65, respectively.   The maximum variance accounted for by the regression equations during this season was 94%.  It is also evident from table 6 that in general OLR based regression equations accounted for relatively low percentage of rainfall variance during the long-rainy season.

The correlation coefficients for the dry seasons of June-August and December-February were generally not significant.  No regression equations were derived for these dry seasons.

Table 7 shows that the maximum variance of the meteorological variables were again accounted for by the regression equations during September-November season.  In general, however, the regression equations accounted for lower proportions of the variance for most of the meteorological variables. The relationships between OLR and

these meteorological variables were even poorer during June-August, March-May and December-February seasons. The incoming radiation, however, had significant relationships with OLR during the dry December-February season. This may be explained in terms of close relationships between OLR and the incoming radiation in clear sky conditions.

It may be concluded from the result from this section that useful estimates of meteorological variables can be derived from OLR records, especially for rainfall over certain locations and seasons. OLR, however, accounted for between 50 and 79% of rainfall variance in most cases. The highest variance of the meteorological variables was explained during September-November season.

## 3.7  SUMMARY AND CONCLUSIONS

The objective of this study was to determine relationships between OLR and several meteorological parameters using correlation and regression analyses. PCA was further used to study the spatial and temporal characteristics of OLR and rainfall.

It is evident from the results of the study that significant correlations existed between OLR and the various meteorological variables. Weak correlations were, however, observed between point records especially over areas with complex orographic patterns, Lake Victoria and coastal regions. Improvement on correlation values were observed when areal records were used.

The largest correlation values which were obtained with point and areal rainfall records were 0.88 and 0.97

respectively. Similarly the largest correlation values which were observed between OLR, and rain-days, moisture budget, cloud cover, incoming radiation and surface temperature were 0.89, 0.89, 0.84, 0.93 and 0.72 respectively. The surface temperature had the weakest correlations at all stations and seasons.

In general, the OLR had the best relationship with all meteorological variables during September-November season.

The patterns of mean OLR values indicated large spatial and temporal fluctuations similar to those of centres of active convection. In most seasons the 240 $WM^{-2}$ OLR isoline generally corresponded to the monthly total rainfall of 50mm. The maximum OLR values were, however, concentrated over the relatively dry areas while the lowest OLR values were concentrated over the highly convective regions.

The results from PCA revealed some similarities in the spatial and temporal characteristics of OLR and rainfall. Three (3) and six (6) spatial modes were dominant in the intermonthly OLR and rainfall records throughout the year, respectively. The three dominant OLR RPC modes accounted for about 89% of OLR variance over East Africa while the six rainfall RPC modes accounted for only 75% of rainfall variance over Kenya. This difference may be an indication of the complex nature of the spatial rainfall characteristics. The PCA results also revealed that some RPC modes were unique for some seasons and regions.

The maximum number of significant seasonal OLR RPC modes, based on Kaiser's criterion were three, four, six and four for the March-May, September-November, June-August and

December-February seasons respectively. The significant RPC modes accounted for over 86% of seasonal OLR variance in all seasons.

Similarly, the maximum number of significant seasonal rainfall RPC modes were seven, six, eleven and eight which accounted for over 80% of seasonal rainfall variance during the respective seasons. The seasons with the best and worst spatial coherence in both rainfall and OLR patterns were September-November and June-August seasons respectively.

Results from regression analysis indicated that useful estimates of meteorological variables can be derived from OLR records, especially rainfall over certain locations and seasons. OLR, however, accounted for between 50 and 79% of rainfall variance in most cases. The highest variance for the meteorological variables were explained during September-November season.

Data availability is one of the major problems in the region. The results from this study provide relationships between OLR and various meteorological variables which may be used to derive useful meteorological information from OLR in the absence of the standard meteorological observations.

## 3.8  SUGGESTIONS FOR FUTURE WORK

The mean OLR maps presented in this study were based on only thirteen (13) years of OLR records. WMO requires all climatological statistics to be based on at least 30 years of continuous records. One of the major future task is to determine whether the statistics obtained with the currently

available data will be the same when the long period records become available in future.

While March-May and September-November are the major rainfall seasons of the region, PCA, correlation and regression analyses revealed that OLR and meteorological variables have the best relationships with the synoptic systems during September-November season. The differences in the patterns of the relationships between OLR and the meteorological variables during the two seasons need further investigation.

The OLR data used in this study was obtained from polar orbiting satellite, which observe a point only twice daily. These may have limitations especially regarding temporal resolutions. The performance of the methods which use data from geosynchronous satellites should be investigated.

It is well known that there is some timelag between the observed strong convections and the raingauge records. The use of continuous hourly records could also enable lagged relationships between OLR and rainfall to be determined.

The single parameter models, like the ones derived in this study, may not be able to incorporate all the characteristics of the meteorological variables. The performance of the methods which utilize satellite data from more than one channel (multispectral) needs some investigation. The skills of the methods which use microwave radiation data may also be investigated.

It should, however, be noted that despite the simplicity of the method used in this study, which considered

only the OLR as the predictor, the results obtained seem to
be very reasonable.

## ACKOWLEDGEMENTS

I would like to extend my gratitude to my supervisors , Professor L.J. Ogallo and Dr. E.K. Anyamba, for their guidance and encouragement throughout this study.  I also wish to thank the Kenya Meteorological Department and WMO-Drought Monitoring Centre (DMC), Nairobi for availing the data used in this study and for allowing me to use their Computer facilities.

My words of appreciation go to my wife, Anjeline Achieng, for her patience throughout the course of this study.

Finally, I would like to thank Miss Tabitha Wakarira Gilbert for typing the manuscript.

**REFERENCES**

Abel, P. and A. Gruber (1979): An improved model for the calculation of longwave flux at 11 $\mu$m. NOAA Technical report NESS 106, 24 pp.

Anyamba. E.K. (1984): On the monthly mean lower tropospheric circulation during 1961/62 floods in East Africa. MSc. Thesis, Dept of Meteor., University of Nairobi, Kenya.

Arkin P.A.(1979): The relationship between fractional coverage of high clouds and rainfall accumulations during GATE over the B-scale Array. Mon.Wea. Rev. 107, 1382-1389.

Arkin, P.A. and Meisner, B.N. (1987): Relationships between large - scale convective rainfall and cold cloud cover over western hemisphere during 1982 - 1984. Mon. Wea. Rev. 115, 51-74.

Arkin, P.A., A.V.R Krishna Rao and R.R Kelkar (1988): Large scale precipitation and outgoing longwave radiation from INSAT -1B during 1986 southwest monsoon season. Journ. Climate 2, 619-628.

Asnani, G.C. (1982): The climate of Africa including feasibility study of climate alert system - Africa Proc. Techn. Conf. on climate - Africa, 25-30 Jan 1982, Arusha, United Republic of Tanzania pp. 107-129.

Asnani G. C. and Kinuthia J.H. (1979): Diurnal variation of precipitation in East Africa. KMD, Res. Rept. 8/79.

Barnston, A.G. and R.E. Livezy (1987): Classification, seasonality and persistence of low frequency circulation patterns. Mon. Wea. Rev. 115, 1083-1126.

Barret. E.C. and Power. C.H. (1986): Satellite cloud and rainfall assessment in Western Sahel. Proc. Twelfth symp. on remomte sensing of environment 4-10 Dec. 1986, Nairobi, Kenya.

Barret T, C.E. G. D'Sousa and C.H. Power (1986): Comparison of two Meteosat based satellite rainfall Monitoring Techniques applied to part of the western sahel. Report of the proc. 6th Meteosat Scientific users meeting, Amsterdam, Netherlands, 25-27 November, 1986 Vol. II.

Barring, L. (1987): spatial patterns of daily rainfall in Central Kenya. Application of Principal Component analysis, common factor analysis and spatial correlations. Journ. Climatology Vol. 7, 267-289.

Basalirwa, C.P.K (1979): Estimation of areal rainfall in some catchments of upper Tana River. MSc. Thesis, Dept. of Meteorology, University of Nairobi, Kenya.

Battacharyaa, G.K. and A.J. Johnson (1977): Statistical concepts and Methods. John Willy & Sons, N.Y.

Bess, T.D, G.L. Smith and T.P. Charlock (1989): A ten-year monthly data set of outgoing longwave radiation from Nimbus - 6 and Nimbus - 7 Satellites. Bull. Amer. Meteor. Soc. 70, 480-489.

Brown, L.H. and J. Cocheme' (1973): A study of the agroclimatology of the highlands of East Africa, WMO, Techn. not. No. 125, WMO, Geneva, 197 pp.

Budyko, I.M. (1969): The effect of Solar radiation variations on the Climate of the earth. Tellus, 21, 611 -619.

Catell, R.B. (1966): The scree test for the number of factors. Multivar Behav. Res. 1, 245-276.

Chow, V.T. (1964): Handbook of applied hydrology. Mc Graw-hill book company, N.Y.

Collier, C.G., D.M. Goddard and B.J. Conway (1989): Real time analysis of precipitation using satellites, ground based radars, conventional observations and numerical model output. Meteorological magazine 118, 1-8.

Craddock, J.M. and Flintoff (1970). Eigenvector representation of Northern hemisphere fields. Quart. Journ. Roy. Met. Soc. 96, 124-129.

Craddock, J.M. and C.R. Flood (1969): Eigenvectors representing the 500 mb geopontential surface over the northern hemisphere. Quart. Journ. Roy. Met. Soc. 95,576-593.

Doneaud, A.A., J.R Miller, J.R. L. Johnson, T.H. Vonder Haar and P. Laybe (1987): The area time integral technique to estimate convective rain volumes over areas applied to satellite data. A preliminary investigation. Journ. Clim. & Applied Meteor. 26,156-169.

Dugdale G.G. and J.R. Milford (1985) Rainfall estimation over the Sahel using Meteosat thermal infrared data. <u>Conf. on parameterization of land surface characteristic. ISL Sc P. Rome, Dec. 1985.</u>

-------- (1989): An application of remote sensing in agriculture, <u>Proc. 484 Easter School in Agricultural Science, University of Nottingham, July, 1989, Butherworth, London,</u> 16 pp.

Dyer, T.G.J. (1975): The assignment of rainfall stations into homogeneous groups. An application of Principal Component analysis. <u>Quart. Journ. Roy. Meteor. Soc. 101,</u> 1005-1013.

EAMD, (1962): The climate seasons of East Africa. <u>E.A.M.D. pamphlet No. 8, Nairobi, Kenya,</u> 1962.

Ellingson, R.G. and R.R. Ferraro JR (1983): An examination of a technique for estimating longwave radiation budget from satellite radiance observations. <u>Journ. Clim. Appl. Meteor., 22,</u> 1416-1423.

Findlator, J. (1968), The month to month variation of winds at low level over East Africa. <u>EAMD Techn. Memo. NO. 12,</u> 27 pp.

Flitcroft, I.D., V. Mcdougall, J.R. Milford and G. Dugdale (1986): The calibration and interpretation of METEOSAT based estimates of Sahelian rainfall. <u>Rept. of Proc. 6th METEOSAT Scientific users meeting, Amsterdam, The Netherlands, 25-27 November, 1986, Volume II.</u>

Fremming, D. (1970): Notes on eastely disturbances affecting East Africa 5-7 Sept 1967, <u>EAMD, Techn. Memo. 13,</u> 13 pp.

Fisher, Sir R.A (1958): <u>Statistical methods for research workers, 13th edition,</u> oliver and Boyd, Ediunburgh: Tweedale court, London: 39A Welbeck Street, W.I., 351 pp.

Fritz, S. and J.S. Winston (1962) synoptic use of radiation measurement from satellite TIROS - II: <u>Mon. Wea. Rev. 90,</u> 1-9.

Garcia, O. (1981): A comparison of two Satellite estimates for GATE. <u>Journ. Appl. Meteor. 20,</u> 430-438.

Gregory, S. (1975): On the delimitation of recent climatic situations. <u>Weather 30,</u> 276-287.

Griffith, J.F. (1958): Climatic zones of East Africa. <u>East African Agricult. J., 23,</u> 179-185.

Griffith, G.G, W.L. Woodley, P.G. Grube, D.W. Martin, J.S. Stout, and D.N. Sikdar (1978): Rain estimation from geosynchronous satellite imagery - visible and infrared studies. Mon. Wea. Rev. 106, 1153 - 1171.

Grimmer, M.,(1963): The space filtering of monthly surface temperature anomaly data in terms of patterns using the emperical orthogonal functions. Quart. Journ. Roy. Meteor. Soc. 89, 395-408.

Gruber, A. and J.S. Winston (1978): Earth atmosphere radiative heating based on NOAA scanning radiometer measurement. Bull. Amer. Meteor. Soc 59, 1570-1573.

Gruber, A and A.F Krueger (1984): The status of NOAA outgoing longwave radiation. Bull. Amer. Meteor. Soc. 65, 958-962.

Harman, H.H. (1967): Modern Factor Analysis. Chicago Univ. Press, 469 pp.

Hartmann, D.L. and D.D. short (1980): On the use of Earth radiation budget statistics for studies of cloud and climate. Journ. Atmos. Sci. 37, 1233-1250.

Hartmann, D.L., and E.E. Recker (1986) Diurnal variations of outgoing longwave radiation in the tropics. Journ. Clim. Appl. Meteor. 25, 800-812.

Heddinguaus T.R. and A.F. Krueger (1981): Annual and interannual variations in outgoing longwave radiation over the tropics. Mon. Wea. Rev. 109, 1208-1218.

Henderson, J.P. (1949): Some aspects of climate in Uganda. EAMD Memo.II. No.5 (1949).

Heinman, P.H., J.D. Martsolf, J.F. Gerber and D. Smith (1987): Combination of manually digitized radar and GOES IR for real-time display of rainfall intensity, Journ. Clim. Appl. Meteor. 26, 1046-1049.

Houghton, J.T. (1979): The future role of observations from Satellites. Quart. Journ. Roy. Met Soc. 105, 1-24.

Hudlow, M. (1979): Mean rainfall pattern for the three phase of GATE. Journ. Appl. Meteor. 18, 1656- 1669.

Janowiak, J.E. (1988): An investigation of interannual rainfall variability in Africa, Journ. Climate 1, 240-255.

Janowiak, J.E, A.F. Krueger and P.A. Arkin (1985): Atlas of outgoing longwave radiation derived from NOAA Satellite data. <u>NOAA No. 6 (1985)</u>, 44 pp.

Johnson, D.M. (1980): An index of Harizona Summer developed through eigenvector analysis. <u>Journ. Appl. Meteor. 19</u>, 849-856.

Johnson, D.H. and H.T. Morth (1960): Tropical Meteorology in Africa. <u>Proc. MUNITALP-WMO joint symposium on tropical Meteorology in Africa</u>, MUNITALP.

Kaiser, H.F.(1959): Computer programme for varimax rotation in factor analysis. <u>Educ. Psychol. Meas. 19</u>, 413-420.

Kaiser, H.F. (1960): The application of electronic computers to factor analysis. <u>Educ. and Psycol. Meas. 20</u>,141-151.

Kasahara, A, A.P. Mizzi, and U.C. Mohanty (1987): Comparison of global diabatic heating rates from FGGE level IIIB analyses with satellite radiation imagery. <u>Mon. Wea. Rev. 115</u>, 2904-2935.

Karl, T.R, A.S. Koscielny and H.F. Diaz (1982): potential errors in the application of principal component (eigenvectors) Analysis to gyophysical data. <u>Journ. App;. Meteor. 21</u>, 1183-1186.

Knutson, T.R., K.M. Wieckmann and J.M. Kutzbach (1986): Global intraseasonal oscillations of outgoing longwave radiation and 250 mb zonal wind during northern hemisphere summer. <u>Mon. Wea. Rev. 114</u>, 605-623.

Kohler, M.A. (1949): On the use of double mass analysis for testing the consistency of Meteorological records and for making required adjustment. <u>Bull. Amer. Met. Soc. 30</u>, 188-189.

Kutzbach, J.E. (1967): Emperical eigenvectors of sea level pressure, surface temperature, and precipitation complexes over North America. <u>Journ. Appl. Meteor. 6</u>, 791-802.

Lau, K. and P.H. Chan (1983): Short term climate variability and atmospheric teleconnections from satellite observed outgoing longwave radiation. Part I. <u>Journ. Atmos. Sci. 40</u>, 2735-2750.

Liebmann, B. and A. Gruber (1988): Annual variation of diurnal cycle of outgoing longwave radiation. <u>Mon. Wea. Rev. 116</u>, 1659-1670.

-------- And D.L. Hartmann (1982): Interannual variation of outgoing IR associated with tropical circulatioon changes during 1974 - 78. Journ. Atmos. Sci. 39, 1153 - 1162.

Linsley, JR. R.K, M.A. Kohler and J.L.H. Paulhus (1949): Applied hydrology. Mc Graw -hill Book Company, N.Y.

Lovejoy, S. and G.L. Austin (1979): The sources of error in rain amount estimating schemes from GOES visible and IR satellite data. Mon. Wea. Rev. 107, 1048-1054.

Lumb, F.E. (1966): Synoptic disturbances causing rainy periods along the East African Coast. Met. magazine 95, 150-159.

Motell, C.E and B.C. Weare (1987): Estimating Tropical Pacific rainfall using digital satellite data. Journ. climate Appl. Meteor. 26, 1436-1446.

Morrissey, M.L. (1986): A statistical analysis of relationships among rainfall, outgoing longwave radiation and the moisture budget during January-March 1979. Mon. Wea. Rev. 114, 931-942.

Mungai, D.N. (1984): Analysis of some seasonal rainfall characteristics in lake Victoria region of Kenya. M.A. Thesis, Department of Geography, University of Nairobi, Kenya.

Murakami, T. (1980): Emperical orthogonal function analysis of satellite - observed outgoing longwave radiation during summer. Mon. Wea. Rev. 108, 205-222.

Negri, A.J. And R.F. Adler (1987a): Infrared and visible satellite rain estimation Part I. A grid cell approach. Journ. Clim. Appl. Meteor. 26, 1553-1564.

---------(1987b): Infrared and visible satellite estimation. Part II. A cloud definition approach. Journ. Clim. Appl. Meteor. 26, 1565-1576.

Nemec, J. (1972): Engineering hydrology. Mc Graw-hill publishing Company, England.

Njau, L.N. (1982): Tropospheric wave disturbances in East Africa. M.Sc Thesis, Department of Meteor. University of Nairobi. Kenya.

North, G.R. (1975): Theory of energy - balance climate model. Journ. Atmos. Sci. 32, 2033-2043.

North, G.R., T.L. Bell and R.E. Cahalan (1982): Sampling errors in the estimation of emperical orthogonal functions. Mon. Wea. Rev. 110, 699-706.

Nyenzi, B.S. (1990): Analysis of the interannual variability of rainfall over East Africa. The second Techn. Conference on Weather Forecasting in East and Southern Africa 3-7 Sept., 1990, Nairobi, Kenya (in press).

Ogallo, L.J. (1980): Time series analysis of rainfall in East Africa, PhD Thesis Dept. Meteor. University of Nairobi, Kenya.

Ogallo L.J. (1981) The nature of homogeneity in rainfall records over East Africa. KMD Res. Rept. NO. 4/81.

Ogallo, L.J. (1986): Stochastic modelling of regional annual rainfall anomalies in East Africa. Journ. Appl. statistics 13, 49-55.

---------(1988): Climatology of rainfall of East Africa. WMO - Tropical Meteorology Research Programme, Rept. NO. 28, pp 136-142.

---------(1989): The spatial and temporal patterns of the East African seasonal rainfall derived from Principal Component Analysis. Intern. Journ. Climatology 9, 145-167.

Ouma, G.O (1988): Estimation of areal rainfall from satellite data. M.Sc. Thesis, Depart. of Meteor., University of Nairobi, Kenya.

Pearson, G.M. and G. Stogaitis (1989) Satellite imagery, interpretation in synoptic and mesoscale Meteorology. Atmospheric Environment service, Canada. 207 pp.

Richards, E. and P. Arkin (1981): On the relationship between satellite observed cloud cover and precipitation. Mon. Wea. Rev. 109,1081-1093.

Richman, M.B. (1981): Obliquely rotated Principal Components and improved Meteorological map typing technique. Journ. Appl. Meteor. 20, 1145-1159.

--------- (1986): Rotation of Principal Components. Journ. Climatology 6, 293-335.

Rinne J., and S.Jarvenoja (1979): Truncation of EOF series representing 500 mb heights. Quart. Journ. Roy. Meteor. Soc. 105, 873-

Rodgers. E. And H. Siddalingaiah (1983): The utilization of Nimbus-7 SMMR measurements to delineate rainfall over land Journ. Clim. Appl. Meteor. 22, 1753-1763.

Salby, M.L. (1989): Climate monitoring from space: Asynoptic sampling considerations. <u>Journ. Climate. 2</u>, 1091-1105.

Shaw, E.M. (1988), <u>Hydrology in practice, 2nd edition</u>, T.J. Press (Padstow) Ltd. Padstow, Cornwall, Britain.

Shin, K. and G.R. North (1988): Sampling error study for rainfall estimate by satellite using a stochastic model. <u>Journ. Appl. Meteor. 27</u>, 1218-1241.

Short, D.A. and J.M. Wallace (1980): Satellite inferred morning to evening cloudiness changes. <u>Mon. Wea. Rev. 108</u>, 1160-1169.

Simpson, J., R. F. Alder, and G.R. North (1988): A proposed Tropical Rainfall ⋅ measuring mission (TRMM) satellite. <u>Bull. Ameri. Meteor. Soc. 69</u>, 278-295.

Slingo, A. R. C. Wilderspin and S. J. Brentnall (1987): Simulation of diurnal cycle of outgoing longwave radiation with an atmospheric GCM. <u>Mon. Wea. Rev. 115</u>, 1451-1457.

Spencer, R.W. (1984): Satellite passive microwave rain rate measurements over croplands during spring, summer and fall. <u>Journ. Clim. Appl. Meteor. 22</u>, 1553-1562.

Stout, J.E., D.W. Martin and D.N. Sikdar (1979): Estimating GATE rainfall with geosynchronous satellite images. <u>Mon. Wea. Rev. 107</u>, 585-598.

Sulakvilidze and Yu.A. Dadali (1965): Multiwavelength radar measurements of precipitation intensity. <u>Proc of 3rd. all union Conf. on radar Meteorology, April 1965, Central Aerological observatory</u>, pp 32-45.

Thiessen, A.H. (1911): Precipitation averages for large areas. <u>Mon. Wea. Rev. 39</u>, 1082-1084.

Thom, H.C.S.(1966): Some methods of climatological analysis. <u>WMO Techn. note. No. 81</u>.

Thompson, B. W. (1957): The diurnal variation of precipitation in British East Africa. <u>EAMD Techn. Memo. NO. 8</u>, 70pp.

Tomsett, J.E. (1969): Average monthly and annual rainfall of E. Africa. <u>EAMD Techn. Memo. No. 14</u>.

Trewartha, G.T. (1961): <u>The earth problem climates</u>, University of Wisconsin Press, Madison, Milwaukee and London.

\-\-\-\-\-\-\-\-\- (1968): <u>An introduction to climate (fourth edition)</u> McGraw - hill Book company, N.Y.

Turpeinen O.M. (1986): Validation of the ESOC precipitation index. <u>Pept. Proc. 6th METEOSAT Scientific users meeting, Amsterdam, Netherlands, 25-27 November, 1986 VoL. II</u>.

\-\-\-\-\-\-\-\-, A. Abidi and W. Belhovanne (1987): Determination of rainfall with ESOC precipitation index. <u>Mon. Wea. Rev. 115</u>, 2699-2706.

\-\-\-\-\-\-\-\-\- And A.A. Diallo (1989): Estimation of rainfall in Burkina Faso using the Esoc precipitation Index <u>Journ. Climate 2</u>, 121-130.

Vonder Haar, T.H. and D.W. Hillger (1986): Lecture notes on the application of Meteorlogical satellites services and data. <u>WMO/TD No. 152</u>, pp 289-297.

Wilheit, T.T., J.S. Theon, W.E. Shenk, L.J. Allison and E.B. Rodgers (1976): Meteorological interpretations of the images from Nimbus - 5 electrically scanned microwave radiometer. <u>Journ. Appl. Meteor. 15</u>, 166-172.

\-\-\-\-\-\-\-\-\- A.T.C. Change, M.S.V. Rao, E.B. Rodgers and J.S. Theon (1977): A satellite technique for quantitatively mapping rainfall rates over oceans. <u>Journ. Appl. Meteor. 16</u>, 551-560.

\-\-\-\-\-\-\-\- (1986): Some comments on passive microwave measurements of rain. <u>Bull. Amer. Meteor. Soc. 67</u>, 1226-1232.

Wannacott, R.J.and T.H.Wanncott (1985): <u>Introductory statistics, 4th edition (1985)</u>, John - Wiley and Sons, N.Y.

WMO (1953): World distribution of thunderstorm days: <u>WMO/OMM-No.21. TP.6</u>.

WMO (1960): Guide to climatological practices. <u>WMO - No 100. TP. 44, Geneva, Switzerland.</u>

\-\-\-\-\-\-\-\-\-\-(1965): Guide to hydrometeorological practices. <u>WMO - No. 168, TP 82, Geneva, Switzerland</u>.

\-\-\-\-\-\-\-\-\-(1966): Statistical analysis and prognosis in Meteorology <u>WMO - No. 178. TP. 88, Techn. note No. 71, WMO, Geneva, Switzerland</u>.

\-\-\-\-\-\-\-\-\-(1970):Guide to hydrometeorological practices. 2nd edition, <u>WMO- No. 168. TP. 82</u>.

\-\-\-\-\-\-\-\-\-(1974):Guide to hydrological practices, 3rd edition, <u>WMO - No. 168, Geneva, Switzerland</u>.

----------(1983):Guide to Climatological practices.  <u>WMO - No. 100. Geneva Switzerland</u>.

Wolter, K.(1989):   Modes of Tropical circulation, Southern oscillation, and Sahel rainfall anomolies.  <u>Journ. Climate  2</u>, 149 - 172.

Yeh, H and K. Liou (1983):   Remote sounding of cloud parameters from a combination of infrared and microwave.  <u>Journ. Clim. Appl. Meteor. 22</u>, 201-213.